

Mechanisms of Sensory Integration Within the Somatosensory Modality and Their Investigation Using Magnetoencephalography

Inaugural-Dissertation

zur Erlangung des Doktorgrades
der Mathematisch-Naturwissenschaftlichen Fakultät
der Heinrich-Heine-Universität Düsseldorf

vorgelegt von

Thomas J. Baumgarten

aus Bad Honnef

Düsseldorf, Dezember 2015

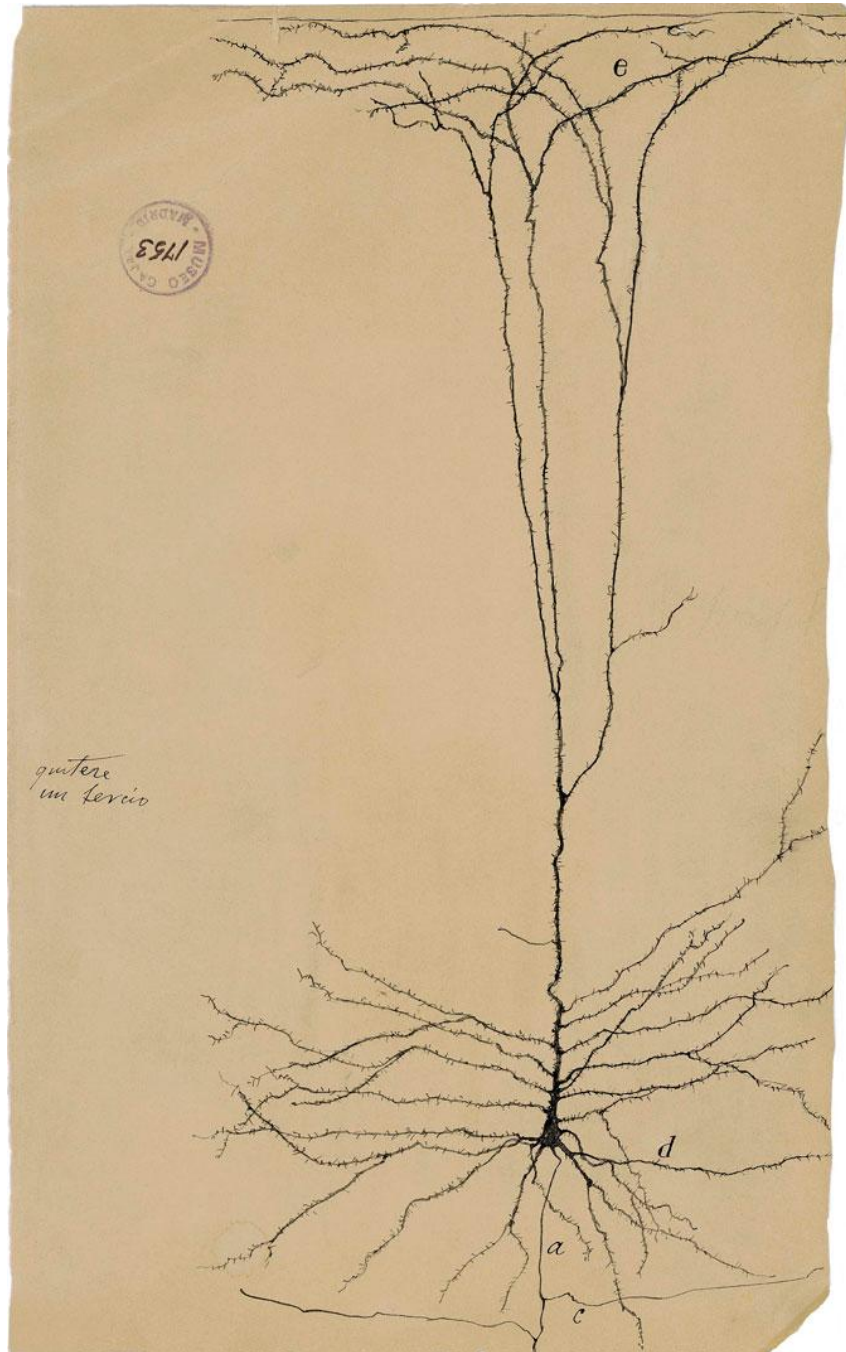
aus dem Institut für Klinische Neurowissenschaften und Medizinische Psychologie
der Heinrich-Heine-Universität Düsseldorf

Gedruckt mit der Genehmigung der
Mathematisch-Naturwissenschaftlichen Fakultät der
Heinrich-Heine-Universität Düsseldorf

Referent: Prof. Dr. Alfons Schnitzler

Korreferent: Prof. Dr. Petra Stoerig

Tag der mündlichen Prüfung: 16.09.2016



Pirámide gigante de la circunvolución frontal ascendente del hombre
Santiago Ramón y Cajal (1899)

Whilst part of what we perceive comes through our senses from the object before us,
another part (and it may be the larger part) always comes out of our own head.

William James (1890)

Table of contents

Glossary	6
Summary	8
Zusammenfassung	11
1 Introduction	14
1.1 The Origin of Extracellularly Measured Electrophysiological Signals	15
1.2 Magnetoencephalography: Measuring Neuromagnetic Signals.....	19
1.3 Neuronal Oscillations in the Human Cerebral Cortex.....	23
1.3.1 Characterizing Neuronal Oscillations.....	24
1.3.2 The Functional Role of Neuronal Oscillations.....	26
1.3.3 Analysis of Neuronal Oscillations Measured by MEG.....	28
1.4 The Somatosensory System	32
1.5 The Functional Role of Neuronal Oscillations in the Alpha and Beta Band	35
1.5.1 Alpha Band Activity	35
1.5.2 Alpha Band Activity in the Somatosensory System	37
1.5.3 Beta Band Activity	38
1.5.4 Beta Activity and its Connection to GABA-Mediated Inhibition	41
1.5.5 Setting the Stage - Alpha and Beta Band Activity in the Prestimulus Epoch....	42
2 Aims and Hypotheses	45
3 Study 1: Prestimulus Alpha Power Influences Tactile Temporal Perceptual Discrimination and Confidence in Decisions (Baumgarten et al., 2014, Cerebral Cortex)	48
3.1 Methods	49

3.2	Results	51
3.3	Discussion	52
3.4	Conclusion	53
4	Study 2: Beta Oscillations Define Discrete Perceptual Cycles in the Somatosensory Domain (Baumgarten et al., 2015, PNAS).....	54
4.1	Methods	55
4.2	Results	55
4.3	Discussion	56
4.4	Conclusion	58
5	Study 3: Beta Peak Frequencies at Rest Correlate with Endogenous GABA/Cr Concentrations in the Left Sensorimotor Cortex (Baumgarten et al., submitted)	59
5.1	Methods	60
5.2	Results	61
5.3	Discussion	61
5.4	Conclusion	63
6	General Discussion	64
7	Outlook.....	68
8	References	71
9	Erklärung	83
10	Danksagung	84
11	Appendix	86

Glossary

BA	Brodman area
CNS	Central nervous system
DICS	Dynamic imaging of coherent sources
ECoG	Electrocorticogram
EEG	Electroencephalogram
EPSP	Excitatory postsynaptic potential
ERF	Event-related field
fMRI	Functional magnetic resonance imaging
GABA	γ -aminobutyric acid
GABA/Cr	GABA-to-creatine ratio
IPSP	Inhibitory postsynaptic potential
LCMV	Linear constraint minimum variance
LFP	Local field potential
LMF	Local magnetic field
MEG	Magnetoencephalography
MRI	Magnetic resonance imaging
MRS	Magnetic resonance spectroscopy
PET	Positron emission tomography
ROI	Region of interest

S1	Primary somatosensory cortex
S2	Secondary somatosensory cortex
SOA	Stimulus onset asynchrony
SQUID	Superconducting quantum interference device
SSSEP	Steady-state somatosensory evoked potential
TMS	Transcranial magnetic stimulation

Summary

Sensory perception is known to critically depend on stimulus characteristics and the perceiver's state of consciousness. It is less known, however, that perception is also modulated by ongoing fluctuations of neuronal activity, which are continuously present in the awake and alert individual. Since the brain is continuously active, incoming sensory information is always superimposed on a preexisting level of neuronal activity. Therefore, it is likely that the state of the brain prior to stimulus presentation influences subsequent stimulus processing and perception.

The present thesis investigated ongoing neuronal oscillations in the somatosensory cortex, which represent a correlate of continuous neuronal activity. Specifically, the connection between neuronal oscillations and the processing and perception of suprathreshold electrotactile stimuli was examined. The major aim was to determine how varying perception of physically identical stimulation was related to different states of oscillatory neuronal activity present before stimulation. Three studies were included in this thesis. All studies analyzed neuromagnetic brain activity measured by magnetoencephalography (MEG). The first two studies examined the connection between the perception of suprathreshold electrotactile stimuli presented in rapid succession and oscillatory power (study 1) or oscillatory phase (study 2) prior to stimulation. To further elucidate the neurochemical basics of oscillatory neuronal activity, the relations between oscillatory neuronal activity and local non-modulated neurotransmitter concentrations measured by magnetic resonance spectroscopy (MRS) were investigated (study 3).

Study 1 analyzed the connection between oscillatory alpha band (8-12 Hz) power present before stimulus presentation and the perception of suprathreshold electrotactile stimuli (i.e., the number of perceived stimuli). Subjects responded whether they perceived two electrotactile stimuli presented in rapid succession as either one single stimulus or two separate stimuli, along with the subjective confidence in their report. Although stimulation was kept physically constant within subjects, perceptual reports varied between the perception of one stimulus or

two stimuli. Alpha band power before stimulus presentation was decreased in the postcentral gyrus and the middle occipital region contralateral to stimulation site when subjects perceived stimulation as two separate stimuli. In addition, a negative linear relation was found between alpha band power and perceptual response rates. Alpha band power levels also were linearly related to confidence ratings. However, the directions of the relations were inversely oriented for trials with differing perceptual reports. In addition, event-related fields (ERFs) time-locked to stimulus presentation were investigated as a correlate of stimulus processing. ERFs of trials with physically identical stimulation differed according to the respective perception of stimulation and thus demonstrated characteristics of a decision variable. ERFs were interpreted in light of current models of perceptual decision making. The results suggest that alpha band power influences how many suprathreshold electrotactile stimuli are perceived and how confident subjects are regarding their perception. Thus, alpha band power seems to modulate the quality of perception.

Study 2 investigated the same paradigm as study 1 but focused on oscillatory phase within the primary somatosensory cortex (S1). In line with study 1, trials in which physically constant stimulation was perceived differently were compared. Before stimulus presentation, oscillatory phase angles in the alpha and low beta band (8-20 Hz) significantly differed between trials with varying perception, with phase angle differences fluctuating around maximum. Based on these results, a model of discrete perceptual cycles was introduced. According to the model, oscillatory cycles of a specific frequency sample incoming somatosensory stimuli, thereby determining the temporal resolution of somatosensory perception. If two stimuli impinge on the somatosensory system together within one cycle, stimulation is perceived as a single stimulus. Vice versa, if each of the two stimuli impinges on the somatosensory system during a separate cycle, stimulation is perceived as two separate stimuli. The specific frequency determining the cycle length was derived from the significant phase angle differences and thus was localized in the alpha and lower beta band. Based on the model, group-level and single-subject perceptual response rates were predicted. The findings provide evidence for a discrete mode of perception in the somatosensory domain, which could so far only be shown for the visual domain.

Study 3 examined the relationship between beta band peak frequency and γ -aminobutyric acid (GABA) concentrations in spatially defined cortical areas. Although various parameters of beta band activity have been previously linked to GABA concentrations, relationships could mostly be shown for movement-related beta band activity and/or pharmacologically modulated GABA concentrations. Beta band peak frequencies measured at rest and non-modulated GABA concentrations assessed with MRS were estimated for left and right sensorimotor and occipital cortices. Within cortices, beta band peak frequencies and GABA concentrations were correlated. A positive linear relation between beta band peak frequency and GABA concentration was determined for the left sensorimotor cortex. Here, subjects showing a higher beta band peak frequency also exhibited a higher local GABA concentration. This spatially specific connection demonstrates that previously reported links between beta band activity and GABA concentrations are also present at rest and regarding non-modulated GABA concentrations.

The studies presented in the course of this thesis demonstrate that parameters of ongoing neuronal oscillatory activity are related to the processing and perception of suprathreshold electrotactile stimuli. Importantly, the findings suggest that the neuronal activity present before stimulus presentation influences the quality of perception of suprathreshold stimuli. In addition, beta band peak frequencies measured at rest correlated with local non-modulated neurotransmitter concentrations. This result provides novel insights into the neurochemical basics underlying neuronal oscillations.

Zusammenfassung

Sensorische Wahrnehmung beruht maßgeblich auf den Eigenschaften der präsentierten Stimuli, sowie auf dem Bewusstseinszustand der wahrnehmenden Person. Weniger bekannt ist allerdings, dass sensorische Wahrnehmung auch durch anhaltende Fluktuationen neuronaler Aktivität beeinflusst wird, die kontinuierlich im wachen Zustand auftreten. Da das Gehirn kontinuierlich aktiv ist, trifft eingehende sensorische Information immer auf ein bereits bestehendes Aktivitätsniveau. Es ist daher wahrscheinlich, dass das zerebrale Aktivitätsniveau welches vor der Präsentation des Stimulus vorliegt, die nachfolgende Verarbeitung und die Wahrnehmung des Stimulus beeinflusst.

Kernstück der vorliegenden Dissertation ist die Untersuchung neuronaler Oszillationen im somatosensorischen Cortex. Dabei wurde die Verbindung zwischen neuronalen Oszillationen und der Wahrnehmung überschwelliger elektrotaktile Stimuli betrachtet. Zentral war hierbei, wie unterschiedliche Wahrnehmungseindrücke, welche durch physikalisch identische Stimulation hervorgerufen wurden, mit dem Zustand neuronaler Oszillationen vor der Stimulation zusammenhängen. Die vorliegende Dissertation umfasst drei Studien, in denen neuromagnetische Hirnaktivität mithilfe der Magnetoenzephalographie analysiert wurde. Die ersten beiden Studien untersuchten die Verbindung zwischen der wahrgenommenen Anzahl elektrotaktile Stimuli, die mit kurzem zeitlichem Abstand hintereinander dargeboten wurden, und dem Leistungsspektrum (Studie 1) oder der Phase (Studie 2) neuronaler Oszillationen vor der Präsentation der Stimuli. Um die neurochemischen Grundlagen neuronaler oszillatorischer Aktivität zu ermitteln, wurde die Verbindung zwischen neuronaler oszillatorischer Aktivität und lokalen nicht-modulierten Neurotransmitterkonzentrationen analysiert (Studie 3).

Studie 1 erforschte die Verbindung zwischen der Wahrnehmung überschwelliger elektrotaktile Stimuli und dem Leistungsspektrum im Alpha Frequenzband (8-12 Hz) vor der Stimulation. Die Versuchspersonen gaben an, ob sie zwei kurz nacheinander dargebotene elektrotaktile Stimuli als einen oder zwei zeitlich distinkte Reize wahrnahmen, sowie die subjektive Sicherheit ihrer jeweiligen Antworten. Obwohl die Stimulation in jedem Versuchsdurchgang physikalisch

identisch war, wurde die Stimulation wechselnd als ein Stimulus oder zwei Stimuli wahrgenommen. Wurde die Stimulation als zwei Reize wahrgenommen, war das Leistungsspektrum im Alpha Frequenzband vor dem Zeitpunkt der Stimulation im Gyrus Postcentralis und im mittleren okzipitalen Cortex kontralateral zur stimulierten Seite vermindert. Zudem zeigte sich ein negativer linearer Zusammenhang zwischen dem Leistungsspektrum im Alpha Frequenzband und der Wahrnehmungsrate. Lineare Zusammenhänge bestanden auch zwischen dem Leistungsspektrum im Alpha Frequenzband und der subjektiven Antwortsicherheit, wobei sich die Richtung dieser Zusammenhänge jedoch zwischen Versuchsdurchgängen mit verschiedener Stimuli-Wahrnehmung unterschied. Ereigniskorrelierte Felder nach (physikalisch identischer) Stimuli-Präsentation unterschieden sich zwischen Versuchsdurchgängen mit unterschiedlicher Stimuli-Wahrnehmung, was eine charakteristische Eigenschaft von Entscheidungsvariablen darstellt. Die Ergebnisse wurden daher im Rahmen aktueller Modelle zur Entscheidungsfindung interpretiert. Die Befunde von Studie 1 zeigen, dass das Leistungsspektrum im Alpha Frequenzband die Wahrnehmung von überschwelligen Reizen und darüber hinaus die subjektive Sicherheit der angegebenen Wahrnehmung qualitativ beeinflusst.

Studie 2 nutzte dasselbe Paradigma wie Studie 1, fokussierte sich allerdings auf die oszillatorische Phase innerhalb des primären somatosensorischen Cortex. Wie in Studie 1 wurden Versuchsdurchgänge verglichen, in denen physikalisch identische Stimulation zu verschiedenen Wahrnehmungseindrücken führte. Vor dem Zeitpunkt der Stimuli-Präsentation unterschieden sich die oszillatorischen Phasenwinkel im Alpha und unteren Beta Frequenzband (8-20 Hz) signifikant zwischen Versuchsdurchgängen mit unterschiedlicher Stimuli-Wahrnehmung. Darauf basierend wurde ein Modell erstellt, welches diskrete Wahrnehmungszyklen innerhalb der somatosensorischen Modalität beschreibt. Hierbei bestimmen Zyklen einer bestimmten Frequenz wie eingehende somatosensorische Stimulus-Repräsentationen zeitlich erfasst und abgetastet werden, wodurch sich die zeitliche Auflösungsfähigkeit somatosensorischer Wahrnehmung ergibt. Falls zwei Stimulus-Repräsentationen innerhalb eines einzelnen Zyklus auf das somatosensorische System treffen, wird die Stimulation als ein einziger Stimulus wahrgenommen. Erreicht jede der zwei Stimulus-

Repräsentationen des somatosensorischen Systems jedoch während eines einzelnen, separaten Zyklus, wird die Stimulation als zwei Stimuli wahrgenommen. Die spezifische Frequenz, welche diese Zyklen bestimmt, wurde aus den signifikanten Unterschieden der Phasenwinkel abgeleitet und lag im Alpha- und niederen Beta-Frequenzband. Basierend auf dem Modell und den empirisch gewonnenen Frequenzen konnten Wahrnehmungsraten für die gesamte Stichprobe, als auch für einzelne Versuchspersonen vorhergesagt werden. Die vorliegenden Ergebnisse sprechen für eine zeitlich diskrete Wahrnehmung innerhalb der somatosensorischen Modalität, was bisher nur für die visuelle Modalität aufgezeigt werden konnte.

Studie 3 untersuchte die Beziehung zwischen der Frequenz innerhalb des Beta-Frequenzbands mit dem höchsten Leistungsspektrum (Gipffrequenz) und der γ -Aminobuttersäure (GABA) Konzentration in lokalen Cortexarealen. Bisher konnten solche Zusammenhänge fast ausschließlich für bewegungsassoziierte oszillatorische Aktivität im Beta-Frequenzband und/oder für pharmakologisch modulierte GABA-Konzentrationen aufgezeigt werden. Innerhalb des linken und rechten sensomotorischen, sowie okzipitalen Cortex wurden die Gipffrequenzen innerhalb des Beta-Frequenzbands während einer Ruheaufgabe und die nicht-modulierten GABA-Konzentrationen mittels Magnetresonanztomographie (MRS) gemessen und miteinander korreliert. Ein positiver linearer Zusammenhang zwischen den Gipffrequenzen innerhalb des Beta-Frequenzbands und den GABA-Konzentrationen konnte für den linken sensomotorischen Cortex festgestellt werden. Somit konnten zuvor berichtete Assoziationen zwischen neuronalen Oszillationen im Beta-Frequenzband und GABA-Konzentrationen auch ohne bewegungsassoziierte Einflüsse und bezüglich nicht-modulierten GABA-Konzentrationen aufgezeigt werden.

Die vorliegenden Studien demonstrieren, dass Parameter fortlaufender neuronaler oszillatorischer Aktivität im Zusammenhang mit der neuronalen Verarbeitung und Wahrnehmung überschwelliger elektrotaktile Stimuli stehen. Dies legt einen qualitativen Einfluss neuronaler oszillatorischer Aktivität auf die Wahrnehmung überschwelliger Stimuli nahe. Zusätzlich konnten nicht-motorische Gipffrequenzen innerhalb des Beta-Frequenzbands mit lokalen nicht-modulierten Neurotransmitterkonzentrationen assoziiert werden, was neuartige Einblicke in die neurochemischen Grundlagen neuronaler Oszillationen ermöglicht.

1 Introduction

One of the most fundamental functions of the brain is the processing and integration of sensory information derived from the outside world. However, the representation of sensory information in the brain does not constitute a simple copy of external information converted into a different format (Buzsáki and Draguhn, 2004). Accordingly, sensory information is not processed mechanistically and identical stimulation can result in different perceptual sensations. Which factors give rise to this perceptual variability and how do they influence the formation of perception? Since the brain is continuously active, sensory input always impinges on an already present level of activity. Therefore, it is likely that the processing and perception of sensory input is modulated by the brain state which is present prior to the emergence of the sensory event (Hebb, 1949).

The present thesis investigates neuronal oscillations in the somatosensory cortex, which represent indicators of continuously ongoing neuronal activity. More specifically, the connection between neuronal oscillations and the perception of electrotactile stimulation is analyzed. By focusing on neuronal oscillations present before stimulus presentation, the influence of ongoing neuronal activity on subsequent stimulus processing and, ultimately, perception is examined. To further elucidate the neurochemical basics of neuronal oscillations, the relation between neuronal oscillations and neurotransmitter concentrations is investigated.

In the course of this introduction, a brief description of the fundamentals of the origin and measurement of electrophysiological signals with a focus on MEG measurements and data analysis will be presented. Based on this, general concepts of neuronal oscillatory activity will be introduced. Subsequently, the human somatosensory system will be described, followed by a focus on the generation and the functional role of oscillatory activity in the somatosensory system. Finally, the core hypotheses and the studies published within the framework of this thesis are presented.

1.1 The Origin of Extracellularly Measured Electrophysiological Signals

Phenomenologically, neuronal oscillations represent cyclic variations in externally measured signals assuming to reflect metrics of brain activity. In order to appropriately interpret the significance of neuronal oscillations, it is fundamental to know how the respective signals are generated in the brain (i.e., which sort of 'brain activity' is represented by the measured signal). Although the major analyses in this thesis focus on the macroscopic level of neuronal activity, a microscopic perspective is necessary to elucidate how cellular-level structures and processes give rise to externally measurable signals of neuronal activity. Therefore, the fundamentals of neuronal information transfer are briefly recapitulated. The components that significantly contribute to externally measurable signals of neuronal activity are highlighted.

Neuronal information transfer critically depends on changes in the membrane permeability for specific ions. When neurotransmitters are released into the synaptic cleft and dock at receptors of a postsynaptic cell, the postsynaptic membrane permeability is altered due to a relative increase of open ion channels within the membrane. Because of different ion concentrations in the intra- and extracellular space, this leads to a transient flow of ions across the postsynaptic membrane according to their chemical concentration gradient. In response, an electrical current is generated in the postsynaptic cell and its membrane potential deviates from its resting potential. In case of an influx of positively charged ions (mostly Na^+), electric current is directed into the neuron and, given the simultaneous input of a sufficient number of presynaptic neurons, eventually gives rise to an excitatory postsynaptic potential (EPSP). Alternatively, an influx of negatively charged ions (mostly Cl^-) or an efflux of positively charged ions (mostly K^+) causes a current that is directed from the intracellular to the extracellular medium, resulting in an inhibitory postsynaptic potential (IPSP; Hansen et al., 2010). Eventually, an EPSP leads to a depolarization of the membrane with the potential shifting towards the neuron's firing threshold. An IPSP leads to a hyperpolarization, thus shifting the potential away from the firing threshold. If the postsynaptic membrane potential is sufficiently depolarized and crosses a specific spiking threshold, an action potential is generated. The action potential then propagates along the neuronal axon to the synaptic knob, determining the release of neurotransmitters into the synaptic cleft. Thereby, the process begins anew in the subsequent, downstream neuron.

Within a specific brain volume, the contributions of electrical current from all active cellular processes superimpose at a given location outside of the active neuron. Here, in the extracellular medium, the superimposed currents generate a potential (V_e ; measured in Volts), defined in respect to a reference potential. V_e can also be compared across two different locations, thereby resulting in an electric field (the negative spatial gradient of V_e ; measured in Volts/distance). This electric field indicates the vectorial electromagnetic forces that act on any charged particle. Consequently, every transmembrane current determines an intra- and extracellular voltage deflection and a corresponding electric field. Such electric fields can be recorded extracellularly, either locally by means of a microelectrode in form of a local field potential (LFP), from subdural grid electrodes directly applied onto the cortical surface as an electrocorticogram (ECoG), or from the scalp as an electroencephalogram (EEG; Buzsáki et al., 2012). Furthermore, transmembrane currents induce a magnetic field, which can be recorded outside of the head by means of magnetoencephalography (MEG; see section 1.2).

Since externally measured electric or magnetic fields result from the superposition of any sort of transmembrane current, it is of major importance to specify the respective contributions of different neuronal processes and neuron types to the extracellular field. This is necessary in order to infer which 'neuronal activity' is represented by an externally measured signal.

Currents generated by neuronal activity can be subdivided into two main categories; axonal action potentials and dendritic post-synaptic potentials (Hall et al., 2014). While action potentials are classically considered as the elemental 'unit of information' in neuronal information transfer, post-synaptic activity presumably provides the major contribution to externally measurable current flow (Hansen et al., 2010; Lopes da Silva, 2013). Partially, this is due to the effect of temporal summation. Extracellular currents from many different sources have to co-occur and temporally overlap in order to induce a signal strong enough to be externally measurable. This temporal overlapping is more likely for relatively slow events (e.g., postsynaptic potentials, which last for tens of milliseconds; Buzsáki, 2006) than for short events like action potentials. Although action potentials generate currents that can be detected extracellularly as spiking activity, the corresponding electrical fields are of short duration (< 2 ms). Thus, action potentials are not considered to significantly contribute to LFP activity

with less than 100 Hz (Buzsáki et al., 2012). Furthermore, because of its low electrical resistance, the extracellular space acts like a low-pass filter. This allows slowly undulating voltages like postsynaptic potentials to propagate farther, compared to fast-rising spikes of action potentials (Buzsáki, 2006).

Additionally, the contribution of postsynaptic currents to externally measured brain signals is considered higher than the contribution of action potentials due to different electrical properties of the two signals. Dendritic current flow due to postsynaptic potentials can be approximated as a current dipole. Current dipoles are represented by two opposite charges with a theoretically infinitely small spatial separation (Buzsáki et al., 2012) and can be interpreted as the spatial center of gravity of momentary cortical activity (Lopes da Silva, 2013). The two opposing charges giving rise to a dipole are created as follows: The movement of positively charged ions from the extracellular into the intracellular space (e.g., at an excitatory synapse) results in a local extracellular sink. Consequently, an electrical current (labeled primary current) builds up along the interior of the postsynaptic cell. In order to balance the extracellular sink, passive ohmic currents (labeled volume or return currents) are generated in the surrounding extracellular medium. These volume currents give rise to an opposing efflux of ions from the cell into the surrounding extracellular space, thereby completing the loop of ionic-flow and preventing any buildup of charge (Hämäläinen et al., 1993; Buzsáki et al., 2012). The respective location of this efflux is labeled a source. Thus, synaptic activity at a given location of the dendritic membrane creates a specific sink-source configuration in the extracellular medium, which can be approximated as current dipole. In contrast, axonal currents due to action potentials create two parallel current dipoles of equal intensity but opposite orientation (one dipole on the leading edge and one dipole on the trailing edge of the action potential peak propagating along the axon), resulting in a quadrupolar current dipole. The electric field strength of a dipole falls off with distance with the rate of $1/(\text{distance})^2$, whereas for a quadrupole, the field strength drops with the rate of $1/(\text{distance})^3$. Thus, the contribution of postsynaptic currents to signals measured at a certain distance can be considered significantly higher (Hall et al., 2014).

In addition to temporal summation and current properties, the geometry and cytoarchitectonical orientation of neuronal sources is highly relevant for the generation of externally measurable signals. Although generally all neuron types are considered to contribute to the extracellular field, the main contribution to EEG and MEG signals is made by pyramidal neurons (Hämäläinen et al., 1993; Hansen et al., 2010; Lopes da Silva, 2013). These cells possess characteristically shaped and orientated long apical dendrites and are located exclusively in the cerebral cortex, in all layers except layer 1. Approximately, pyramidal neurons constitute about 70-85 % of the total cortical neuronal population. Therefore, they have been considered the principal neuron of the cerebral cortex (DeFelipe and Fariñas, 1992). The cytoarchitectonical organization of neurons is relevant for their contribution to the extracellular field, because the spatial distance between sink and source determines the ion flow in the extracellular medium and thus, the strength of the dipole (Hari et al., 2010; Buzsáki et al., 2012). Active pyramidal neurons generate strong dipoles along their main axis due to their characteristic thick apical dendrites, as there is a substantial distance between sink and source. Consequently, the resulting electric field can be measured across a large distance, which is why it is termed an open field. On the contrary, neurons with spherically symmetrically orientated dendrites create a closed field and thus contribute far less to the extracellularly measured field (Hansen et al., 2010). Furthermore, it has to be taken into account that externally measured brain signals reflect neuronal population activity; i.e., the summated post-synaptic potentials of a multitude of coherently active neurons. Therefore, the collective orientation of the active neurons is of major importance. Pyramidal neurons are arranged analogous to a palisade; i.e., the main axes of the dendritic trees are positioned parallel to each other and the cells are oriented perpendicular to the cortical surface. This geometry allows for the efficient superposition of synchronously active dipoles, giving rise to relatively large LFPs (Buzsáki et al., 2012; Hall et al., 2014). Finally, the gyrification of the cerebral cortex leads to a dense concentration of the apical dendrites of pyramidal cells in the concave side of a gyrus. By this, the current density is enhanced, which in turn amplifies the externally measurable signal (Buzsáki et al., 2012).

Taken together, the systematic temporal co-activation of a multitude of neurons, as well as their specific spatial organization, generates electrical fields (or, in case of MEG measurements,

magnetic fields) of sufficient magnitude to be externally measured. By means of an inserted microelectrode these signals can be recorded locally as LFPs. LFPs are mainly generated by the superposition of synchronized transmembrane currents, spatially averaged over hundreds to thousands of neurons in close vicinity (several hundred μm) of the electrode tip (Katzner et al., 2009; Wang, 2010). LFPs and their magnetic counterparts, local magnetic fields (LMFs), can be seen as microscopic core elements that give rise to EEG and MEG signals. The neuronal sources generating the respective signals are considered to be essentially the same (Lopes da Silva, 2013). However, there are significant differences regarding the measured signals. While EEG measures electrical potential differences between electrodes applied on the scalp (Baillet et al., 2001) and thus can be interpreted as the macroscopic equivalent of a LFP, the signal measured by MEG is physically different. This is addressed in more detail in the following section.

1.2 Magnetoencephalography: Measuring Neuromagnetic Signals

In contrast to LFPs and EEG, MEG does not measure the electric field determined by neuronal currents, but the magnetic field over the scalp induced by these currents. The strength of a magnetic field is determined by the distance, strength and geometry of the current distribution. Magnetic fields can be calculated with the help of Maxwell's equations (Maxwell, 1865), given that the primary current source and the conductivity of the surrounding medium are known (Hämäläinen et al., 1993). Because magnetic fields are always orientated orthogonally to the underlying primary currents, only dipoles orientated tangentially to the cortex surface give rise to magnetic fields that are measurable outside of the head. In contrast, radially oriented dipoles produce silent magnetic fields that cannot be measured outside the head (Hämäläinen et al., 1993). As a consequence, fissural neuronal activity is considered the major generator of MEG signals (see Fig. 1 for a schematic representation). From this and the electric properties of different transmembrane currents specified in the previous section, it follows that MEG signals primarily originate from dendritic current flow due to synchronous postsynaptic potentials in a population of coherently active pyramidal neurons orientated perpendicular to the cortical surface (i.e., within cortical fissures; Hämäläinen et al., 1993; Hari et al., 2010; Hall et al., 2014).

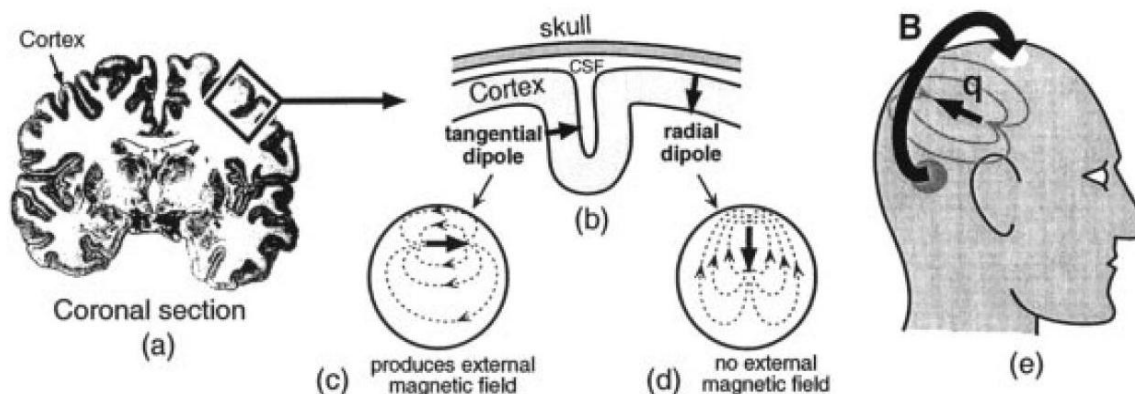


Figure 1: Schematic representation of the origin of MEG signals. (a) Coronal slice of the human brain. The cortical surface is represented by dark color. (b) Close-up on the cortical surface. Primary currents (black arrows) flow perpendicular to the cortical surface. Depending on their position in gyri and sulci, the currents flow either tangentially or radially relative to the head. (c) Tangentially oriented currents produce externally visible magnetic fields that can be measured outside the head. (d) Radial currents produce silent magnetic fields. Consequently, no magnetic fields can be measured outside the head. (e) The magnetic field induced by the exemplary dipole \mathbf{q} exits and reenters the scalp. Adapted from Vrba and Robinson, 2001.

Neuromagnetic signals as measured by MEG are direct correlates of neuronal activity. Therefore, they offer a more direct insight into ‘brain activity’ compared to indirect metrics (e.g., functional magnetic resonance imaging (fMRI) blood-oxygen-level dependent contrast and positron emission tomography (PET) glucose-metabolism). This advantage is accompanied by a high temporal resolution, which is limited only by the sampling speed of the system and can reach up to 12,000 Hz in modern MEG systems (Hall et al., 2014). Consequently, neuronal activity can be recorded on a millisecond timescale, enabling a detailed investigation of the temporal dimension of neuronal processes. In contrast, the spatial localization of the signal sources poses an inherent challenge in MEG measurements. This is due to the electromagnetic inverse problem; i.e., the estimation of source currents within the head given only externally measured signals. Because inverse problems are ill-posed and have no unique solution (i.e., a multitude of different source configurations can create a given signal), it is necessary to include certain theoretical constraints and assumptions about the underlying sources in the source model (Hämäläinen et al., 1993). Accordingly, the localization of neuronal sources in MEG

measurements always depends on the validity of the a priori defined assumptions and simplifications (e.g., the simplified representation of primary currents as current dipoles; Baillet et al., 2001). The topic of source localization is addressed in more detail in section 1.3.3.3. Nonetheless, MEG offers a higher spatial accuracy than EEG. Because in both methods, neuronal signals are measured outside of the head, the signals have to pass the intermediary layers of tissue (e.g., liquor, skull and scalp). These tissues exhibit inhomogeneous electrical conductivity, which modulate externally measured signals. Thus, the externally recorded signal represents a distorted image of the underlying sources. Since magnetic fields are far less distorted by the different tissues than electric fields, the modeling of extra-cranial fields holds a potentially higher spatial accuracy for MEG compared to EEG (Baillet et al., 2001; Hall et al., 2014). Under favorable conditions, the average spatial accuracy of MEG is considered to be around a few millimeters (Hämäläinen et al., 1993).

Another point determining the spatial resolution of MEG is the distance between sensor and signal source. In general, the further the recording sensor is positioned from the current source, the greater the spatial averaging of the signal; i.e., the more indistinct the measured signal becomes regarding the events at the current source (Buzsáki et al., 2012). This general principle holds true also for macroscopic measurements of brain activity, specifically for MEG. Since in MEG the sensors are located outside of the skull and thus in considerable distance to the current sources (approximately 4-5 cm), the degree of spatial averaging is relatively high. Thus, MEG recordings are biased towards the representation of synchronized activity, since non-synchronized sources are canceled out due to spatial averaging (Uhlhaas et al., 2009). Consequently, a large population of neurons has to be synchronously active to generate a visible MEG signal. Neuromagnetic signals as measured by MEG typically range from $50\text{-}500 \cdot 10^{-15} \text{ T}$ (Hämäläinen et al., 1993). The extent of cortical activity (i.e., the number of synchronously active neurons) that is necessary to generate signals of such magnitude is estimated to be around 40 mm^2 of cortical surface (Chapman et al., 1984), which corresponds to approximately 10,000-50,000 neurons (Murakami and Okada, 2006).

Because neuromagnetic activity produces signals with low field strength, MEG systems require highly sensitive sensors. Currently, the only sensor that is able to reliably measure such small

signals is the superconducting quantum interference device (SQUID; Zimmerman et al., 1970). To further increase sensitivity, special pickup coils are coupled to the SQUIDS. These coils detect the neuromagnetic fields and route the signal to the SQUIDS (see Vrba and Robinson, 2001 for a detailed review on SQUID technology). To guarantee such high levels of sensitivity, SQUIDS and pickup coils have to possess superconductivity, which is achieved by placing the sensors in liquid helium ($4.2^{\circ}\text{K}/ -268.95^{\circ}\text{C}$ at sea level; Reite and Zimmerman, 1978). Modern systems comprise several hundred sensors arranged in a head-size shaped cavity. Sensors and cryogenic agent rest within a vacuum-isolated container called a dewar, which is placed inside an external casing (Fig. 2).



Figure 2: Frontal view of an exemplary MEG system. The photo shows the Elekta Neuromag Vector View 306 Channel MEG system (Elekta Oy, Helsinki, Finland) of the Institute of Clinical Neuroscience and Medical Psychology at the University Clinic of Düsseldorf. The neuromagnetic field is detected by pickup coils built into the helmet-shaped cavity. Coils, SQUID sensors and cryogenic agent are fitted within the dewar, which is placed in a composite fiberglass-synthetic made gantry. The subject is seated in a movable chair with the head placed within the cavity. Alternatively, the gantry can be tilted backwards to measure subjects in a supine position.

A considerable problem is the separation of neuromagnetic signals from external magnetic noise. Since the neuromagnetic fields are extremely small, they are superimposed by other magnetic signals of higher magnitude, provided that these signals are not specifically filtered out and rejected. Noise signals can be of biological (e.g., muscle contraction) or non-biological (e.g., moving magnetic objects) origin. Therefore, MEG systems rely on different mechanisms to reduce external magnetic noise. One mechanism is provided by the special superconducting pickup coils or flux transformers, which guide the magnetic signal to the SQUID sensors. Often, the coils are constructed in a specific configuration with two coils positioned in series, either horizontally (planar) or vertically (axial). Such gradiometer coils measure the magnetic field gradient selectively across the device-dimension (i.e., in longitudinal or latitudinal direction,

respectively). Consequently, the system is most sensitive to spatially inhomogeneous signals of nearby sources and insensitive to spatially uniform signals of distant sources (Hämäläinen et al., 1993). In addition, MEG systems are placed in special magnetically shielded rooms. These rooms are encased with specific metals suppressing external magnetic noise, thereby shielding the sensors. Supplementary to these hardware-based mechanisms of noise reduction, there are various software-based processing tools available for noise filtering and cancellation (Vrba and Robinson, 2001).

After briefly describing the origin and measurement of electrophysiological and neuromagnetic signals, the next section will focus on the fundamental characteristics, basic functions and analysis of neuronal oscillations.

1.3 Neuronal Oscillations in the Human Cerebral Cortex

Neuronal oscillations represent rhythmic variations in the synchronous activity of neuronal populations over a wide temporal and spatial range. The periodicity of oscillatory signals is generated by both cellular mechanisms as well as circuit properties in neuronal networks (see section 1.3.1 for details). Within networks, rhythmic synchronization of neurons emerges from the dynamic interaction between excitation and inhibition, relying heavily on the influence of inhibitory interneurons (Wang, 2010). These variations in neuronal activity can be measured locally in form of LFPs or more globally in form of EEG or MEG signals. Regarding the measured signal, neuronal oscillations are considered to result from periodic fluctuations in membrane potentials mainly caused by postsynaptic potentials (Gray and Singer, 1989) and thus represent cyclic changes in neuronal excitability (Fries, 2005; Thut et al., 2012; Jensen et al., 2014). Importantly, neuronal excitability can be understood in an afferent and efferent sense; i.e., it determines the sensitivity to afferent synaptic input as well as the probability for efferent output (Fries, 2005). Although the connection between neuronal excitability and neuronal oscillations has already been postulated since the early days of electrophysiology (Bishop, 1933; Lindsley, 1952), it has only recently been experimentally verified by studies directly linking neuronal firing rates (i.e., neuronal excitability) to specific points in the cycle of ongoing fluctuations in LFP and EEG recordings (Lakatos et al., 2005). However, the relationship between

the firing pattern of individual cells and oscillatory population activity is of stochastic nature. Individual neurons participating in oscillating populations do not have to show strictly oscillatory output themselves, since they do not regularly discharge at every single cycle (Singer, 2013).

Synchronization and Oscillations

Synchronization and oscillations are no phenomena restricted to neuronal activity, but can be found in various biological and non-biological systems. A classic example of oscillations in biological systems is the cardiac rhythm. In non-biological systems, the swinging pendulum of a clock is often used to illustrate oscillatory processes. In general, oscillations can be understood as the periodic repetition of similar patterns in the time domain, ranging from highly regular to highly irregular periodicity (Singer, 2013). These repeating periodic variations (i.e., cycles) produce rhythms, which often interact with the environment and thereby generate the effect of synchronicity. Synchronicity is defined as the precise co-occurrence of events in the time domain; i.e., if multiple events co-occur at the same point in time. The state of synchronicity is achieved by synchronization, defined as an “adjustment of rhythms of oscillatory objects due to their weak interaction” (Pikovsky et al., 2001). This is also visible in the word’s origin from the Greek words *Χρόνος* (*chronos*, i.e., time) and *σύν* (*syn*, i.e., common). Literally, “synchronous” therefore means “occurring in the same time”.

1.3.1 Characterizing Neuronal Oscillations

Neuronal oscillations are unambiguously characterized by three specific parameters. The maybe most fundamental one is frequency, defined as the amount of cycles elapsed within the time span of one second (measured in Hz). Frequency defines different oscillatory bands. In the human brain, oscillatory activity covers a wide range from approximately 0.5 Hz to 500 Hz (Buzsáki and Draguhn, 2004) and can be divided into delta (<2 Hz), theta (4-7 Hz), alpha (8-12 Hz), beta (13-30 Hz), low gamma (30-60 Hz), high gamma (60-90 Hz; Singer, 2013) and high frequency oscillations (>100 Hz). However, it is important to note that the boundaries between different frequency bands are loosely defined and a subject of ongoing debate. The main rationale for the distinction of different frequency bands is that they are often associated with

different functional brain states (Klimesch, 1999; Kopell et al., 2000). The present thesis focuses on oscillations in the alpha and beta band, which are described in detail in the sections 1.5.1 and 1.5.3, respectively.

A further important parameter of neuronal oscillations is power. Oscillatory power is defined as the square of the Fourier amplitude of a signal (Buzsáki et al., 2012). Power variations are considered to result from an increase or decrease in the synchronization of the underlying neuronal population. Additionally, power is related to the number of synchronously active neurons (Pfurtscheller and Lopes da Silva, 1999). Power can be used to approximate the number of EPSPs arriving in a given neuronal population at a given time point (Varela et al., 2001). Interestingly, the frequency of neuronal oscillations is inversely related to their power; i.e., signals with high frequency usually exhibit a lower power compared to low frequency signals (Freeman et al., 2000). Because power is proportional to the number of synchronously active neurons, this $1/f$ power ratio implies an important functional property of neuronal oscillations. Generally, oscillations in higher frequency bands (e.g., gamma oscillations) are assumed to be restricted to smaller neuronal networks, hence supporting local computation, whereas slow oscillations are more often associated with larger cortical networks (Pfurtscheller and Lopes da Silva, 1999; Buzsáki and Draguhn, 2004). In line with this, neuronal networks operating at low frequency are considered to influence local high frequency networks in a hierarchical, top-down fashion (Lakatos et al., 2005; Lakatos et al., 2008).

Oscillatory phase explicitly defines at which point of a cycle an oscillating signal is at a given time point. It represents a cyclic parameter and ranges from $0-2\pi$ or alternatively from $0-360^\circ$. Phase determines the timing of neuronal firing and thus defines discrete windows of excitation and inhibition with high temporal resolution (Busch et al., 2009; Mathewson et al., 2011).

The properties of neuronal oscillations are determined by both cellular and network characteristics (Wang, 2010). Oscillatory firing patterns are also known from single neurons (Llinas, 1988). This suggests the existence of mechanisms generating oscillatory output that are largely independent from network properties. Such intrinsic oscillatory properties of single neurons enable them to act as pacemaker, thus shaping oscillatory activity within networks. For

single neurons to establish synchronicity in neuronal networks, it is of critical importance how neurons temporally adjust their firing according to their phasic synaptic input (Wang, 2010). Passive membrane properties like specific leak conductance act as a low-pass filter for incoming signals. In contrast, voltage-gated active membrane channels determine the high-pass filtering qualities of neurons (Wang, 2010). The combination of these two opposite mechanisms can tune neurons towards specific filtering properties and frequency preferences, enabling them to select afferent information by its frequency (Buzsáki and Draguhn, 2004). On the other hand, synchronous oscillations result from an interaction of excitatory and inhibitory network components. Here, synaptic inhibition (either by means of inhibitory interneurons or by reciprocal feedback inhibition) is considered a main factor determining the temporal structure of network activity (Uhlhaas et al., 2009; Wang, 2010). In line with the significant influence of synaptic inhibition on the generation of synchronous oscillations, γ -aminobutyric acid (GABA) is considered to have an important impact on the generation of neuronal oscillations (Wang, 2010). GABAergic inhibitory interneurons are connected to excitatory neurons by feedforward and feedback loops and thus are able to temporally adjust ongoing network activity (Lopes da Silva, 2013). The influence of GABA on oscillatory activity (with focus on the beta band) will be further addressed in section 1.5.4. Finally, physical parameters like synaptic delay time and axon conduction speed define the temporal limits of information transfer within neuronal networks (Buzsáki and Draguhn, 2004). By this, neuronal oscillations are restricted to certain frequency ranges.

1.3.2 The Functional Role of Neuronal Oscillations

Oscillatory activity is a fundamental characteristic of neuronal signals (Gray, 1994) and a well preserved phenomenon in the evolution of the mammalian brain (Buzsáki, 2006). This suggests that neuronal oscillations are important for neuronal information transfer. However, the specific functions underlying neuronal oscillations remain speculative. Scientific interest in neuronal oscillations has rekindled in the last decades. This is mainly owing to the possibility to non-invasively measure neuronal oscillations, thus enabling experiments with human subjects on a large scale. The corresponding results show that neuronal oscillations are directly connected to perception and behavior (reviewed in Buzsáki, 2006; Thut et al., 2012), which

contradicts their initial evaluation as a mere epiphenomenon of neuronal activity. Due to the recent prominence of neuronal oscillations within the neuroscientific community, multiple theories addressing the potential functions of neuronal oscillations have been formulated. These theories range from particular functions of selective frequency bands in specific cortex areas to fundamental mechanisms of information transfer attributed to oscillatory activity. Subsequently, a short overview regarding global functions related to oscillatory activity in the human brain will be given. The more specific role of neuronal oscillations in the alpha and beta band will be described in section 1.5.

The cerebral cortex is estimated to comprise at least 10^{10} neurons, densely interconnected by approximately 10^{14} synapses (Hämäläinen et al., 1993). Although the 'neuron doctrine' (i.e., the concept that single neurons represent the elemental structural and functional units of the brain) can be considered as one of the core principles of modern neuroscience (Cajal, 1888; reviewed in Yuste, 2015), it is evident that neurons do not work in isolation. Rather, neurons dynamically form multiple functionally coherent assemblies across different cortical areas that operate in parallel (Hebb, 1949). This leads to the question how such functionally distinct and constantly changing assemblies are integrated in order to achieve a coherent representation of the perceived environment and, consequently, an effective behavioral output. Since synchronization of neuronal assemblies in oscillatory activity is a dynamic process (i.e., the properties of oscillations and the participating neurons can change rapidly over time, as opposed to 'hard-wired' anatomical connections), neuronal oscillations are considered an important mechanism enabling dynamic communication between neuronal assemblies (Lopes da Silva, 2013). Thus, neuronal oscillations are presumed to represent a link between single neuron activity and rigid neuroanatomical connections on the one side and a dynamical cognitive workspace and complex behavioral output on the other side (Buzsáki and Draguhn, 2004).

Fundamentally, neuronal synchronization allows for the collective subthreshold modulation of membrane potentials in defined neuronal populations (Lopes da Silva, 2013). Within synchronous populations, coherent modulations determine the periods where neurons are responsive to incoming signals and, in turn, are able to emit signals themselves. Because

synchronously oscillating neurons are susceptible to afferent input only during narrow time windows, the saliency of signals arriving during these time windows is enhanced (relative to signals arriving outside of these time windows; Uhlhaas et al., 2009). Likewise, in a synchronized neuronal population, outputs are restricted to narrow time windows. In downstream target neurons, this results in a coherent summation of signals, thereby amplifying the incoming signals and increasing their efficacy (Buzsáki and Draguhn, 2004; Fries, 2009). Thus, activity within synchronized assemblies is recursively entrained and the synchronous network is internally stabilized. Consequently, the synchronization of neuronal discharges within a network allows for the dynamic formation of selective functional relationships (Engel et al., 2001). In other words, synchronization within neuronal assemblies increases the chance that the encoded information (e.g., sensory representations) is grouped, selectively routed for further joint processing and segregated from information encoded in differently synchronized networks (Singer, 1999; 2013). Similarly, neuronal oscillations are considered an essential mechanism for the dynamic communication between different neuronal assemblies. By synchronizing and locking their phases, different neuronal assemblies can align their time windows of high excitability. In this way, temporal relations can be systematically coordinated between distinct neuronal assemblies. Consequently, communication between phase-locked neuronal populations is established (Fries, 2005; 2009).

1.3.3 Analysis of Neuronal Oscillations Measured by MEG

The technique of MEG is especially suited for the analysis of neuronal oscillations. Since neuronal oscillations rely on the accurate timing of synchronously firing neuronal populations, a high temporal resolution is necessary to reliably measure oscillatory signals. Furthermore, the high temporal resolution of MEG can be used to investigate oscillatory signals with high frequency content. The raw signal output of an MEG measurement is a time series of scalars for each sensor, representing variations in magnetic field strength or magnetic field gradient as a function of time. Usually, the first analysis step is the preprocessing of the raw signal. Preprocessing involves various filtering methods, by which the signal is cleaned from components unrelated to neuromagnetic activity. These components are known as artifacts and can be of biological (e.g., eye movement) and non-biological (e.g., power line noise) origin

(Mitra and Pesaran, 1999; Braeutigam, 2013). Further important preprocessing steps include filtering (i.e., restricting the signal to specific frequency components), the rejection of noisy or broken sensors and detrending (i.e., correction of linear power changes in the data) (Gross et al., 2013). Based on the preprocessed signal, different analysis methods can be applied. The respective choice of analysis methods thus depends on the available data, the present experimental paradigm and, ultimately, the hypothesis.

1.3.3.1 Event-related Fields

Event-related fields (ERFs) are the magnetoencephalographic analogue of the well-established electroencephalographic event-related potentials. The core assumption of event-related approaches is the existence of neuronal responses that exhibit a systematic temporal relationship (i.e., are time-locked) to a given event (e.g., the presentation of a stimulus). Under such conditions, the response is labeled an 'evoked response'. These responses are assumed to remain stable over multiple repetitions, but are contaminated by neuronal activity systematically unrelated to the event (i.e., the noise). The onset of the event is defined as a fixed time point. Multiple repetitions of the event are recorded and temporally aligned with regard to the onset time point. Subsequently, the signals are averaged. By this, the activity unrelated to the event is averaged out. Consequently, the neuronal responses systematically related to the event are enhanced relative to the activity unrelated to the event (i.e., the signal-to-noise ratio is enhanced). Based on these properties, poststimulus ERFs are often interpreted as neuronal correlates of stimulus processing (Jones et al., 2007). Thus, the latency and the amplitude of poststimulus ERFs can be interpreted regarding their relation to factors like stimulus type or intensity (Braeutigam, 2013).

1.3.3.2 Spectral Decomposition

One of the fundamental properties of oscillations is their periodicity. Because they occur periodically, it is efficient to transform oscillatory signals from the time domain to the frequency domain. This is achieved by means of a Fourier transformation, which decomposes the signal into multiple sinusoidal functions, thus allowing an estimation of the signal at a specific frequency (reviewed in Mitra and Pesaran, 1999). Contrary to ERFs, which include all frequency

components, the output of a Fourier analysis yields phase and amplitude values as a function of frequency. Additionally, phase and amplitude values can also be computed as a function of time. This is achieved by means of a time-frequency analysis, where a window function is translated in time across the signal. Thereby, temporal changes regarding the frequency components in the data can be investigated. While ERFs only identify signal components with a stable temporal relationship between the neuronal response and the respective event, a time-frequency analysis can also identify those signal components with a temporal jitter regarding the event onset. Time-frequency analyses are especially important for analyzing signal components that are present only in specific frequencies and for transient signals not phase-locked to the respective event (labeled 'induced' responses).

1.3.3.3 Source Reconstruction

Source reconstruction is applied to estimate the neuronal current sources that underlie the externally measured signals. Unfortunately, the task of source reconstruction is intrinsically problematic in the sense that it is severely underdetermined. There are far more possible neuronal sources (in the order of 10,000) than available sensors (in the order of 100; Baillet et al., 2001). The problem arising from this constellation is that a given sensor-level signal can be caused from a multitude of neuronal current generators. Additionally, even with theoretically optimal data quality and a theoretically infinite number of sensors, the possibility remains that there are neurophysiologically relevant currents which cannot be measured by the sensors (Braeutigam, 2013). This 'inverse problem' (i.e., the estimation of current sources from externally measured fields) is ill-posed and has non-unique solutions. Thus, the solution requires a priori assumptions in form of physiological constraints and mathematical simplifications (Baillet et al., 2001; Vrba and Robinson, 2001). The common approach to solve the inverse problem is to first address the 'forward problem'; i.e., to define which externally measured fields result from a given set of neuronal sources. The computation of the forward model requires several components. First, it is necessary to construct a head model, which specifies the spatial and conductor properties of the subjects' head. Therefore, the head model integrates the geometric information of the respective brain volume and a model of the conductor properties of the tissues between brain and scalp surface. Regarding the geometric

information, up-to-date measurements usually implement realistic head models, which rely on individual anatomical information obtained by magnetic resonance imaging (MRI) measurements. Regarding the conductor properties, a simple single-shell model (Nolte, 2003) is sufficient for MEG measurements (Baillet et al., 2001). Subsequently, the brain volume is spatially discretized by placing a grid of evenly spaced discrete points within the volume. Furthermore, the sensor positions relative to each other as well as relative to the brain have to be specified. The head model and the sensors are then linked by means of a lead field. The lead field specifies which sensor signal pattern is generated by a given source with unitary amplitude, given various discrete locations within the source volume. Finally, the source model is constructed, which estimates and quantifies the underlying current density distribution (Gross et al., 2013). Based on these components, the forward model is calculated. The inverse problem is then addressed by taking the inverse of the forward problem; i.e., sensor level signals are traced back to source activity. As stated above, the inverse problem has an unlimited number of solutions. Therefore, it is necessary to impose certain constraints in order to reduce the number of possible solutions. This is done by different computational approaches, e.g., minimum norm estimate, least-squares source estimation and beamforming approaches (reviewed in Baillet et al., 2001).

The experiments presented in the course of this thesis make extensive use of the beamforming approach. In general, beamformers are used to discriminate between signals from a given point of interest and other signal components (Baillet et al., 2001). Therefore, it is assumed that MEG sensor activity can be derived from a fixed and finite set of current dipoles within the brain volume. Using a spatial filter, neuronal activation is estimated for each dipole location as the weighted sums of sensor data, independently of all other locations. The aim is to adjust the respective sensor weightings in order to maximally explain the neuronal activation at a certain location and to minimize neuronal activation from other locations. After determining the respective spatial filter, the underlying neuronal source at a given position can be reconstructed from the sensor level activity (Braeutigam, 2013). Different versions of beamformers exist. The studies presented in the framework of this thesis apply both dynamic imaging of coherent sources (DICS; Gross et al., 2001) and linear constraint minimum variance (LCMV) beamformers

(van Veen et al., 1997). DICS beamformers operate on frequency domain data, whereas LCMV beamformers operate on time domain data.

1.4 The Somatosensory System

The somatosensory system is responsible for three different functions: proprioception, interoception and exteroception. Proprioception describes the perception of body posture and body movements and is central to provide sensory feedback in order to enable precise motor activity. Interoception is the sensory function within the viscera (i.e., the internal organ systems). In contrast to the other functions, interoception mainly operates unconsciously, but is nonetheless important for the regulation of autonomic processes. Exteroception describes the perception of external stimuli on the skin. Exteroception comprises the sense of touch (e.g., pressure, vibration), thermoception and pain (Kandel et al., 2000). Since the current thesis focuses on electrotactile stimulation, this section will concentrate on exteroception or, more specifically, on tactile perception.

The sensation of touch is mediated by specialized mechanoreceptors, which are sensitive to physical deformation due to pressure on or stretching of tissue in their receptive field. From the receptors, sensory information is conveyed by dorsal root ganglion neurons (Fig. 3). Although the subjective impression is often described as being similar to mechanical stimulation, electrotactile stimulation is considered to rely on a different conduction of sensory information. The applied electric current is presumed to directly stimulate afferent nerve fibers (Butikofer and Lawrence, 1978; Kaczmarek et al., 1991), thus bypassing the mechanoreceptors. Perception of electrotactile stimulation ranges from touch to pain, depending on stimulation parameters like voltage, current, location of stimulation and hydration of the skin (Kaczmarek et al., 1991). Thus, it can be assumed that electrotactile stimulation affects multiple nerve fibers mediating different senses of exteroception (e.g., touch and pain; Kandel et al., 2000). The present thesis focuses on the processing of electrotactile stimulation in the brain (omitting peripheral information transfer) and the included experiments solely involve non-painful electrotactile stimulation, which subjects described as highly similar to the perception of touch. Therefore, information processing of electrotactile stimuli will be treated synonymously to tactile

stimulation at the level of the central nervous system (CNS; i.e., from the level of the dorsal root ganglion neuron onward).

In the dorsal root ganglion neurons, somatosensory information is encoded into action potentials, which are transmitted to the CNS (Kandel et al., 2000). The fibers of the dorsal root ganglion neurons enter the spinal cord on the ipsilateral side with regard to the stimulation site and ascend to the medulla, where they decussate on the contralateral side (Fig. 3). This fiber bundle is labeled the medial lemniscus and ascends further to the ventral posterior nucleus in the thalamus. From the level of the thalamus, somatosensory information is conveyed to the primary somatosensory cortex (S1) in the postcentral gyrus (Fig. 3). Classically, S1 was considered to encompass Brodmann Areas (BA) 1-3. However, BA 3b is currently interpreted as the primary target for tactile input (Kandel et al., 2000). Here, tactile information from the contralateral side of the body is somatotopically organized, thereby representing different body parts proportionally to the respective density of receptor innervation (Kandel et al., 2000). Consequently, the representation of the fingers in S1 is far larger than the representation of the thighs (despite the fact that the thighs cover a bigger surface area), which in turn determines the high discriminative sense of touch in the fingers. Notably, S1 incorporates multiple somatotopic maps. Basic properties of tactile perception are encoded within BA 3. Higher-order processing of tactile information is located in BA 1 and the combination of proprioceptive and tactile information occurs in BA 2 (Kandel et al., 2000). The secondary somatosensory cortex (S2) lies on the parietal operculum and covers BA 43. S2 receives major input from S1 but is also densely interconnected between hemispheres. Functionally, S2 is considered as a higher order somatosensory area which is relevant for object recognition by touch, spatial feature discrimination and the comparison of somatosensory stimuli (Kandel et al., 2000).

Ascending dorsal column–medial lemniscal pathway to primary sensory cortex

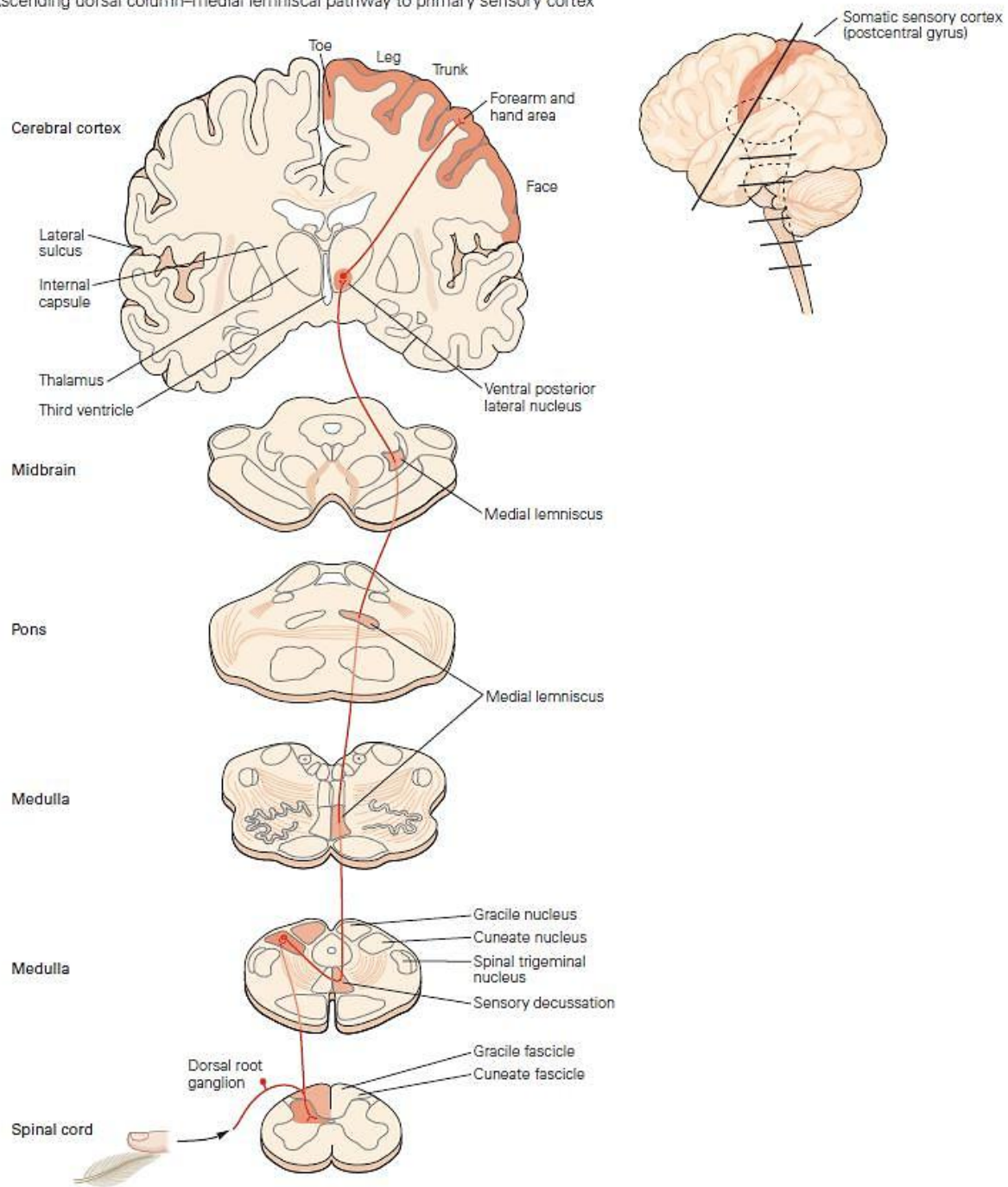


Figure 3: The neuronal afferent pathway for tactile information. Red: The medial lemniscus which conveys the sensory information of touch. Tactile information is recorded by specific mechanoreceptors in the skin and is conveyed to the CNS by means of dorsal root ganglion cells. Within the CNS, the fibers decussate on the level of the medulla, ascend further to the ventral posterior nucleus in the thalamus and finally project to the primary somatosensory cortex. Adapted and modified from Kandel et al., 2000.

1.5 The Functional Role of Neuronal Oscillations in the Alpha and Beta Band

The characteristics and potential functions of neuronal oscillations in general have been previously addressed in section 1.3. Subsequently, the specific functions of alpha and beta band oscillations will be presented, along with a particular focus on the somatosensory system.

1.5.1 Alpha Band Activity

The alpha band is commonly defined as the frequency band between 8-12 Hz (Womelsdorf and Fries, 2007; Raichle, 2010; Lange et al., 2014), resulting in a cycle length of about 80-120 ms. Alpha band activity resembles the most prominent rhythm in the human cortex, often visible in ongoing unprocessed EEG and MEG recordings. Oscillatory activity in the alpha band occurs both spontaneously and continuously in human sensory cortices and is most visible in parietal and occipital areas (Manshanden et al., 2002). This prominence also explains why the alpha band rhythm was the first neuronal rhythm to be scientifically described by Berger in 1929 (Berger, 1929). Because of Berger's finding that the occipital alpha band amplitude increases in response to the closing of the eyes (Berger, 1929), high alpha band activity was initially thought to be related to states of low arousal (Adrian and Matthews, 1934). In line with this interpretation, subsequent studies reported decreases in alpha band power during various activities (e.g., voluntary movement) compared to resting baseline (Pfurtscheller and Aranibar, 1977). Vice versa, alpha band power increases could be demonstrated in sensory cortices associated with modalities not essential for the current task (Koshino and Niedermeyer, 1975). Based on these findings, alpha band activity was interpreted as an electroencephalic correlate of brain idling (Pfurtscheller et al., 1996a). In this sense, brain areas exhibiting high alpha band power were understood as currently inactive, whereas brain areas demonstrating low alpha power were considered as currently activated and engaged.

In the last decades, the interpretation of alpha band activity as an indicator of passive idling has been largely replaced with a more active role of alpha activity. This novel perspective results from studies demonstrating alpha band effects that do not agree with a merely passive conception of the alpha rhythm. One point supporting a more active role is the active top-down modulation of alpha band activity in response to attentional changes. In bimodal attention

tasks, alpha band power increases in occipital sensors when attention is focused on somatosensory stimulation, whereas alpha band power increases in sensorimotor sensors when attention was focused on visual stimulation (Anderson and Ding, 2011; Bauer et al., 2012). Importantly, occipital alpha band power exceeds baseline levels when attention is directed to somatosensory stimulation (Anderson and Ding, 2011). This increase above baseline levels suggests an attention-related process actively inhibiting visual processing, rather than mere passive idling. Likewise, the orientation of attention to a specific spatial location (e.g., the left or right hemifield) leads to decreases in alpha band power in sensors over the corresponding contralateral brain region (Thut et al., 2006; Busch and VanRullen, 2010; Jones et al., 2010). In line with results from multimodal studies, alpha band power in sensory areas ipsilateral to the attended spatial location is increased relative to baseline (Jones et al., 2010), thus supporting active modulation of sensory information processing. Furthermore, the relative lateralization asymmetry of alpha band power is predictive of the reaction time needed to respond to target presentation, which suggests alpha band power lateralization indicates spatial attentional focus (Thut et al., 2006). These results demonstrate an active top-down influence on alpha band activity, which is fundamentally different from passive idling. In agreement with an active role of the alpha rhythm, increased alpha band activity is present during the retention interval of memory tasks (Başar et al., 2000) and thus associated with active task demands. Here, the level of the alpha band increase even expands with increasing memory load (Jensen, 2002). Finally, neuromodulatory studies demonstrate that cortical excitability fluctuates along with ongoing alpha band rhythm. In a transcranial magnetic stimulation (TMS) study, Romei and colleagues (2008a) determined the individual minimal stimulation amplitude by which visual phosphenes could be elicited. This minimum stimulation amplitude positively correlated with individual alpha band power at rest; i.e., higher stimulation amplitude was necessary to induce visual phosphenes during states of high alpha band power (Romei et al., 2008a). Likewise, this relation could be demonstrated within subjects on a single-trial basis (Romei et al., 2008b). In line with this, the active entrainment of neuronal visual cortex activity to the alpha band rhythm impaired the detection of visual near-threshold stimuli. This stimulation effect was specific for the stimulated hemisphere; i.e., visual detection was impaired only in the visual field contralateral to the stimulated hemisphere. In contrast, visual detection in the ipsilateral visual

field was enhanced (Romei et al., 2010). Thus, high alpha band activity exerts an inhibitory influence on cortical activity and thereby modulates perception. Taken together, these results disagree with the role of alpha band oscillations as a correlate of passive brain idling.

In response, novel theories have been put forward that suggest a more active role of alpha band activity in sensory and cognitive processing. These theories include the inhibition-timing hypothesis (Klimesch et al., 2007) and the gating by inhibition hypothesis (Jensen and Mazaheri, 2010). Both theories view alpha band activity as an active and top-down controlled inhibitory mechanism dynamically shaping the functional architecture of the brain. Ongoing alpha band activity is understood as a sensory gating mechanism that regulates information processing between sensory and higher-order cortex areas. Increased alpha band activity selectively inhibits task-irrelevant areas and connections. In contrast, low alpha band activity in task-relevant cortex areas enables efficient information processing, thereby actively routing the flow of information. Thus, an interference of currently irrelevant information is prevented and the processing of currently important (e.g., attentionally focused) information is facilitated. However, it seems that low alpha band power in sensory cortices is not per se related to an enhanced stimulus processing, in the sense that the perceived stimulation agrees with the presented stimulation. Rather, low alpha power seems to indicate a higher excitability of sensory cortices, which can also result in an increased tendency of illusory perception (Romei et al., 2008a; Romei et al., 2008b ; Lange et al., 2013).

1.5.2 Alpha Band Activity in the Somatosensory System

Oscillatory activity within the alpha frequency band in the sensorimotor cortex was first mentioned in 1952 (Gastaut, 1952) and was considered a component of the sensorimotor mu rhythm (Schnitzler et al., 2000). Sensorimotor alpha band activity is assumed to originate mainly from the hand area of the somatosensory cortex (Salmelin and Hari, 1994). Following tactile stimulation, somatosensory alpha band activity is suppressed (Bauer et al., 2006). Although it can be considered a somatosensory rhythm due to its origin, the somatosensory alpha band rhythm is decreased during movement and shows a strong increase after movement (Salmelin and Hari, 1994). Most studies investigating the functions of alpha band activity focus on the

visual domain. Current theories, however, do not differentiate the role of alpha band activity across modalities (Jensen and Mazaheri, 2010). This is confirmed by experimental results showing effects in the somatosensory domain that are generally comparable to the visual domain. Accordingly, attentional effects on alpha band activity have been documented also for the somatosensory modality. After the presentation of attentional cues that reliably signaled if a tactile target stimulus would appear at the left or right hand, somatosensory alpha band power lateralized (i.e., higher alpha band power was visible in the somatosensory cortex ipsilateral to the attended side, and lower alpha power was visible in the somatosensory cortex contralateral to the attended side; Haegens et al., 2011a; van Ede et al., 2011). With decreasing reliability of the attentional cue, the alpha band lateralization also decreased. Furthermore, the level of alpha band lateralization also predicted the behavioral performance (i.e., response accuracy and response speed) of the subjects (Haegens et al., 2011a). In line with findings from the visual modality, the cue-related ipsilateral alpha band increases exceeded baseline alpha band power levels, whereas the contralateral decreases were lower than baseline alpha band power levels (Haegens et al., 2012). Taken together, the function of alpha band activity within the somatosensory system seems comparable to the role of alpha band activity in the visual domain. Likewise, alpha band activity is currently interpreted as a mechanism for sensory gating and inhibition of task-irrelevant areas, which can be actively modulated in a top-down manner (e.g., by means of attention).

1.5.3 Beta Band Activity

Classically, beta band activity is defined as neuronal oscillatory activity in the frequency band from 13-30 Hz (Jenkinson and Brown, 2011; Kilavik et al., 2013). Beta band oscillations are most prominent over rolandic areas (i.e., the sensorimotor cortex). Historically, beta band activity was first described by Berger in 1931. By means of ECoG in epileptic patients, Jasper and Penfield were the first to locate the source of beta band activity in the sensorimotor cortex and to describe the close connection between beta band activity and movement (Jasper and Penfield, 1949).

Since then, the link between sensorimotor beta band activity and movement has been consistently replicated and extended. Sensorimotor beta band power decreases during movement execution and changes in isometric muscle contraction (Doyle et al., 2005; Kilavik et al., 2012), both for self-paced and stimulus-triggered movements (Gaetz et al., 2010). Beta band decreases in sensorimotor cortices have even been observed as a consequence of motor imagery, in the absence of actual movement (Schnitzler et al., 1997; de Lange et al., 2008). Decreases in beta band activity related to movement have been reported to occur bilaterally in both hemispheres (Salmelin and Hari, 1994), while other studies demonstrated a stronger beta band decrease contralaterally to the moved effector (Jurkiewicz et al., 2006). After movement termination, beta band activity in motor areas typically increases transiently, which is labeled beta rebound (Kilavik et al., 2013). Based on the abovementioned results, initial theories attributed beta band activity to be a correlate of motor cortex idling (Pfurtscheller et al., 1996b). However, the interpretation of beta band activity as a correlate of motor idling does not agree with results that show a rapid increase in sensorimotor beta band power when a prepared movement is held back (Zhang et al., 2008; Wheaton et al., 2009). Likewise, power increases in the beta band are present during states of postural maintenance and stabilization (e.g., object holding; Baker et al., 1997; Spinks et al., 2008). Novel theories on the function of beta band activity within the motor cortex therefore interpret beta band activity as an internal index representing the likelihood for the execution of novel voluntary actions. In this sense, suppression of beta band activity is thought to represent the state of readiness of the motor system (Jenkinson and Brown, 2011).

Importantly, sensorimotor beta band decreases are not only present during movement, but also during and after tactile stimulation (Cheyne et al., 2003; Gaetz and Cheyne, 2006; Bauer et al., 2006; Lange et al., 2011). Sources of beta band decreases could be differentiated between finger, toe and lip stimulation and thus demonstrated a somatotopical organization in somatosensory cortices (Gaetz and Cheyne, 2006). Similar to the beta band rebound after motor termination, sensorimotor beta band activity increased after the initial beta band power decrease resulting from tactile stimulation (Cheyne et al., 2003; Bauer et al., 2006). These

results suggest that beta band activity is also important for the processing of somatosensory information and thereby not exclusively related to motor activity.

The notion that beta band activity is not restricted to motor-related processes is further supported by beta band effects reported for cognitive paradigms. In the cognitive domain, beta band effects could be demonstrated for a variety of different task dimensions, ranging from perceptual decision tasks (e.g., Haegens et al., 2011b) to memory tasks (e.g., Siegel et al., 2009). The wide range of task dimensions for which effects in the beta band have been shown make it difficult to attribute a single consistent function to oscillatory activity in the beta band. Consequently, beta band oscillations have been labeled as the frequency band which functional role is least well understood (Engel and Fries, 2010). However, recent theories aim to integrate the results from cognitive paradigms along with the results from motor and movement-related tasks and give rise to novel holistic interpretations of beta band activity. These theories interpret beta-band activity as a correlate of increased top-down control, as compared to stimulus driven bottom-up control (Buschman and Miller, 2007; Siegel et al., 2012). A similar view was expressed in a seminal paper from Engel and Fries (Engel and Fries, 2010), who conceptualized beta band activity as a mechanism generally promoting the status quo. In other words, states of high beta band activity are interpreted as a correlate of maintaining the existing state, likewise in motor and cognitive domains. In the motor domain this is represented by increased beta power during postural maintenance (reviewed in Kilavik et al., 2013) and, vice versa, decreased beta band activity as correlate of motor readiness (Jenkinson and Brown, 2011). In cognitive domains, increased beta band represents involvement and preponderance of top-down processes and their respective content compared to stimulus-driven bottom-up influence. This interpretation is supported by studies showing progressive beta band decreases during evidence accumulation in decisional paradigms (Donner et al., 2009), which represents a stimulus-driven process. Vice versa, beta band increases during delay periods in memory tasks (Siegel et al., 2009). Here, the delay period is characteristic for top-down controlled maintenance of the memory set. Furthermore, beta band activity differentiates between endogenously driven and stimulus driven choices in visual search tasks (Pesaran et al., 2008).

Taken together, beta band effects are consistently reported and most established for movement-related tasks. However, changes in beta band activity are also increasingly demonstrated for a variety of sensory and cognitive (i.e., non-motor) paradigms. Because of the diversity of these findings, the specific role of the beta rhythm is still a subject of debate. Current theories, however, attribute high beta band activity as a correlate of the maintenance of the status quo, likewise in motor and cognitive domains.

1.5.4 Beta Activity and its Connection to GABA-Mediated Inhibition

As already mentioned in section 1.3, synaptic GABAergic inhibition plays an important role for the determination of the temporal structure of neuronal oscillations in general (Wang, 2010). This connection between GABAergic inhibition and oscillatory neuronal activity has been extensively investigated for the beta band. The generation of beta band rhythms in neuronal populations relies on the balance between the excitatory influence of pyramidal neurons and the inhibitory influence of interneurons. Here, GABA_A-mediated inhibition is considered as the central pacemaker within these networks and thus as the determinant of the frequency with which the neurons constituting the network oscillate (Whittington et al., 2000a; 2000b). In line with these findings, both neuronal modeling approaches and animal models demonstrate that GABAergic interneuronal activity is central for the generation of beta band activity in neuronal networks (Jensen et al., 2005; Roopun et al., 2006; Yamawaki et al., 2008). In humans, pharmacological intervention studies reported effects on sensorimotor beta band activity after the administration of GABAergic agents, mostly benzodiazepines (Jensen et al., 2005; Hall et al., 2010; Muthukumaraswamy et al., 2013). Since the primary effect of benzodiazepines is considered to be an increase of the conductance of GABA_A-mediated currents (Jensen et al., 2005), the results from pharmacological studies further support a link between GABAergic inhibition and beta band oscillatory activity. Finally, due to the emergence of magnetic resonance spectroscopy (MRS), which allows in vivo neurotransmitter concentrations to be measured non-invasively, the investigation of the neurochemical underpinnings of oscillatory activity has seen substantial progress in the last decade. MRS studies supported previous findings on the connection between GABAergic inhibition and beta band oscillations, with results indicating linear relationships between beta band power and GABA concentrations ins

sensorimotor cortices (e.g., Gaetz et al., 2011). However, the majority of current combined MEG-MRS studies only focus on a small set of parameters of oscillatory activity (e.g., solely on movement-related beta band activity).

In summary, there is extensive evidence that GABA-mediated inhibition is an important modulator of sensorimotor beta band activity. However, most evidence results from animal studies, modeling approaches or studies that modulated GABA concentration by means of pharmacological intervention. Although the relationship between local, non-modulated GABA concentrations and beta band activity has recently been addressed by studies applying MRS, the full range of this relationship has yet to be determined.

1.5.5 Setting the Stage - Alpha and Beta Band Activity in the Prestimulus Epoch

The classical experimental approach in neuroscience involves the repeated presentation of a stimulus. Then, the brain signals related to stimulus processing and perception (i.e., signals that appear temporally after stimulus presentation) are analyzed. Thus, the brain activity during the time window before stimulus presentation (subsequently labeled the prestimulus epoch) is often not considered for further investigation. This prestimulus neuronal activity, which resembles the state of the brain prior to stimulus processing, is usually either subtracted from the stimulus-related signal (i.e., the signal is baseline-corrected) or completely ignored. In this regard, it is important to note that sensory information is not processed mechanistically in the brain; i.e., the same stimulation can be processed differently and thus may result in different stimulus perception. This is most evident for bistable, ambiguous or near-threshold stimulation. Since afferent sensory input always impinges on a continuously active system, it seems likely that the brain state before and during stimulus presentation influences the subsequent stimulus processing and perception (Hebb, 1949). To investigate this assumption, it is necessary to identify measurable indices of ongoing brain activity. In this regard, ongoing neuronal oscillations represent promising candidate measures. Consequently, it is likely that neuronal oscillations in the prestimulus period influence the perception of subsequently presented stimuli.

In line with this assumption, there are consistent results showing that sensory processing and perception is modulated and predicted by prestimulus fluctuations of oscillatory activity. The influence of prestimulus oscillatory activity on subsequent neuronal processing and perception has been most extensively investigated for alpha band activity. For example, perception of near-threshold stimuli is significantly influenced by prestimulus alpha band power in the visual (Ergenoglu et al., 2004; Hanslmayr et al., 2007; van Dijk et al., 2008; Mazaheri et al., 2009; Wyart and Tallon-Baudry, 2009) and somatosensory (Linkenkaer-Hansen et al., 2004; Jones et al., 2010; Zhang and Ding, 2010) domain. In this regard, low prestimulus alpha band power in sensory cortex areas seems to facilitate the perception of near-threshold stimuli (e.g., van Dijk et al., 2008), whereas other studies report the highest perception rates to be associated with intermediate alpha power levels (e.g., Linkenkaer-Hansen et al., 2004). Although the vast majority of studies investigate the effect of prestimulus alpha band activity on near-threshold stimuli, there are indications that the influence of prestimulus alpha band power also extends to the perception of supra-threshold stimuli (Lange et al., 2012). In addition to power effects, the phase of ongoing alpha band oscillations in the prestimulus epoch likewise modulates subsequent perception (Busch et al., 2009; Mathewson et al., 2009). Studies report that shortly before visual stimulus presentation, prestimulus alpha band phase was concentrated in phase angles that significantly differed between trials where a near-threshold stimulus was either perceived or missed (Busch et al., 2009). Thus, perceptual thresholds for the detection of visual stimuli seem to temporally fluctuate along with alpha band phase. Finally, prestimulus alpha band activity not only modulates the perception of sensory stimulation, but also event-related potentials evoked by the stimulation (Jones et al., 2010; Anderson and Ding, 2011; Lange et al., 2012). Since event-related potentials are related to stimulus processing (Jones et al., 2007), this modulation of event-related potentials by prestimulus activity demonstrates the influence of the prestimulus brain state on neuronal stimulus processing.

Various studies showing prestimulus alpha band effects could also demonstrate an influence of prestimulus beta band activity on the neuronal processing of sensory information. Lange and colleagues (Lange et al., 2012) demonstrated that prestimulus beta band power in primary and secondary somatosensory cortices predicted the temporal perception of tactile stimulation.

Furthermore, high levels of prestimulus beta band power facilitated illusory perception in cross-modal visual-auditory paradigms, the McGurk effect (Keil et al., 2012) and the sound-induced flash illusion (Keil et al., 2014). Likewise, beta band activity in the prestimulus period seems to influence the perception of near-threshold tactile stimuli. For the sensorimotor cortex, best perceptual detection rates were associated during intermediate levels of beta band power, whereas in parietal areas, the best perceptual detection rates were found during high levels of beta band power (Linkenkaer-Hansen et al., 2004). In agreement with results on alpha band activity, prestimulus beta band activity also modulated the amplitude of stimulus-related evoked components (Jones et al., 2009; Anderson and Ding, 2011). These results demonstrate that perception, especially in the somatosensory domain, is markedly influenced by prestimulus beta band power.

However, perceptual variance despite identical stimulation could be potentially explained by fluctuations in the activity or output of the sensory organs. Yet, recent studies demonstrated that the necessary stimulation amplitude to induce phosphenes by TMS (without any form of visual stimulation) were dependent on ongoing alpha band oscillations in the occipital cortex (Romei et al., 2008a; 2008b). Because TMS stimulation in such paradigms avoids the stimulation of sensory organs, the reported variations in perception cannot be systematically caused by the sensory organs. Likewise, top-down related modulations like the covert direction of attention are known to significantly influence perception. In turn, such attentional shifts are related to changes in ongoing brain activity or, more specifically, alpha band oscillations (see section 1.5.1). Thus, variances in the perception of identical stimulation are more likely to result from ongoing changes in brain activity than from fluctuations in sensory organs.

In summary, the abovementioned results demonstrate that the state of the brain before stimulation is an important factor for the processing and perception of sensory information. Specifically, prestimulus oscillatory activity in the alpha and beta band within sensory cortices has been repeatedly reported to be related to stimulus processing and perception.

2 Aims and Hypotheses

The studies presented within the scope of this thesis focus on neuronal oscillations in the somatosensory cortex. In particular, the studies examine two major aspects of somatosensory oscillatory neuronal activity. Primarily, the influence of prestimulus neuronal oscillations on the sensory integration and subsequent perception of somatosensory stimulation is investigated. In addition, the neurochemical basics of neuronal oscillations in the somatosensory cortex are analyzed.

Prestimulus neuronal oscillations (i.e., ongoing rhythmic fluctuations of neuronal activity, which are present prior to stimulus presentation) and their connection to stimulus perception have only recently emerged as a topic of neuroscientific investigation (Engel et al., 2001). Most studies addressing the influence of prestimulus neuronal oscillations on perception focus on the visual domain. Thus, various aspects regarding the functional role of prestimulus neuronal oscillations for somatosensory perception remain to be investigated. For example, those studies investigating the connection between somatosensory perception and prestimulus neuronal oscillations mostly use paradigms with near-threshold stimulation, with subjects reporting whether they either perceive somatosensory stimulation or not (e.g., Zhang et al., 2008; Jones et al., 2010). Such paradigms allow investigating which neuronal processes are relevant for the perception of near-threshold stimulation and in which state these neuronal processes enable or prohibit subsequent perception. Here, the respective neuronal processes are interpreted analogue to an on/off switch, since stimulation is either perceived or not. Hence, because subject responses are restricted to perceived vs. not perceived, such experiments cannot determine if neuronal processes influence how (i.e., the quality) stimulation is perceived. Such a qualitative influence could modulate the features of the perceived stimulation (e.g., the intensity or amount) in contrast to determining if a percept arises at all.

Furthermore, the fundamental mechanisms giving rise to neuronal oscillatory activity in the somatosensory cortex have yet to be fully determined. Here, local neurotransmitter concentrations presumably offer valuable insights into the generation of neuronal oscillations.

GABAergic inhibition is assumed to represent a key factor for the generation of oscillatory neuronal activity, both in general and specifically for beta band oscillations (see sections 1.3.1 and 1.5.4). Thus, the analysis of local GABA concentrations in somatosensory areas in connection to parameters of oscillatory activity should provide useful information on the mechanisms underlying somatosensory oscillatory activity.

The current thesis addresses the question if prestimulus neuronal oscillations influence the quality of perception and stimulus processing by investigating mechanisms of sensory integration in the somatosensory system. Therefore, suprathreshold electro tactile stimuli were presented in rapid temporal succession and subjects should report whether they perceived one single stimulus or two separate stimuli (subsequently labeled temporal perceptual discrimination). The present thesis aims at elucidating if prestimulus oscillatory activity in the alpha and beta band determines the temporal resolution of tactile perception (i.e., how many stimuli are perceived in a given time interval). In addition, the connection between sensorimotor GABA concentrations and parameters of neuronal oscillatory activity are examined. In detail, the included studies focus on:

Study1: Investigating the influence of prestimulus oscillatory alpha band activity on the subsequent temporal perceptual discrimination of electro tactile stimulation. Subjects were presented with two consecutive suprathreshold tactile stimuli separated by an individually determined stimulus onset asynchrony (SOA) while their neuromagnetic brain activity was measured with MEG. Although the physical stimulation parameters remained constant for each subject, the stimulation was perceived as one single stimulus in approximately half of the trials and as two separate stimuli in the other half of the trials. Prestimulus alpha power was contrasted between trials with differing perceptual reports (i.e., perceived one stimulus vs. two stimuli). It was hypothesized that low levels of alpha band power enhance temporal perceptual discrimination and facilitate the perception of two separate stimuli. Furthermore, the study examined the influence of prestimulus alpha band power on subjects' confidence in their perceptual reports. Finally, the study compared poststimulus ERFs between trials

with different perceptual reports and interpreted the findings in light of current decision making models.

Study2: Identifying the role of prestimulus oscillatory phase within S1 for the discrete perceptual sampling of electrotactile stimuli. Prestimulus phase was contrasted between trials with differing perceptual reports (i.e., perceived one stimulus vs. two stimuli). It was hypothesized that oscillatory phase in the beta frequency band in S1 differs between trials with varying perceptual response and thus could predict subsequent stimulus perception. Results were integrated into a model describing how the temporal resolution of the somatosensory system is defined by perceptual cycles in the beta band, which determine discrete perceptual sampling in the somatosensory domain.

Study3: Determining the connection between beta band peak frequency and GABA concentration in sensorimotor and occipital cortex areas. Beta band peak frequency was measured at rest (i.e., without movement) by means of MEG, whereas non-modulated GABA concentration (i.e., not modulated by pharmacological agents) was measured by MRS in healthy human subjects. A linear relation between beta band peak frequency and GABA concentration in sensorimotor cortex areas was hypothesized.

In summary, the present thesis investigated how prestimulus oscillatory activity in the somatosensory system determines temporal perceptual discrimination of tactile stimuli. In order to further elucidate the neurochemical basics of neuronal oscillations in the somatosensory cortex, the connection between local GABAergic neurotransmitter concentrations and sensorimotor oscillatory activity was examined.

3 Study 1: Prestimulus Alpha Power Influences Tactile Temporal Perceptual Discrimination and Confidence in Decisions (Baumgarten et al., 2014, Cerebral Cortex)

Study 1 (Appendix 1) investigated the influence of prestimulus alpha band power on the temporal perceptual discrimination of electrotactile stimuli. Prestimulus alpha band power modulates poststimulus evoked responses (Jones et al., 2010; Anderson and Ding, 2011), which are related to neuronal stimulus processing (Jones et al., 2007). Accordingly, prestimulus alpha band power in sensory cortex areas correlates with reported perception (Linkenkaer-Hansen et al., 2004; van Dijk et al., 2008; Romei et al., 2010). Although the connection between prestimulus alpha band activity and neuronal stimulus processing or perception has been repeatedly demonstrated for visual, but also somatosensory stimulation, various aspects remain unclear. The influence of prestimulus alpha band activity on subjective confidence in perceptual reports is largely unknown. Furthermore, the majority of studies investigating prestimulus alpha band power effects on subsequent perception use near-threshold stimuli (e.g., Linkenkaer-Hansen et al., 2004; Zhang et al., 2008; Jones et al., 2010). Such paradigms only allow for the investigation of perceived vs. non-perceived stimulation but prohibit examining if prestimulus oscillations also modulate perception qualitatively (i.e., the perceived amount or intensity of stimulation). In order to investigate if prestimulus alpha band activity influences perception qualitatively, the present study used suprathreshold stimuli. Subjects thus always perceived the electrotactile stimulation, but had to report how many stimuli they perceived, as well as the subjective confidence regarding their perception. It was hypothesized that low levels of alpha band power enhance tactile temporal discrimination and facilitate the perception of two temporally separate stimuli.

Stimulus perception can be viewed as a process of (perceptual) decision making (Gold and Shadlen, 2007). According to this theoretical framework, sensory evidence provided by the stimulus is accumulated in a decision variable. If sensory evidence is sufficiently strong, this decision variable accumulates over time and at some point crosses a theoretical decision bound,

determining the choice of a specific decisional option (Ratcliff and McKoon, 2008; Kiani and Shadlen, 2009). Neuronal correlates of decision variables have been found in poststimulus event-related potentials (VanRullen and Thorpe, 2001; Philiastides et al., 2006; O'Connell et al., 2012). Given the known connection between prestimulus oscillatory activity and poststimulus evoked responses, study 1 investigated if prestimulus oscillatory activity influences neuronal correlates of perceptual decision making.

3.1 Methods

Sixteen subjects participated in the study. Suprathreshold electrotactile pulses were presented at the left index finger. In the main experimental condition, two subsequent pulses were presented, with pulses being separated by a subject-specific SOA (labeled intermediate SOA). This intermediate SOA was adjusted so that subjects perceived one stimulus in about half of the trials, whereas in the other half subjects perceived two stimuli. Hence, within subjects, physically identical stimulation resulted in varying perception across trials. After stimulation, subjects were asked to report their respective perception (i.e., one or two stimuli) and their confidence in the perceptual report by a button press with the index or middle finger of the right hand (Fig. 4). During the experiment, ongoing neuromagnetic activity was recorded by means of MEG.

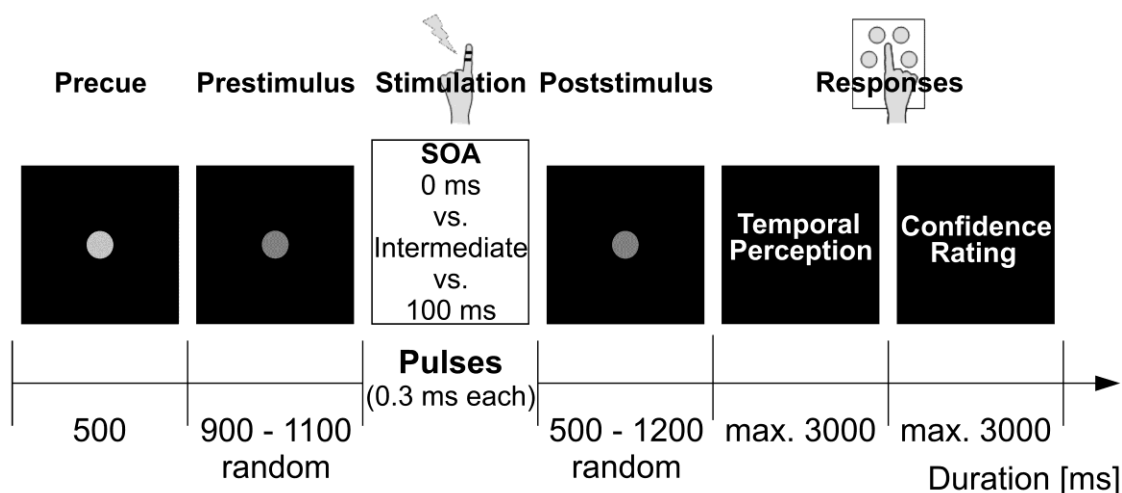


Figure 4: Paradigm of study 1. A central fixation dot indicated the start of the trial. After 500 ms, luminance decreased and signaled the beginning of a jittered prestimulus epoch (900-1100 ms). Subsequently, electrotactile stimulation was applied to the left index finger with varying SOAs. Stimulation was followed by a jittered poststimulus interval (500-1200 ms), after which subjects reported their perception and subjective confidence in the previous perceptual report by button-press. Adapted and modified from Baumgarten et al., 2014.

Trials with intermediate SOA were sorted according to their perceptual response (perceived one stimulus vs. two stimuli) and grouped in two perceptual conditions. Time-frequency analysis with a spectral focus on the alpha band (8-12 Hz) and a temporal focus on the prestimulus epoch (900-0 ms before onset of the first stimulus) was performed on neuromagnetic data. Power estimates for both perceptual conditions were compared to assess any significantly different sensors and time points. Sensor-level power estimates were projected to source-level by means of a DICS beamformer approach (Gross et al., 2001). In a post hoc analysis, alpha band power in all trials with intermediate SOA was averaged across time points and sensors showing a significant difference between perceptual conditions. Trials were divided into five bins according to their average alpha band power. Normalized average perception rates were calculated for each bin and linear and quadratic functions were fitted to the data. A similar approach was selected to assess relationships between alpha band power and confidence ratings, although analyses were separated between perceptual conditions. To analyze any influence of prestimulus alpha band activity on neuronal correlates of decision variables, a model of perceptual decision making was adopted (Fig. 4B of Appendix 1). Decision bounds

were defined as poststimulus ERFs computed from unambiguous control conditions with trials nearly always perceived as one or two stimuli, respectively. For time points of significant difference between the ERFs of the control conditions, amplitude values and confidence values of trials with intermediate SOA divided by prestimulus alpha power (high vs. low) and perceptual response (one vs. two perceived stimuli) were compared according to the decision making model.

3.2 Results

In trials with intermediate SOA, alpha band power was significantly lower when subjects correctly perceived stimulation as two separate stimuli. Power differences were evident in the prestimulus epoch (900-250 ms before onset of the first stimulus) in anterior/somatosensory and parieto-occipital sensors contralateral to stimulation site. The underlying cortical sources were located in the contralateral postcentral gyrus and the contralateral middle occipital region (Fig. 2 of Appendix 1). A significant negative linear relation was found between averaged prestimulus alpha power and temporal perception; i.e., the probability to perceive stimulation as two separate stimuli increased with decreasing prestimulus alpha power. Likewise, linear relations were found between prestimulus alpha power and confidence ratings, however, the direction of the relations was opposite in both perceptual conditions. A significant negative linear relation was found for trials where stimulation was perceived as two separate stimuli and a strong trend towards a positive linear relation was found for trials where stimulation was perceived as one stimulus (Fig. 3 of Appendix 1). Poststimulus ERFs showed characteristics of a decision variable at ~150 ms after stimulus onset. Poststimulus ERFs of trials with intermediate SOA differed with respect to subjects' perception and prestimulus alpha power (Fig. 4 of Appendix 1). Amplitude values of poststimulus ERFs monotonically decreased from two perceived stimuli with low alpha power levels to one perceived stimulus with high alpha power levels in agreement with the postulated decision making model. Likewise, the distribution of average confidence values of trials with intermediate SOA agreed with the proposed model predictions (Fig. 5 of Appendix 1).

3.3 Discussion

Study 1 demonstrated that prestimulus alpha band power (8-12 Hz) is related to the temporal perceptual discrimination of suprathreshold tactile stimuli. Low prestimulus alpha power in the contralateral postcentral gyrus and the contralateral middle occipital region facilitated the perception of two separate stimuli. Prestimulus alpha band power was linearly related to subjects' confidence ratings, with the direction of relations inversely orientated depending on stimulus perception. Finally, poststimulus ERFs reflected the subjects' perceptual responses and confidence, not sensory evidence. Thus, ERFs represented potential neuronal correlates of decisional processes. Amplitude values of poststimulus ERFs were in accordance with the proposed decisional model. Confidence values in trials with intermediate SOA could be explained by the distance of the respective ERFs to the decision bounds. Finally, poststimulus ERFs were modulated by prestimulus alpha band power.

The present results are in line with theories that interpret alpha band power as a perceptual gating mechanism by means of functional inhibition of task-irrelevant areas (Jensen and Mazaheri, 2010) and as an indicator of cortical excitability (Thut et al., 2006; Romei et al., 2008b; Lange et al., 2013). Beyond that, study 1 demonstrates that prestimulus alpha band power does not operate like a binary switch alternating between inhibition and excitation. Rather, alpha band power gradually influences perception, since it modulates how many suprathreshold stimuli are perceived as well as the subjective quality (i.e., confidence rating) of the perception.

Alpha band power significantly differed in the postcentral gyrus (presumably S1) and the contralateral middle occipital region. Power differences in the alpha band in S1 are known to be present in tasks where identical tactile stimulation results in varying perception (Zhang et al., 2008; Lange et al., 2012) and agree with the role of alpha band activity as indicator of cortical excitability. Power differences in the contralateral middle occipital region were not expected as a consequence of tactile stimulation. However, it is known that tasks involving shifts in spatial attention cause a suppression of alpha band power in cortical areas not directly related to presented stimulus modality (Bauer et al., 2006; 2012). Although spatial attention was not

systematically modified in the present study, occipital power differences can be interpreted as a correlate of global attention. This is supported by the finding that the poststimulus ERF effects related to perceptual decision making could only be replicated for the anterior/somatosensory sensor cluster and not for the parieto-occipital sensor cluster when both clusters were analyzed separately.

Finally, prestimulus alpha power modulated the confidence subjects had in their perceptual reports. The inversely orientated directions of the relations between prestimulus alpha power and the confidence ratings for the two different perceptual conditions can be explained by the proposed decision model. Confidence ratings of trials with intermediate SOA were determined by the distance from the respective ERFs (i.e., the decision variable) to the decision bounds (e.g., low prestimulus alpha band power increased confidence in trials perceived as two separate stimuli because the distance between the decision variable and the decision bound for two perceived stimuli decreased; Fig. 4B in Appendix 1). Prestimulus alpha power presumably modulates the starting point of the decision variable (de Lange et al., 2013). Thus, the prestimulus brain state can influence the outcome of perceptual decisions, with increasing influence when sensory evidence is weak or ambiguous.

3.4 Conclusion

Prestimulus alpha band power is related to the temporal perceptual discrimination of electrotactile stimulation. Furthermore, prestimulus alpha band power shows a connection to the subjective confidence subjects have in their perceptual reports, which can be explained by a decision making model. The results suggest that prestimulus alpha band power qualitatively influences stimulus processing and subsequent perception; i.e., by influencing the amount of perceived stimuli and the subjective confidence in the perceptual report.

4 Study 2: Beta Oscillations Define Discrete Perceptual Cycles in the Somatosensory Domain (Baumgarten et al., 2015, PNAS)

Study 2 (Appendix 2) focused on the role of prestimulus oscillatory phase in S1 for the discrete perceptual sampling of electrotactile stimuli. Although subjective experience indicates that perception is continuous, there is growing evidence suggesting discrete processing of sensory input (e.g., Varela et al., 1981; Chakravarthi and VanRullen, 2012). A discontinuous processing mode is thought to rely on discrete perceptual cycles sampling incoming sensory stimulation, with discrete stimuli arriving within a single perceptual cycle being perceived as single event (VanRullen and Koch, 2003). Since the theory of discrete perceptual cycles assumes that perceptual sampling is based on ongoing internal neurophysiological processes providing a temporal reference frame (Busch et al., 2009), neuronal oscillations have been considered a promising candidate measure for the determination of perceptual cycles. These assumptions have been corroborated by studies suggesting that parieto-occipital alpha band phase defines cycles of perception in the visual domain (Dugué et al., 2011; Romei et al., 2012; Jensen et al., 2014). However, it remains to be demonstrated that discrete perceptual sampling is not domain-specific for the visual domain but also present in other sensory modalities. Furthermore, if discrete perceptual sampling is present in multiple sensory domains, it is critical to determine whether different sensory domains operate on the same temporal reference frame (i.e., if perceptual sampling in all modalities relies on alpha band cycles). Since different modalities operate on different time scales (e.g., Gebhard and Mowbray, 1959), there are indications against the notion of a common temporal reference frame.

Based on findings on perceptual cycles in the visual domain, the present study hypothesized that discrete perceptual sampling exists in the somatosensory domain. Prestimulus ongoing oscillatory phase in the beta band in S1 was hypothesized to differ across trials in which subsequently presented electrotactile stimuli were perceived as either one single or two separate sensory events. If the perception of two subsequently presented stimuli as either one stimulus or two stimuli would be related to phase angle differences in ongoing neuronal

oscillations, this would suggest that oscillatory phase is relevant for the discrete temporal sampling of sensory information.

4.1 Methods

Study 2 was based on the same data set as study 1 (see 3.1 for details on subjects and paradigm). In summary, subjects received suprathreshold electrotactile stimulation of the left index finger. In the main condition, subjects received two subsequent pulses separated by a subject-specific SOA (labeled intermediate SOA) determined to result in a distribution of ~50% of trials perceived as one stimulus and ~50% of trials perceived as two stimuli.

To focus the analysis of neuromagnetic data on S1, a virtual sensor was constructed by means of an LCMV beamformer (van Veen et al., 1997; Fig. 2A of Appendix 2). Based on the resulting spatial filter, source level virtual sensor data was reconstructed from single-trial time courses of MEG sensor data. Oscillatory phase was calculated for virtual sensor data by applying a discrete Fourier transform. For each trial, this resulted in a complex number for every time-frequency element, from which phase angles were calculated. Trials with intermediate SOA were sorted according to the perceptual response (perceived one stimulus vs. two stimuli) and placed in two different perceptual conditions. Perceptual conditions were compared to determine statistically significant phase angle differences. To investigate to what extent the respective perception of one or two stimuli was associated with different phase angles, trials were divided into six equally spaced bins according to their oscillatory phase angle. For each bin, the normalized perceptual response rate was calculated. Based on the phase angle differences between perceptual conditions, a model of perceptual cycles was derived (Fig. 3 of Appendix 2). Group-level and single-subject level perceptual response rates were predicted based on this model.

4.2 Results

Phase angles in S1 significantly differed between perceptual conditions in the prestimulus epoch (530-90 ms before stimulus onset) for frequencies in the alpha and beta band (8-20 Hz; Fig. 2B of Appendix 2). Hence, in this time-frequency range phase angle differences between

perceptual conditions were significantly larger than randomly distributed phases and fluctuated around the maximum phase angle difference (i.e., π). These phase angle differences could not be explained by power differences between perceptual conditions. The influence of phase accounted for up to 13% points of perceptual variability (Fig. 2D of Appendix 2). The proposed model of perceptual cycles (Fig. 3 of Appendix 2) was derived from the resulting phase angle differences between perceptual conditions and the theory of perceptual framing (Varela et al., 1981; VanRullen et al., 2011; 2014). The model states that the temporal resolution of perception is defined by an oscillatory cycle of a specific frequency. If two stimuli both impinge on the sensory system within one cycle, stimulation is perceived as one single stimulus. If two stimuli impinge on the sensory system within two separate cycles (i.e., each single stimulus within a separate cycle), stimulation is perceived as two separate stimuli. From the resulting phase angle differences, the critical frequency band determining the length of the perceptual cycle lies in the alpha and lower beta band. Based on this model, perceptual response rates could be successfully predicted on group level (Fig. 4 of Appendix 2) and single-subject level (Fig. S2 of Appendix 2).

4.3 Discussion

Study 2 suggests that somatosensory perception operates in a discrete mode and that somatosensory stimulation is sampled by discrete perceptual cycles. These perceptual cycles are determined by the alpha and, in particular, the lower beta band. This result was based on the finding that alpha and beta band phase angles in S1 predicted whether two suprathreshold stimuli were perceived as one single stimulus or two separate stimuli. Accordingly, a model was put forward which explained the mechanisms of discrete sampling by means of perceptual cycles. Perceptual response rates could be predicted successfully based on the model propositions.

In general, studies addressing the topic of discrete perceptual sampling remain scarce, with present studies mainly addressing the visual domain (Varela et al., 1981; Chakravarthi and VanRullen, 2012). The present results demonstrate that discrete perceptual sampling is no domain-specific visual phenomenon, but is also present in the somatosensory domain. In the

visual domain, discrete cycles in perception and attentional updating are considered to be determined by alpha band cycles (Busch and VanRullen, 2010; Jensen et al., 2014). The present model is in line with these findings, albeit somatosensory perception seems to be defined by alpha and, in particular, beta band cycles. These domain-specific characteristics are in agreement with a prominent role of beta band oscillations in somatosensory processing (Jones et al., 2010; Haegens et al., 2011b; Lange et al., 2012), whereas alpha band oscillations are central for visual perception (Romei et al., 2008b; Wyart and Tallon-Baudry, 2009). Furthermore, these domain-specific differences are in accordance with studies investigating steady-state somatosensory evoked potentials (SSSEPs). SSSEP amplitudes are highest for a stimulation frequency of approximately 18-26 Hz (i.e., in the beta band; Snyder, 1992; Tobimatsu et al., 1999; Haegens et al., 2011b). By such a stimulation frequency, every single tactile stimulus would be placed within a separate beta cycle. This in turn would increase SSSEP amplitude and facilitate perception.

The present results indicate that the phase of ongoing neuronal oscillations differs between perceptual conditions and is central to the temporal sampling of sensory information. However, the present study does not claim that specific phase (i.e., the peak or trough of a cycle) is either beneficial or hindering for perception. Effects of specific phase on perception have previously been addressed for different modalities (e.g., Varela et al., 1981; Busch et al., 2009; Mathewson et al., 2009; Dugué et al., 2011; Ng et al., 2012;), whereas evidence for the influence of oscillatory phase on the temporal sampling of sensory information remains scarce and only focuses on the visual domain (e.g., Varela et al., 1981).

Taken together, there is notable evidence that sensory information is processed in a phasic mode. The question remains, however, why subjective experience does not match such a discrete sampling mode, but rather resembles a seamless perceptual stream. The mechanisms of how the brain transforms discretely sampled sensory information into this seamless percept still remain to be revealed. Nonetheless, there are reports of situations where these mechanisms fail to work (Dubois and VanRullen, 2011), for example in akinetopsia (Horton and Trobe, 1999; Tsai and Mendez, 2009) and after the ingestion of lysergic acid diethylamide (Abraham, 1983; Kawasaki and Purvin, 1996).

4.4 Conclusion

Study 2 investigated the relationship between oscillatory phase in S1 and the perceptual sampling of electrotactile stimulation. Oscillatory phase angles in the alpha and lower beta band significantly differed between perceptual conditions. Based on these results, a model of perceptual cycles was presented. This model states that cycles in the alpha and lower beta band represent neurophysiological correlates of somatosensory perceptual cycles. The results demonstrate that discrete perceptual sampling is no domain-specific visual phenomenon, but also exists in the somatosensory domain.

5 Study 3: Beta Peak Frequencies at Rest Correlate with Endogenous GABA/Cr Concentrations in the Left Sensorimotor Cortex (Baumgarten et al., submitted)

Study 3 (Appendix 3) investigated the relationship between beta band peak frequency (i.e., the frequency within the beta band exhibiting the highest power) and GABA concentration in sensorimotor and occipital cortices. Prominent beta band activity can be measured in the human sensorimotor cortex both at rest and after movement (Murthy and Fetz, 1996; Salmelin and Hari, 1994; Kilavik et al., 2013). Furthermore, beta band power and phase is related to somatosensory perception (e.g., Bauer et al., 2006; Gaetz and Cheyne, 2006; Baumgarten et al., 2015). Although the majority of studies addressing beta band activity focus on beta band power, beta band peak frequency has been shown to be a functionally relevant parameter (Kilavik et al., 2012). For example, beta band peak frequency differs during movement or stimulation of lower versus upper limbs, thus distinguishing between different somatotopic representations (Neuper and Pfurtscheller, 2001).

GABAergic inhibition is generally considered an important factor for the generation of neuronal oscillations in neuronal networks (Wang, 2010). Specifically for the beta band, GABA_A-mediated inhibition is assumed to act as the central pacemaker within neuronal networks, thereby determining the oscillatory frequency within the network (Whittington et al., 2000a; 2000b). The connection between beta band activity and GABA concentration is further supported by animal studies and computational neuronal models (Jensen et al., 2005; Roopun et al., 2006; Yamawaki et al., 2008). Direct experimental evidence for this link in humans results from pharmacological modulation studies demonstrating that GABAergic compounds modulate beta band power (Jensen et al., 2005; Hall et al., 2010; Gaetz et al., 2011; Muthukumaraswamy et al., 2013) and peak frequency (Jensen et al., 2005) both at rest and during movement. Although these pharmacological modulation studies provide causal evidence for the influence of GABAergic agents on beta band activity, these studies do not provide information about selective regional GABA concentrations. Thus, the quantitative relation between local GABA

concentration and measures of oscillatory activity remains to be determined. Recently, in vivo estimation of neurotransmitter concentrations in spatially defined cortical areas has become possible by means of MRS. Studies applying MRS that targeted sensorimotor cortex areas demonstrate linear relationships between sensorimotor GABA and post-movement beta band power, although no relationship could be determined for post-movement beta band peak frequency (Gaetz et al., 2011).

Taken together, current studies consistently report a general relationship between GABA concentration and beta band power. Results regarding beta band peak frequency however, are less consistent. In addition, most studies addressing this topic measured beta band activity related to motor activity, with few findings available for beta band activity at rest. Study 3 thus investigated if beta band peak frequency during rest (i.e., without movement) is correlated with non-modulated GABA concentration in sensorimotor and occipital cortices. It was hypothesized that a linear relation between beta band peak frequency and GABA concentration is present in sensorimotor cortices, but not in occipital control regions.

5.1 Methods

15 healthy subjects participated in the study. The subjects were selected from a sample of healthy controls that was previously reported in a study from Oeltzschner et al. (2015). An assessment of handedness was conducted by means of a bi-manual performance test. 12 subjects were categorized as clearly right-handed and 3 subjects showed no clear hand preference. MRS data was recorded for three voxels ($3 \times 3 \times 3 \text{ cm}^3$) in MRS regions of interest (ROIs) placed in the left and right sensorimotor and occipital cortex (Fig. 1A of Appendix 3). For the subsequent analysis of neurotransmitter concentrations, the GABA-to-creatine ratio (GABA/Cr) was selected (Mullins et al., 2014). GABA/Cr values were compared across MRS ROIs by means of a one-factor repeated measures ANOVA. Ongoing neuromagnetic data was recorded via MEG during two sessions. In the first session, subjects visually focused a fixation dot (eyes open condition; EO), whereas in the second session subjects closed their eyes but remained awake (eyes closed condition; EC). In addition, both conditions were merged into a combined condition (EC+EO). MEG ROIs corresponding to the respective MRS ROIs were defined

by a selection of left and right sensorimotor and occipital sensors (Fig. 2A of Appendix 3). For each subject, peak frequencies in the beta band (15-30 Hz) were computed for each MEG ROI. Beta band peak frequencies were compared across MEG ROIs by means of a two-factor repeated measures ANOVA (main factors: MEG ROI and condition). Potential relationships between neurotransmitter concentrations and parameters of oscillatory activity were assessed by correlating GABA/CR concentration and beta band peak frequency for each condition (EC, EO, EC+EO) within corresponding ROIs.

5.2 Results

For GABA/Cr concentrations, no significant differences were found between the three MRS ROIs (Fig. 1B of Appendix 3). For beta band peak frequencies, a significant main effect for the factor MEG ROI was found, with beta peak frequencies significantly higher in both left and right sensorimotor sensors than in occipital sensors (Fig. 2C of Appendix 3). No significant differences were found for the factor condition. Likewise, no significant interaction between the factors MEG ROI and condition was found. Significant positive linear relations between GABA/Cr concentration and beta band peak frequency, computed for all conditions (EC, EO, EC+EO), were found for the left sensorimotor cortex (Fig. 3A of Appendix 3). After partializing out the effect of handedness, relations for the left sensorimotor cortex remained significant for beta band peak frequency computed for the conditions EO and EC+EO. For the right sensorimotor and occipital cortex, no significant relations between GABA/Cr concentration and beta band peak frequency were found.

5.3 Discussion

Study 3 demonstrated a significant positive linear relationship between non-modulated GABA/Cr concentration and beta band peak frequency measured at rest in left sensorimotor cortex areas. Thus, subjects with higher GABA/Cr concentration exhibited higher beta band peak frequencies in the left sensorimotor cortex. For right sensorimotor and occipital cortex areas, no relationship was found. The present results are in agreement with previous studies generally

indicating a connection between beta band activity and GABA concentration (e.g., Roopun et al., 2006; Hall et al., 2010; Gaetz et al., 2011; Muthukumaraswamy et al., 2013). Importantly, the current results provide evidence that the connection between beta band activity and GABA concentration is also present at rest.

The significant difference of beta band peak frequencies between sensorimotor and occipital sensors is in line with the prominent role of beta band activity in the sensorimotor cortex (see chapter 1.5.3 and Salmelin and Hari, 1994; Kilavik et al., 2013). This offers a possible explanation why no significant relation between beta band peak frequency and GABA/Cr concentration was found for occipital areas. However, this interpretation cannot explain why no relation could be determined for the right sensorimotor cortex. Although handedness was considered a probable cause for the hemispherically asymmetric relation, results remained virtually unchanged after correcting for handedness. Nonetheless, handedness is known to determine asymmetries in hand representation within the sensorimotor cortex (Volkman et al., 1998; Sörös et al., 1999; Triggs et al., 1999), which in turn might result in hemispheric differences in GABA/Cr concentration and/or beta band generators. The fact that GABA/Cr values were not found to be different for left and right sensorimotor cortices might relate to the rather large voxel size of the MRS analysis. These voxel sizes did not allow for a separate estimation of neurotransmitter concentration for motor and somatosensory cortex. Consequently, MRS measurements in the right sensorimotor cortex might have quantified GABA/Cr concentrations that are relatively more unrelated to beta band generators, compared to the left sensorimotor cortex. This issue has to be addressed by studies using more spatially fine-grained analyses and investigating both left and right-handed samples of equal size.

Of further interest is the connection of GABA concentration and beta peak frequency on a functional and behavioral level. Higher GABA concentration in sensorimotor areas has been related to lower frequency discrimination thresholds for tactile stimulation (Puts et al., 2011). Thus, higher GABA concentrations resulted in a higher temporal resolution regarding tactile perception. These findings were interpreted as that due to higher levels of inhibition, neurons in the somatosensory cortex would be able to adjust their firing pattern to cycles of the respective stimulus frequencies, thereby lowering frequency discrimination thresholds. This can be related

to the influence of somatosensory beta band activity on the temporal sampling of tactile stimuli demonstrated in study 2 (Baumgarten et al., 2015). Here, beta band phase predicted tactile temporal discrimination, and the specific frequency within the beta band showing the largest phase angle differences successfully predicted perceptual response rates (Fig. S2 of Appendix 2). Thus, current findings suggest that GABA concentrations and beta band activity within the sensorimotor cortex are related to the temporal resolution of tactile perception.

5.4 Conclusion

Study 3 investigated if local non-modulated GABA/Cr concentrations are related to beta band peak frequencies at rest in sensorimotor and occipital cortex areas. Positive linear relations between GABA/Cr concentration and beta band peak frequency were found for the left sensorimotor cortex. These results suggest that the previously reported connection between GABA concentration and beta band power also extends to beta band peak frequency. The findings further provide evidence that sensorimotor beta band activity is linked to local sensorimotor GABA concentration. Finally, the results demonstrate that the previously reported connection between beta band activity and GABA concentrations are also present at rest and regarding non-modulated GABA concentrations.

6 General Discussion

The present thesis focused on neuronal oscillatory activity in the somatosensory cortex. The first two studies aimed at investigating the role of ongoing neuronal oscillatory activity in the alpha and beta band during the prestimulus interval for the temporal perceptual discrimination of electrotactile stimuli. Empirical evidence for the relationship between different parameters of prestimulus neuronal oscillatory activity and stimulus processing and perception was presented. Based on these experimental findings, theoretical models were provided that elucidated potential mechanisms of how the current brain state (in form of ongoing prestimulus oscillatory activity) determines perception. The third study examined the connection between parameters of oscillatory activity measured at rest and local non-modulated neurotransmitter concentrations. Locally specific connections between beta band peak frequency and non-modulated GABA concentrations were demonstrated.

Study 1 and 2 relied on a simple, yet efficient paradigm. By presenting subjects with stimulation that was physically constant but produced varying perceptual reports across trials, a comparison between trials with different perceptual reports eliminated systematical stimulation effects. Here, varying perception resulted from ambiguity in the temporal dimension due to individually selected SOAs. The primary impact is the finding that prestimulus oscillatory activity is not only central to neuronal stimulus processing and perception, but that neuronal stimulus processing and perception are gradually modulated by prestimulus oscillatory activity. This gradual influence is reflected in a qualitative modulation of perception, which study 1 and 2 demonstrated for the temporal perceptual discrimination of consecutive electrotactile stimuli. Hence, prestimulus oscillations do not only determine whether a (near-threshold) stimulus is perceived or not, but also how (suprathreshold) stimuli are perceived.

Both study 1 and 2 were based on the same experimental paradigm and raw data sets. Yet, it is important to note that they investigate two different parameters of neuronal oscillatory activity (oscillatory power and phase). Although both studies find the respective parameter to differ between trials with constant stimulation but varying perception, there are fundamental

differences between the respective analysis approaches. Study 1 focused on the alpha band and investigated power differences over all sensors. In contrast, study 2 applied a virtual sensor approach and solely focused on neuromagnetic activity originating from S1. Furthermore, the power effects demonstrated in study 1 begin earlier (900 ms before stimulus onset) than the phase angle effects of study 2 (530 ms before stimulus onset). This is likely due to the intrinsic differences between power and phase. Oscillatory phase provides fine grained windows of excitation and inhibition (Busch et al., 2009; Mathewson et al., 2011) and is therefore suited as correlate of quickly fluctuating processes (i.e., perceptual cycles). Power changes, however, reflect the size and synchronization of an active neuronal population (Pfurtscheller and Lopes da Silva, 1999). This is further supported by theories attributing (alpha) power differences as a neuronal correlate of top down mechanisms like attention (Jensen and Mazaheri, 2010).

Of further interest is the question why prestimulus power and phase effects presented in the first two studies are not present up to the time point of stimulus presentation. Here, one could argue that prestimulus effects which influence subsequent perception should be most visible immediately before stimulus presentation. However, this phenomenon has been frequently reported across modalities and for power as well as phase effects (e.g., Busch et al., 2009; Lange et al., 2012; Hanslmayr et al., 2013). Although so far no definitive reason for this well-replicated finding is known, it can be speculated about different causes. One reason could be that prestimulus effects immediately before stimulus presentation are masked by neuronal activity related to stimulus processing. Since such stimulus-related activity can be considered to have a higher signal-to-noise ratio than ongoing prestimulus activity, a masking of the prestimulus signal from the stimulus-related signal would appear reasonable. Alternatively, it could be assumed that prestimulus effects in the alpha and beta frequency band are modulated by an underlying rhythm with lower frequency. For example, activity in the alpha and beta band could be locked to the phase of underlying ongoing theta oscillations (4-7 Hz) with cycle durations around 140-250 ms (Singer, 2013). Consequently, power or phase in the alpha and beta band should fluctuate according to the phase of underlying rhythm. Provided that the underlying rhythm is also systematically related to stimulus perception, power or phase differences between perceptual conditions in the alpha and beta band should likewise fluctuate according

to the phase of underlying rhythm. Power or phase differences between perceptual conditions would therefore reach significance only during those time points when the phase difference between perceptual conditions in the underlying theta rhythm is maximal. This would determine that power or phase differences in the alpha and beta band would be discernible periodically, instead of being present throughout the prestimulus period. Interestingly, recent studies reported that behavioral performance and neuronal correlates of stimulus processing in a visual change detection tasks fluctuated at a 4 Hz rhythm (Landau and Fries, 2012; Landau et al., 2015).

Taken together, the first two studies show that the prestimulus brain state as expressed in ongoing neuronal oscillations influences how subsequently presented stimulation is perceived. The results of the study 1 are in agreement with current theories on the role of alpha band activity as a sensory gating mechanism that regulates information processing (Klimesch et al., 2007; Jensen and Mazaheri, 2010). However, study 1 critically extends current theories by showing that prestimulus alpha band changes also qualitatively influence perception. Study 2 demonstrates that beta band activity is not only central to movement-related tasks and the maintenance of the status quo, but also influences the perception of somatosensory stimulation. Importantly, study 2 provides empirical support for the theory of discrete perceptual sampling of sensory information, a concept which had already been proposed decades ago (e.g., Stroud, 1956; Varela et al., 1981) but since then has received surprisingly little scientific interest. Finally, study 2 could demonstrate that discrete perceptual sampling is no domain-specific visual phenomenon and that perceptual cycles exist also in the somatosensory modality.

Finally, the present thesis demonstrates a connection between non-modulated neurotransmitter concentrations and neuronal oscillatory parameters at rest. Study 3 presented linear positive relations between GABA/Cr concentrations and beta band peak frequency in the left sensorimotor cortex. By investigating beta band peak frequency not related to motor activity and local non-modulated GABA concentrations, study 3 extended previous findings regarding the connection of beta band activity and GABA concentrations. However, a significant relation was only found for the left sensorimotor cortex. Future studies are necessary to clarify

if the connection between beta band peak frequency and GABA concentration generally exhibits hemispheric asymmetries and which factors (e.g., handedness) contribute to this imbalance.

In sum, the present thesis makes important scientific contributions regarding the functions and neurochemical basics of somatosensory neuronal oscillations. Novel findings regarding the role of prestimulus low frequency band oscillatory activity for somatosensory stimulus processing and perception are demonstrated. The included studies show that ongoing variations in the state of the brain are connected to the way how somatosensory stimulation is perceived. In addition, parameters of oscillatory activity at rest are related to local non-modulated neurochemical concentrations. Finally, the thesis emphasizes that MEG and current analysis techniques represent powerful tools to investigate ongoing brain activity and the temporal dimension of stimulus processing.

7 Outlook

The abovementioned results demonstrate comprehensive evidence for the role of prestimulus oscillatory activity for the processing and perception of suprathreshold electrotactile stimulation. Additionally, locally specific connections between neuronal oscillatory activity and non-modulated neurotransmitter concentrations are presented. Various avenues regarding potential future research options emanate from these findings.

An important limitation of the presented studies is their correlative nature. Strictly speaking, since ongoing oscillatory activity was not experimentally modified, it cannot be deduced that prestimulus activity causally influenced subsequent perception. However, previous studies in which oscillatory parameters were experimentally manipulated were able to demonstrate that perception is causally modulated by oscillatory power (e.g., Romei et al., 2008a; 2008b; 2010) and phase (e.g., Neuling et al., 2012; Romei et al., 2012). Taking these findings into account, it seems highly likely that prestimulus oscillatory activity also causally influences the perception of suprathreshold stimuli. To further strengthen this assumption, however, future studies are needed in which similar paradigms are combined with neuromodulatory mechanisms. Potential established mechanisms include TMS (e.g., Romei et al., 2008a; 2008b; 2010) as well as transcranial alternating current stimulation (Zaehle et al., 2010) and transcranial direct current stimulation (Neuling et al., 2012). Nonetheless, it has to be considered that such neuromodulatory approaches create additional difficulties and artifacts in MEG measurements. An additional option to experimentally manipulate oscillatory parameters is provided by sensory stimulation. Sensory stimulation has been shown to reset oscillatory phase in sensory cortices (Lakatos et al., 2007; Romei et al., 2012). Attentional cueing by sensory stimulation cyclically influences perceptual detection, which in turn is attributed to underlying oscillatory phase (Landau and Fries, 2012; Landau et al., 2015). Thus, the reset of oscillatory phase in S1 by a somatosensory stimulus would theoretically enable to more directly test the theory of perceptual cycles addressed in study 2. The time interval between the phase resetting stimulation and the presentation of the first stimulus should determine at which phase of the perceptual cycle the first stimulus impinges on the somatosensory system. The phase of the

perceptual cycle at which the second stimulus would arrive can be derived from the SOA and the perceptual cycle length. According to the theory of somatosensory perceptual cycles presented in study 2, temporal perceptual discrimination rates should be a cyclic function of the temporal distance between reset stimulus and first target stimulus. These cyclic fluctuations should be present within a frequency of the beta band.

Study 1 examined the relationship between ongoing prestimulus alpha band power and poststimulus ERFs, which were interpreted as neuronal correlates of stimulus processing. In line with this approach, it would also be interesting to investigate the effect of prestimulus oscillations on different parameters representing stimulus processing, in particular gamma band activity (Fries, 2009). Although stimulus-induced gamma band activity has been demonstrated mostly for visual stimulation (e.g., Hoogenboom et al., 2006), recent studies also reported gamma band activity in somatosensory cortex areas in response to tactile stimulation (e.g., Rossiter et al., 2013; Jamali and Ross, 2014).

In addition, it would be interesting to investigate the influence of prestimulus oscillations on the perception of more naturalistic stimuli (e.g., mechanical stimulation instead of electrotactile stimulation). Although naturalistic stimuli are more demanding in terms of their presentation, the potential results could emphasize the influence of ongoing neuronal oscillations on everyday perception. Despite concerns that naturalistic stimulation might result in smaller and more smeared effects of stimulus processing, there is evidence that such an approach is feasible (e.g., Smith et al., 2006).

Furthermore, network analyses of those brain areas involved in temporal perceptual discrimination would offer an intriguing possibility to study the neuronal networks involved in perceptual decision making. Since current decision making models generally assume the decision process to consist of separate, functionally and temporally distinguishable subprocesses (e.g., evidence accumulation, response preparation; Gold and Shadlen, 2007), network analyses could yield important results on how the brain encodes and integrates these subprocesses to form a specific decisional outcome. For time series data with high temporal resolution (as provided by MEG), various established connectivity metrics are available (Lachaux

et al., 1999; Schoffelen and Gross, 2009). As demonstrated by the results of study 1, differences between perceptual conditions are not restricted to sensory cortices. This is further supported by findings reporting that global network features indicating the integration of the somatosensory cortex into a distributed network differ between hits and misses in a tactile detection task (Weisz et al., 2014).

Finally, future studies addressing the connection between parameters of oscillatory activity and local neurotransmitter concentrations would benefit from smaller MRS voxel sizes. Smaller voxels would allow for the differentiated analysis of functionally distinct cortical areas (e.g., motor vs. somatosensory cortex) and thus allow for a more fine grained spatial analysis of neurotransmitter distribution. Currently, smaller voxel sizes are possible, but come at the cost of a longer measurement duration or higher field strength (Puts and Edden, 2012). However, with the emergence and increasing use of 7T MRI scanners, smaller MRS voxels in combination with feasible measurement time might become possible in the near future.

Taken together, the findings presented in the scope of this thesis provide important information about the functional role and neurochemical basics of somatosensory neuronal oscillations. However, compared to the existing knowledge regarding neuronal oscillations and the many questions that remain to be addressed, the present findings resemble only a small piece in the ongoing endeavor to elucidate the general purpose of neuronal oscillations in the brain.

8 References

- Abraham, H.D. (1983). Visual phenomenology of the LSD flashback. *Arch Gen Psychiatry* 40(8):884–889.
- Adrian, E.D., and Matthews, B.H.C. (1934). The Berger rhythm: potential changes from the occipital lobes in man. *Brain* 57:355–385.
- Anderson, K.L., and Ding, M. (2011). Attentional modulation of the somatosensory mu rhythm. *Neuroscience* 180:165–180.
- Baillet, S., Mosher, J., and Leahy, R. (2001). Electromagnetic brain mapping. *IEEE Signal Process Mag* 18(6):14–30.
- Baker, S.N., Olivier, E., and Lemon, R.N. (1997). Coherent oscillations in monkey motor cortex and hand muscle EMG show task-dependent modulation. *J Physiol* 501(1):225–241.
- Başar, E., Başar-Eroğlu, C., Karakaş, S., and Schürmann, M. (2000). Brain oscillations in perception and memory. *Int J Psychophysiol* 35(2–3):95–124.
- Bauer, M., Kennett, S., and Driver, J. (2012). Attentional selection of location and modality in vision and touch modulates low-frequency activity in associated sensory cortices. *J Neurophysiol* 107(9):2342–2351.
- Bauer, M., Oostenveld, R., Peeters, M., and Fries, P. (2006). Tactile spatial attention enhances Gamma-band activity in somatosensory cortex and reduces low-frequency activity in parieto-occipital areas. *J Neurosci* 26(2):490–501.
- Baumgarten, T.J., Schnitzler, A., and Lange, J. (2014). Prestimulus alpha power influences tactile temporal perceptual discrimination and confidence in decisions. *Cereb Cortex* 10.1093/cercor/bhu247.
- Baumgarten, T.J., Schnitzler, A., and Lange, J. (2015). Beta oscillations define discrete perceptual cycles in the somatosensory domain. *Proc Natl Acad Sci U S A* 112(39):12187–12192.
- Berger, H. (1929). Über das Elektrenkephalogramm des Menschen. *Archiv f. Psychiatrie* 87(1):527–570.
- Bishop, G. (1933). Cyclic changes in excitability of the optic pathway of the rabbit. *Am J Physiol* 103(1):213–224.
- Braeutigam, S. (2013). Magnetoencephalography: Fundamentals and established and emerging clinical applications in radiology. *ISRN Radiol* 2013:529463.
- Busch, N.A., Dubois, J., and VanRullen, R. (2009). The phase of ongoing EEG oscillations predicts visual perception. *J Neurosci* 29(24):7869–7876.
- Busch, N.A., and VanRullen, R. (2010). Spontaneous EEG oscillations reveal periodic sampling of visual attention. *Proc Natl Acad Sci U S A* 107(37):16048–16053.

- Buschman, T.J., and Miller, E.K. (2007). Top-down versus bottom-up control of attention in the prefrontal and posterior parietal cortices. *Science* 315(5820):1860–1862.
- Butikofer, R., and Lawrence, P.D. (1978). Electrocutaneous nerve stimulation-I: Model and experiment. *IEEE Trans Biomed Eng* 25(6):526–531.
- Buzsáki, G. (2006). Rhythms of the Brain. New York: Oxford Univ Press.
- Buzsáki, G., Anastassiou, C.A., and Koch, C. (2012). The origin of extracellular fields and currents — EEG, ECoG, LFP and spikes. *Nat Rev Neurosci* 13(6):407–420.
- Buzsáki, G., and Draguhn, A. (2004). Neuronal oscillations in cortical networks. *Science* 304(5679):1926–1929.
- Cajal, S.R.y. (1888). Estructura de los centros nerviosos de las aves. *Revis Trim Histol Norm Pat*(1):1–10.
- Chakravarthi, R., and VanRullen, R. (2012). Conscious updating is a rhythmic process. *Proc Natl Acad Sci U S A* 109(26):10599–10604.
- Chapman, R.M., Ilmoniemi, R.J., Barbanera, S., and Romani, G.L. (1984). Selective localization of alpha brain activity with neuromagnetic measurements. *Electroencephalogr Clin Neurophysiol* 58(6):569–572.
- Cheyne, D., Gaetz, W., Garnero, L., Lachaux, J.-P., Ducorps, A., Schwartz, D., and Varela, F.J. (2003). Neuromagnetic imaging of cortical oscillations accompanying tactile stimulation. *Brain Res Cogn Brain Res* 17(3):599–611.
- de Lange, F.P., Jensen, O., Bauer, M., and Toni, I. (2008). Interactions between posterior gamma and frontal alpha/beta oscillations during imagined actions. *Front Hum Neurosci* 2(7).
- de Lange, F.P., Rahnev, D.A., Donner, T.H., and Lau, H. (2013). Prestimulus oscillatory activity over motor cortex reflects perceptual expectations. *J Neurosci* 33(4):1400–1410.
- DeFelipe, J., and Fariñas, I. (1992). The pyramidal neuron of the cerebral cortex: Morphological and chemical characteristics of the synaptic inputs. *Prog Neurobiol* 39(6):563–607.
- Donner, T.H., Siegel, M., Fries, P., and Engel, A.K. (2009). Buildup of choice-predictive activity in human motor cortex during perceptual decision making. *Curr Biol* 19(18):1581–1585.
- Doyle, L.M.F., Yarrow, K., and Brown, P. (2005). Lateralization of event-related beta desynchronization in the EEG during pre-cued reaction time tasks. *Clin Neurophysiol* 116(8):1879–1888.
- Dubois, J., and VanRullen, R. (2011). Visual trails: Do the doors of perception open periodically? *PLoS Biol* 9(5):e1001056.
- Dugué, L., Marque, P., and VanRullen, R. (2011). The phase of ongoing oscillations mediates the causal relation between brain excitation and visual perception. *J Neurosci* 31(33):11889–11893.
- Engel, A.K., and Fries, P. (2010). Beta-band oscillations — signalling the status quo? Cognitive neuroscience. *Curr Opin Neurobiol* 20(2):156–165.

- Engel, A.K., Fries, P., and Singer, W. (2001). Dynamic predictions: Oscillations and synchrony in top-down processing. *Nat Rev Neurosci* 2(10):704–716.
- Ergenoglu, T., Demiralp, T., Bayraktaroglu, Z., Ergen, M., Beydagi, H., and Uresin, Y. (2004). Alpha rhythm of the EEG modulates visual detection performance in humans. *Brain Res Cogn Brain Res* 20(3):376–383.
- Freeman, W.J., Rogers, L.J., Holmes, M.D., and Silbergeld, D.L. (2000). Spatial spectral analysis of human electrocorticograms including the alpha and gamma bands. *J Neurosci Methods* 95(2):111–121.
- Fries, P. (2005). A mechanism for cognitive dynamics: neuronal communication through neuronal coherence. *Trends Cogn Sci* 9(10):474–480.
- Fries, P. (2009). Neuronal Gamma-band synchronization as a fundamental process in cortical computation. *Annu Rev Neurosci* 32(1):209–224.
- Gaetz, W., and Cheyne, D. (2006). Localization of sensorimotor cortical rhythms induced by tactile stimulation using spatially filtered MEG. *NeuroImage* 30(3):899–908.
- Gaetz, W., Edgar, J.C., Wang, D.J., and Roberts, T. (2011). Relating MEG measured motor cortical oscillations to resting γ -Aminobutyric acid (GABA) concentration. *NeuroImage* 55(2):616–621.
- Gaetz, W., MacDonald, M., Cheyne, D., and Snead, O.C. (2010). Neuromagnetic imaging of movement-related cortical oscillations in children and adults: Age predicts post-movement beta rebound. *NeuroImage* 51(2):792–807.
- Gastaut, H. (1952). Electroencephalographic study of the reactivity of rolandic rhythm. *Rev Neurol (Paris)* 87(2):176–182.
- Gebhard, J.W., and Mowbray, G.H. (1959). On discriminating the rate of visual flicker and auditory flutter. *Am J Psychol* 72(4):521–529.
- Gold, J.I., and Shadlen, M.N. (2007). The neural basis of decision making. *Annu Rev Neurosci* 30(1):535–574.
- Gray, C. (1994). Synchronous oscillations in neuronal systems: Mechanisms and functions. *J Comput Neurosci* 1(1-2):11–38.
- Gray, C.M., and Singer, W. (1989). Stimulus-specific neuronal oscillations in orientation columns of cat visual cortex. *Proc Natl Acad Sci U S A* 86(5):1698–1702.
- Gross, J., Baillet, S., Barnes, G.R., Henson, R.N., Hillebrand, A., Jensen, O., Jerbi, K., Litvak, V., Maess, B., Oostenveld, R., Parkkonen, L., Taylor, J.R., van Wassenhove, V., Wibral, M., and Schoffelen, J.M. (2013). Good practice for conducting and reporting MEG research. *NeuroImage* 65:349–363.
- Gross, J., Kujala, J., Hamalainen, M., Timmermann, L., Schnitzler, A., and Salmelin, R. (2001). Dynamic imaging of coherent sources: Studying neural interactions in the human brain. *Proc Natl Acad Sci U S A* 98(2):694–699.

- Haegens, S., Händel, B.F., and Jensen, O. (2011a). Top-down controlled Alpha band activity in somatosensory areas determines behavioral performance in a discrimination task. *J Neurosci* 31(14):5197–5204.
- Haegens, S., Luther, L., and Jensen, O. (2012). Somatosensory anticipatory alpha activity increases to suppress distracting input. *J Cogn Neurosci* 24(3):677–685.
- Haegens, S., Nácher, V., Hernández, A., Luna, R., Jensen, O., and Romo, R. (2011b). Beta oscillations in the monkey sensorimotor network reflect somatosensory decision making. *Proc Natl Acad Sci U S A* 108(26):10708–10713.
- Hall, E.L., Robson, S.E., Morris, P.G., and Brookes, M.J. (2014). The relationship between MEG and fMRI. *NeuroImage* 102, Part 1:80–91.
- Hall, S.D., Barnes, G.R., Furlong, P.L., Seri, S., and Hillebrand, A. (2010). Neuronal network pharmacodynamics of GABAergic modulation in the human cortex determined using pharmaco-magnetoencephalography. *Hum Brain Mapp* 31(4):581–594.
- Hämäläinen, M., Hari, R., Ilmoniemi, R.J., Knuutila, J., and Lounasmaa, O.V. (1993). Magnetoencephalography—theory, instrumentation, and applications to noninvasive studies of the working human brain. *Rev Mod Phys* 65:413–497.
- Hansen P, Kringelbach M, Salmelin R (2010). MEG: An introduction to methods. New York: Oxford Univ Press.
- Hanslmayr, S., Aslan, A., Staudigl, T., Klimesch, W., Herrmann, C.S., and Bäuml, K.-H. (2007). Prestimulus oscillations predict visual perception performance between and within subjects. *NeuroImage* 37(4):1465–1473.
- Hanslmayr, S., Volberg, G., Wimber, M., Dalal, S.S., and Greenlee, M.W. (2013). Prestimulus oscillatory phase at 7 Hz gates cortical information flow and visual perception. *Curr Biol* 23(22):2273–2278.
- Hari, R., Parkkonen, L., and Nangini, C. (2010). The brain in time: insights from neuromagnetic recordings. *Ann N Y Acad Sci* 1191(1):89–109.
- Hebb, D.O. (1949). The organization of behavior. New York: Wiley.
- Hoogenboom, N., Schoffelen, J.-M., Oostenveld, R., Parkes, L.M., and Fries, P. (2006). Localizing human visual gamma-band activity in frequency, time and space. *NeuroImage* 29(3):764–773.
- Horton, J.C., and Trobe, J.D. (1999). Akinetopsia from nefazodone toxicity. *Am J Ophthalmol* 128(4):530–531.
- Jamali, S., and Ross, B. (2014). Sustained changes in somatosensory gamma responses after brief vibrotactile stimulation. *NeuroReport* 25(7):537–541.
- Jasper, H., and Penfield, W. (1949). Electrocorticograms in man: Effect of voluntary movement upon the electrical activity of the precentral gyrus. *Eur Arch Psychiatry Clin Neurosci* 183(1-2):163–174.

- Jenkinson, N., and Brown, P. (2011). New insights into the relationship between dopamine, beta oscillations and motor function. *Trends Neurosci* 34(12):611–618.
- Jensen, O. (2002). Oscillations in the Alpha band (9–12 Hz) increase with memory load during retention in a short-term memory task. *Cereb Cortex* 12(8):877–882.
- Jensen, O., Gips, B., Bergmann, T.O., and Bonnefond, M. (2014). Temporal coding organized by coupled alpha and gamma oscillations prioritize visual processing. *Trends Neurosci* 37(7):357–369.
- Jensen, O., Goel, P., Kopell, N., Pohja, M., Hari, R., and Ermentrout, B. (2005). On the human sensorimotor-cortex beta rhythm: Sources and modeling. *NeuroImage* 26(2):347–355.
- Jensen, O., and Mazaheri, A. (2010). Shaping Functional Architecture by Oscillatory Alpha Activity: Gating by Inhibition. *Frontiers Hum Neurosci* 4:186.
- Jones, S.R., Kerr, C.E., Wan, Q., Pritchett, D.L., Hämäläinen, M., and Moore, C.I. (2010). Cued spatial attention drives functionally relevant modulation of the Mu rhythm in primary somatosensory cortex. *J Neurosci* 30(41):13760–13765.
- Jones, S.R., Pritchett, D.L., Sikora, M.A., Stufflebeam, S.M., Hämäläinen, M., and Moore, C.I. (2009). Quantitative analysis and biophysically realistic neural modeling of the MEG Mu rhythm: Rhythmogenesis and modulation of sensory-evoked responses. *J Neurophysiol* 102(6):3554–3572.
- Jones, S.R., Pritchett, D.L., Stufflebeam, S.M., Hämäläinen, M., and Moore, C.I. (2007). Neural correlates of tactile detection: A combined Magnetoencephalography and biophysically based computational modeling study. *J Neurosci* 27(40):10751–10764.
- Gold, J.I., and Shadlen, M.N. (2007). The neural basis of decision making. *Annu Rev Neurosci* 30(1):535–574.
- Jurkiewicz, M.T., Gaetz, W.C., Bostan, A.C., and Cheyne, D. (2006). Post-movement beta rebound is generated in motor cortex: Evidence from neuromagnetic recordings. *NeuroImage* 32(3):1281–1289.
- Kaczmarek, K.A., Webster, J.G., Bach-y-Rita, P., and Tompkins, W.J. (1991). Electrotactile and vibrotactile displays for sensory substitution systems. *IEEE Trans Biomed Eng* 38(1):1–16.
- Kandel, E.R., Schwartz, J.H., Jessel, T.M., Siegelbaum, S.A., and Hudspeth, A.J. (2000). Principles of neural science. Fifth edition. New York: McGraw-Hill Education.
- Katzner, S., Nauhaus, I., Benucci, A., Bonin, V., Ringach, D.L., and Carandini, M. (2009). Local origin of field potentials in visual cortex. *Neuron* 61(1):35–41.
- Kawasaki, A., and Purvin, V. (1996). Persistent palinopsia following ingestion of lysergic acid diethylamide (LSD). *Arch Ophthalmol* 114(1):47–50.
- Keil, J., Müller, N., Hartmann, T., and Weisz, N. (2014). Prestimulus beta power and phase synchrony influence the sound-induced flash illusion. *Cereb Cortex* 24(5):1278–1288.
- Keil, J., Müller, N., Ihssen, N., and Weisz, N. (2012). On the variability of the McGurk effect: Audiovisual integration depends on prestimulus brain states. *Cereb Cortex* 22(1):221–231.

- Kiani, R., and Shadlen, M.N. (2009). Representation of confidence associated with a decision by neurons in the parietal cortex. *Science* 324(5928):759–764.
- Kilavik, B.E., Ponce-Alvarez, A., Trachel, R., Confais, J., Takerkart, S., and Riehle, A. (2012). Context-related frequency modulations of macaque motor cortical LFP Beta oscillations. *Cereb Cortex* 22(9):2148–2159.
- Kilavik, B.E., Zaepffel, M., Brovelli, A., MacKay, W.A., and Riehle, A. (2013). The ups and downs of beta oscillations in sensorimotor cortex. *Exp Neurol* 245:15–26.
- Klimesch, W. (1999). EEG alpha and theta oscillations reflect cognitive and memory performance: a review and analysis. *Brain Res Brain Res Rev* 29(2–3):169–195.
- Klimesch, W., Sauseng, P., and Hanslmayr, S. (2007). EEG alpha oscillations: The inhibition–timing hypothesis. *Brain Res Rev* 53(1):63–88.
- Kopell, N., Ermentrout, G.B., Whittington, M.A., and Traub, R.D. (2000). Gamma rhythms and beta rhythms have different synchronization properties. *Proc Natl Acad Sci U S A* 97(4):1867–1872.
- Koshino, Y., and Niedermeyer, E. (1975). Enhancement of rolandic Mu-rhythm by pattern vision. *Electroencephalogr Clin Neurophysiol* 38(5):535–538.
- Lachaux, J.P., Rodriguez, E., Martinerie, J., and Varela, F.J. (1999). Measuring phase synchrony in brain signals. *Hum Brain Mapp* 8(4):194–208.
- Lakatos, P., Chen, C.M., O’Connell, M.N., Mills, A., and Schroeder, C.E. (2007). Neuronal oscillations and multisensory interaction in primary auditory cortex. *Neuron* 53(2):279–292.
- Lakatos, P., Karmos, G., Mehta, A.D., Ulbert, I., and Schroeder, C.E. (2008). Entrainment of neuronal oscillations as a mechanism of attentional selection. *Science* 320(5872):110–113.
- Lakatos, P., Shah, A.S., Knuth, K.H., Ulbert, I., Karmos, G., and Schroeder, C.E. (2005). An oscillatory hierarchy controlling neuronal excitability and stimulus processing in the auditory cortex. *J Neurophysiol* 94(3):1904–1911.
- Landau, A.N., and Fries, P. (2012). Attention samples stimuli rhythmically. *Curr Biol* 22(11):1000–1004.
- Landau, A.N., Schreyer, H.M., van Pelt, S., and Fries, P. (2015). Distributed attention is implemented through Theta-rhythmic Gamma modulation. *Curr Biol* 25(17):2332–2337.
- Lange, J., Halacz, J., van Dijk, H., Kahlbrock, N., and Schnitzler, A. (2012). Fluctuations of prestimulus oscillatory power predict subjective perception of tactile simultaneity. *Cereb Cortex* 22(11):2564–2574.
- Lange, J., Keil, J., Schnitzler, A., van Dijk, H., and Weisz, N. (2014). The role of alpha oscillations for illusory perception. *Behav Brain Res* 271(100):294–301.
- Lange, J., Oostenveld, R., and Fries, P. (2011). Perception of the touch-induced visual double-flash illusion correlates with changes of rhythmic neuronal activity in human visual and somatosensory areas. *NeuroImage* 54(2):1395–1405.

- Lange, J., Oostenveld, R., and Fries, P. (2013). Reduced occipital Alpha power indexes enhanced excitability rather than improved visual perception. *J Neurosci* 33(7):3212–3220.
- Lindsley, D. (1952). Psychological phenomena and the electroencephalogram. *Electroencephalogr Clin Neurophysiol* 4(4):443–456.
- Linkenkaer-Hansen, K., Nikulin, V.V., Palva, S., Ilmoniemi, R.J., and Palva, J.M. (2004). Prestimulus oscillations enhance psychophysical performance in humans. *J Neurosci* 24(45):10186–10190.
- Llinas, R.R. (1988). The intrinsic electrophysiological properties of mammalian neurons: insights into central nervous system function. *Science* 242(4886):1654–1664.
- Lopes da Silva, F. (2013). EEG and MEG: Relevance to neuroscience. *Neuron* 80(5):1112–1128.
- Manshanden, I., de Munck, J.C., Simon, N.R., and Lopes da Silva, Fernando H (2002). Source localization of MEG sleep spindles and the relation to sources of alpha band rhythms. *Clin Neurophysiol* 113(12):1937–1947.
- Mathewson, K.E., Gratton, G., Fabiani, M., Beck, D.M., and Ro, T. (2009). To see or not to see: Prestimulus phase predicts visual awareness. *J Neurosci* 29(9):2725–2732.
- Mathewson, K.E., Lleras, A., Beck, D.M., Fabiani, M., Ro, T., and Gratton, G. (2011). Pulsed out of awareness: EEG Alpha oscillations represent a pulsed inhibition of ongoing cortical processing. *Front Psychol* 2. 10.3389/fpsyg.2011.00099
- Maxwell, J.C. (1865). A dynamical theory of the electromagnetic field. *Philos Trans R Soc Lond* 155:459–512.
- Mazaheri, A., Nieuwenhuis, I.L.C., van Dijk, H., and Jensen, O. (2009). Prestimulus alpha and mu activity predicts failure to inhibit motor responses. *Hum Brain Mapp* 30(6):1791–1800.
- Mitra, P.P., and Pesaran, B. (1999). Analysis of Dynamic Brain Imaging Data. *Biophys J* 76(2):691–708.
- Mullins, P.G., McGonigle, D.J., O’Gorman, R.L., Puts, N.A., Vidyasagar, R., Evans, C.J., and Edden, R.A. (2014). Current practice in the use of MEGA-PRESS spectroscopy for the detection of GABA. *NeuroImage* 86:43–52.
- Murakami, S., and Okada, Y. (2006). Contributions of principal neocortical neurons to magnetoencephalography and electroencephalography signals. *J Physiol* 575(3):925–936.
- Murthy, V.N., and Fetz, E.E. (1996). Oscillatory activity in sensorimotor cortex of awake monkeys: synchronization of local field potentials and relation to behavior. *J Neurophysiol* 76(6):3949–3967.
- Muthukumaraswamy, S.D., Myers, J.F.M., Wilson, S.J., Nutt, D.J., Lingford-Hughes, A., Singh, K.D., and Hamandi, K. (2013). The effects of elevated endogenous GABA levels on movement-related network oscillations. *NeuroImage* 66:36–41.
- Neuling, T., Rach, S., Wagner, S., Wolters, C.H., and Herrmann, C.S. (2012). Good vibrations: Oscillatory phase shapes perception. *NeuroImage* 63(2):771–778.

- Neuper, C., and Pfurtscheller, G. (2001). Event-related dynamics of cortical rhythms: frequency-specific features and functional correlates. *Int J Psychophysiol* 43(1):41–58.
- Ng, B.S.W., Schroeder, T., and Kayser, C. (2012). A precluding but not ensuring role of entrained low-frequency oscillations for auditory perception. *J Neurosci* 32(35):12268–12276.
- Nolte, G. (2003). The magnetic lead field theorem in the quasi-static approximation and its use for magnetoencephalography forward calculation in realistic volume conductors. *Phys Med Biol* 48(22):3637.
- O'Connell, R.G., Dockree, P.M., and Kelly, S.P. (2012). A supramodal accumulation-to-bound signal that determines perceptual decisions in humans. *Nat Neurosci* 15(12):1729–1735.
- Oeltzschner, G., Butz, M., Baumgarten, T.J., Hoogenboom, N., Wittsack, H.J., and Schnitzler, A. (2015). Low visual cortex GABA levels in hepatic encephalopathy: links to blood ammonia, critical flicker frequency, and brain osmolytes. *Metab Brain Dis* 30(6):1429–1438.
- Pesaran, B., Nelson, M.J., and Andersen, R.A. (2008). Free choice activates a decision circuit between frontal and parietal cortex. *Nature* 453(7193):406–409.
- Pfurtscheller, G., and Aranibar, A. (1977). Event-related cortical desynchronization detected by power measurements of scalp EEG. *Electroencephalogr Clin Neurophysiol* 42(6):817–826.
- Pfurtscheller, G., and Lopes da Silva, F.H. (1999). Event-related EEG/MEG synchronization and desynchronization: basic principles. *Clin Neurophysiol* 110(11):1842–1857.
- Pfurtscheller, G., Stancák, A., Jr., and Neuper, C. (1996a). Event-related synchronization (ERS) in the alpha band — an electrophysiological correlate of cortical idling: A review. *Int J Psychophysiol* 24(1–2):39–46.
- Pfurtscheller, G., Stancák, A., Jr., and Neuper, C. (1996b). Post-movement beta synchronization. A correlate of an idling motor area? *Electroencephalogr Clin Neurophysiol* 98(4):281–293.
- Philiastides, M.G., Ratcliff, R., and Sajda, P. (2006). Neural representation of task difficulty and decision making during perceptual categorization: A timing diagram. *J Neurosci* 26(35):8965–8975.
- Pikovsky, A., Rosenblum, M., and Kurths, J. (2001). Synchronization. A universal concept in nonlinear sciences. Cambridge: Cambridge Univ Press.
- Puts, N.A.J., and Edden, R.A.E. (2012). In vivo magnetic resonance spectroscopy of GABA: A methodological review. *Prog Nucl Magn Reson Spectrosc* 60:29–41.
- Puts, N.A.J., Edden, R.A.E., Evans, C.J., McGlone, F., and McGonigle, D.J. (2011). Regionally specific human GABA concentration correlates with tactile discrimination thresholds. *J Neurosci* 31(46):16556–16560.
- Raichle, M.E. (2010). Two views of brain function. *Trends Cogn Sci* 14(4):180–190.
- Ratcliff, R., and McKoon, G. (2008). The diffusion decision model: Theory and data for two-choice decision tasks. *Neural Comput* 20(4):873–922.
- Reite, M., and Zimmerman, J. (1978). Magnetic phenomena of the central nervous system. *Annu Rev Biophys Bioeng* 7(1):167–188.

- Romei, V., Brodbeck, V., Michel, C., Amedi, A., Pascual-Leone, A., and Thut, G. (2008a). Spontaneous fluctuations in posterior Alpha-band EEG activity reflect variability in excitability of human visual areas. *Cereb Cortex* 18(9):2010–2018.
- Romei, V., Gross, J., and Thut, G. (2010). On the role of prestimulus Alpha rhythms over occipitoparietal areas in visual input regulation: Correlation or causation? *J Neurosci* 30(25):8692–8697.
- Romei, V., Gross, J., and Thut, G. (2012). Sounds reset rhythms of visual cortex and corresponding human visual perception. *Curr Biol* 22(9):807–813.
- Romei, V., Rihs, T., Brodbeck, V., and Thut, G. (2008b). Resting electroencephalogram alpha-power over posterior sites indexes baseline visual cortex excitability. *Neuroreport* 19(2):203–208.
- Roopun, A.K., Middleton, S.J., Cunningham, M.O., LeBeau, F.E.N., Bibbig, A., Whittington, M.A., and Traub, R.D. (2006). A beta2-frequency (20–30 Hz) oscillation in nonsynaptic networks of somatosensory cortex. *Proc Natl Acad Sci U S A* 103(42):15646–15650.
- Rossiter, H.E., Worthen, S.F., Witton, C., Hall, S.D., and Furlong, P.L. (2013). Gamma oscillatory amplitude encodes stimulus intensity in primary somatosensory cortex. *Front Hum Neurosci* 7:362.
- Salmelin, R., and Hari, R. (1994). Spatiotemporal characteristics of sensorimotor neuromagnetic rhythms related to thumb movement. *Neuroscience* 60(2):537–550.
- Schnitzler, A., Gross, J., and Timmermann, L. (2000). Synchronised oscillations of the human sensorimotor cortex. *Acta Neurobiol Exp (Wars)* 60(2):271–287.
- Schnitzler, A., Salenius, S., Salmelin, R., Jousmäki, V., and Hari, R. (1997). Involvement of primary motor cortex in motor imagery: A neuromagnetic study. *NeuroImage* 6(3):201–208.
- Schoffelen, J.M., and Gross, J. (2009). Source connectivity analysis with MEG and EEG. *Hum Brain Mapp* 30(6):1857–1865.
- Siegel, M., Donner, T.H., and Engel, A.K. (2012). Spectral fingerprints of large-scale neuronal interactions. *Nat Rev Neurosci* 13(2):121–134.
- Siegel, M., Warden, M.R., and Miller, E.K. (2009). Phase-dependent neuronal coding of objects in short-term memory. *Proc Natl Acad Sci U S A* 106(50):21341–21346.
- Singer, W. (1999). Neuronal synchrony: A versatile code for the definition of relations? *Neuron* 24(1):49–65.
- Singer, W. (2013). Cortical dynamics revisited. *Trends Cogn Sci* 17(12):616–626.
- Smith, M.L., Gosselin, F., and Schyns, P.G. (2006). Perceptual moments of conscious visual experience inferred from oscillatory brain activity. *Proc Natl Acad Sci U S A* 103(14):5626–5631.
- Snyder, A.Z. (1992). Steady-state vibration evoked potentials: description of technique and characterization of responses. *Electroencephalogr Clin Neurophysiol* 84(3):257–268.

- Sörös, P., Knecht, S., Imai, T., Gürtler, S., Lütkenhöner, B., Ringelstein, E., and Henningsen, H. (1999). Cortical asymmetries of the human somatosensory hand representation in right- and left-handers. *Neurosci Letters* 271(2):89–92.
- Spinks, R.L., Kraskov, A., Brochier, T., Umiltà, M.A., and Lemon, R.N. (2008). Selectivity for grasp in local field potential and single neuron activity recorded simultaneously from M1 and F5 in the awake macaque monkey. *J Neurosci* 28(43):10961–10971.
- Stroud, J.M. (1956). The fine structure of psychological time. In: Information theory in psychology (Editor: Quastler, H.), 174–205. Chicago: Free Press.
- Thut, G., Miniussi, C., and Gross, J. (2012). The functional importance of rhythmic activity in the brain. *Curr Biol* 22(16):R658-R663.
- Thut, G., Nietzel, A., Brandt, S.A., and Pascual-Leone, A. (2006). α -band electroencephalographic activity over occipital cortex indexes visuospatial attention bias and predicts visual target detection. *J Neurosci* 26(37):9494–9502.
- Tobimatsu, S., Zhang, Y.M., and Kato, M. (1999). Steady-state vibration somatosensory evoked potentials: physiological characteristics and tuning function. *Clin Neurophysiol* 110(11):1953–1958.
- Triggs, W.J., Subramaniam, B., and Rossi, F. (1999). Hand preference and transcranial magnetic stimulation asymmetry of cortical motor representation. *Brain Res* 835(2):324–329.
- Tsai, P.H., and Mendez, M.F. (2009). Akinetopsia in the posterior cortical variant of Alzheimer disease. *Neurology* 73(9):731–732.
- Uhlhaas, P., Pipa, G., Lima, B., Melloni, L., Neuenschwander, S., Nikolic, D., and Singer, W. (2009). Neural synchrony in cortical networks: history, concept and current status. *Front Integr Neurosci* 3. 10.3389/neuro.07.017.2009
- van Dijk, H., Schoffelen, J.M., Oostenveld, R., and Jensen, O. (2008). Prestimulus oscillatory activity in the alpha band predicts visual discrimination ability. *J Neurosci* 28(8):1816–1823.
- van Ede, F., de Lange, F., Jensen, O., and Maris, E. (2011). Orienting attention to an upcoming tactile event involves a spatially and temporally specific modulation of sensorimotor Alpha- and Beta-band oscillations. *J Neurosci* 31(6):2016–2024.
- van Veen, B.D., van Drongelen, W., Yuchtman, M., and Suzuki, A. (1997). Localization of brain electrical activity via linearly constrained minimum variance spatial filtering. *IEEE Trans Biomed Eng* 44(9):867–880.
- VanRullen, R., Busch, N.A., Drewes, J., and Dubois, J. (2011). Ongoing EEG phase as a trial-by-trial predictor of perceptual and attentional variability. *Front Psychol* 2:60. 10.3389/fpsyg.2011.00060
- VanRullen, R., and Koch, C. (2003). Is perception discrete or continuous? *Trends Cogn Sci* 7(5):207–213.
- VanRullen, R., and Thorpe, S.J. (2001). The time course of visual processing: From early perception to decision-making. *J Cogn Neurosci* 13(4):454–461.

- VanRullen, R., Zoefel, B., and Ilhan, B. (2014). On the cyclic nature of perception in vision versus audition. *Philos Trans R Soc Lond B Biol Sci* 369(1641):20130214.
- Varela, F., Lachaux, J.P., Rodriguez, E., and Martinerie, J. (2001). The brainweb: Phase synchronization and large-scale integration. *Nat Rev Neurosci* 2(4):229–239.
- Varela, F.J., Toro, A., Roy John, E., and Schwartz, E.L. (1981). Perceptual framing and cortical alpha rhythm. *Neuropsychologia* 19(5):675–686.
- Volkman, J., Schnitzler, A., Witte, O.W., and Freund, H.J. (1998). Handedness and asymmetry of hand representation in human motor cortex. *J Neurophysiol* 79(4):2149–2154.
- Vrba, J., and Robinson, S.E. (2001). Signal processing in magnetoencephalography. *Methods* 25(2):249–271.
- Wang, X.J. (2010). Neurophysiological and computational principles of cortical rhythms in cognition. *Physiol Rev* 90(3):1195–1268.
- Weisz, N., Wühle, A., Monittola, G., Demarchi, G., Frey, J., Popov, T., and Braun, C. (2014). Prestimulus oscillatory power and connectivity patterns predispose conscious somatosensory perception. *Proc Natl Acad Sci U S A* 111(4):E417-E425.
- Wheaton, L., Fridman, E., Bohlhalter, S., Vorbach, S., and Hallett, M. (2009). Left parietal activation related to planning, executing and suppressing praxis hand movements. *Clin Neurophysiol* 120(5):980–986.
- Whittington, M.A., Traub, R.D., Kopell, N., Ermentrout, B., and Buhl, E.H. (2000a). Inhibition-based rhythms: experimental and mathematical observations on network dynamics. *Int J Psychophysiol* 38(3):315–336.
- Whittington, M.A., Faulkner, H.J., Doheny, H.C., and Traub, R.D. (2000b). Neuronal fast oscillations as a target site for psychoactive drugs. *Pharmacol Ther* 86(2):171–190.
- Womelsdorf, T., and Fries, P. (2007). The role of neuronal synchronization in selective attention. *Curr Opin Neurobiol* 17(2):154–160.
- Wyart, V., and Tallon-Baudry, C. (2009). How ongoing fluctuations in human visual cortex predict perceptual awareness: Baseline shift versus decision bias. *J Neurosci* 29(27):8715–8725.
- Yamawaki, N., Stanford, I.M., Hall, S.D., and Woodhall, G.L. (2008). Pharmacologically induced and stimulus evoked rhythmic neuronal oscillatory activity in the primary motor cortex in vitro. *Neuroscience* 151(2):386–395.
- Yuste, R. (2015). From the neuron doctrine to neural networks. *Nat Rev Neurosci* 16(8):487–497.
- Zaehle, T., Rach, S. and Herrmann, C.S. (2010). Transcranial alternating current stimulation enhances individual Alpha activity in human EEG. *PLoS ONE* 5(11):e13766.
- Zhang, Y., Chen, Y., Bressler, S.L., and Ding, M. (2008). Response preparation and inhibition: The role of the cortical sensorimotor beta rhythm. *Neuroscience* 156(1):238–246.
- Zhang, Y., and Ding, M. (2010). Detection of a weak somatosensory stimulus: Role of the prestimulus Mu rhythm and its top-down modulation. *J Cogn Neurosci* 22(2):307–322.

Zimmerman, J.E., Thiene, P., and Harding, J.T. (1970). Design and operation of stable rf-biased superconducting point-contact quantum devices, and a note on the properties of perfectly clean metal contacts. *J Appl Phys* 41(4):1572–1580.

9 Erklärung

Ich versichere an Eides Statt, dass die Dissertation von mir selbständig und ohne unzulässige fremde Hilfe unter Beachtung der „Grundsätze zur Sicherung guter wissenschaftlicher Praxis an der Heinrich-Heine-Universität Düsseldorf“ erstellt worden ist. Die Dissertation wurde in der vorliegenden oder in ähnlicher Form noch bei keiner anderen Institution eingereicht. Ich habe bisher keine erfolglosen Promotionsversuche unternommen.

Düsseldorf, den

Thomas J. Baumgarten

10 Danksagung

Zunächst möchte ich mich bei meinem Doktorvater Herrn Prof. Dr. Alfons Schnitzler für die Möglichkeit bedanken, meine Promotion an Ihrem Institut durchführen zu können. Vielen Dank für die anhaltende Unterstützung und kontinuierliche Förderung, welche ich an Ihrem Institut erfahren habe.

Weiterhin möchte ich mich herzlich bei Frau Prof. Dr. Petra Stoerig für die Zweitbetreuung der vorliegenden Doktorarbeit bedanken. Darüber hinaus auch ein großes Dankeschön für die wertvollen und prägenden Erfahrungen, die ich während meiner Studienzeit in Ihren Vorlesungen und Seminaren sammeln konnte und denen mein Interesse an den Neurowissenschaften maßgeblich zu verdanken ist.

Ein allgemeines Dankeschön möchte ich an das gesamte Institut für Klinische Neurowissenschaften und Medizinische Psychologie der Heinrich-Heine-Universität Düsseldorf aussprechen. Die Herzlichkeit und der ausgesprochen positive gemeinsame Umgang welchen ich hier erfahren habe, haben meine Zeit in diesem Institut sehr bereichert.

Besonders erwähnt sei an dieser Stelle noch Herr Dr. David Petri. Schön, dass wir nach dem Studium die Promotion noch gemeinsam gewagt haben. Auch Herrn Dr. Georg Oeltzschner sei herzlich für eine produktive Zusammenarbeit im Rahmen des SFB974 gedankt, welche wir erfolgreich auf der OHBM2015 unter Beweis stellen konnten. David, Schorsch, es freut mich zu sehen, dass das Humboldtsche Bildungsideal noch gelebt wird! Herrn Dr. Markus Butz möchte ich für seinen wertvollen Rat, seine Zeit und seinen nicht zu trübenden Frohsinn und Enthusiasmus danken (Du zeigst uns, dass Düsseldorf immer noch im Rheinland liegt). Frau Prof. Dr. Pollok sei zudem für ihre Hilfe bei meinem Einstieg in die Lehrtätigkeit gedankt, wovon ich sehr profitiert habe.

Weiterhin ein großer Dank an alle Versuchspersonen, welche sich die Zeit genommen haben bei meinen Experimenten teilzunehmen. Ohne Euch wäre dies alles nicht möglich gewesen.

Im Sinne der Listenkonformität möchte ich ein besonderes Dankeschön an meine Kolleginnen Frau Dr. Ariane Keitel und Frau Dr. Anne Klepp aus dem großartigen Room 41 richten. Vielen Dank für Eure ungebrochene fachliche Unterstützung, kleinen und großen Alltagshilfen und dafür, dass in unserem Büro immer die Menschlichkeit die Oberhand behalten hat. Am meisten allerdings, danke für Eure Geduld! Lasst uns hoffen, dass die Bildungslücke in Room 41 bald geschlossen wird. Ihr seid maßgeblich daran beteiligt, dass ich (fast) jeden Tag gerne zur Arbeit gehe. Weiterhin auch ein großes Dankeschön an meine frühere Kollegin Frau Dr. Claudia Wach.

Bezüglich meines Arbeitsgruppenleiters und Mentors Herrn Dr. Joachim Lange weiß ich gar nicht, wo ich anfangen soll mich zu bedanken. Danke, dass Du mir so viel über so vieles beigebracht hast. Danke für Deine Geduld, Deine kontinuierliche Unterstützung und Deine stete Erreichbarkeit. Auch wenn ich das (glücklicherweise) während meiner Promotion nie anders kennengelernt habe, weiß ich doch, dass dies nicht selbstverständlich ist. In diesem Sinne: „Es gibt keine Probleme, sondern nur Herausforderungen!“

Abschließend möchte ich meiner Familie danken. Ein besonderer Dank für anhaltende außerfachliche Unterstützung und Präsenz geht dabei an meinen Bruder. Und an meine Eltern, einen tiefen Dank dafür, dass Ihr mir die besten Voraussetzungen und das bedingungslose Vertrauen geschenkt habt, ohne welche ich das alles niemals geschafft hätte.

11 Appendix

The present work is based on:

Appendix 1:

Baumgarten, T.J., Schnitzler, A., and Lange, J. (2014). Prestimulus alpha power influences tactile temporal perceptual discrimination and confidence in decisions. *Cerebral Cortex*. [Epub ahead of print]. DOI: 10.1093/cercor/bhu247.

Impact factor (2014): 8.665

Personal contribution: 80% (data acquisition, data analysis, data interpretation, manuscript writing, manuscript revision)

Appendix 2:

Baumgarten, T.J., Schnitzler, A., and Lange, J. (2015). Beta oscillations define discrete perceptual cycles in the somatosensory domain. *Proceedings of the National Academy of Sciences of the United States of America*. 112(39): 12187-12192.

Impact factor (2014): 9.674

Personal contribution: 80% (data acquisition, data analysis, data interpretation, manuscript writing, manuscript revision)

Appendix 3:

Baumgarten, T.J., Oeltzschner, G., Hoogenboom, N., Wittsack, H.J., Schnitzler, A., and Lange J. Beta peak frequencies at rest correlate with endogenous GABA/Cr concentrations in the left sensorimotor cortex.

Submitted to PLoS One

Personal contribution: 70% (MEG data acquisition, data analysis, data interpretation, manuscript writing)

Other aspects are taken from:

Oeltzschner, G., Butz, M., Baumgarten, T.J., Hoogenboom, N., Wittsack, H.J., and Schnitzler, A. (2015). Low visual cortex GABA levels in hepatic encephalopathy: links to blood ammonia, critical flicker frequency, and brain osmolytes. *Metabolic Brain Disease*. 30(6):1429–1438

ORIGINAL ARTICLE

Prestimulus Alpha Power Influences Tactile Temporal Perceptual Discrimination and Confidence in Decisions

Thomas J. Baumgarten, Alfons Schnitzler, and Joachim Lange

Institute of Clinical Neuroscience and Medical Psychology, Medical Faculty, Heinrich-Heine-University Düsseldorf, 40225 Düsseldorf, Germany

Address correspondence to Thomas J. Baumgarten, Institute of Clinical Neuroscience and Medical Psychology, Medical Faculty, Heinrich-Heine-University Düsseldorf, 40225 Düsseldorf, Germany. Email: thomas.baumgarten@med.uni-duesseldorf.de

Abstract

Recent studies have demonstrated that prestimulus alpha-band activity substantially influences perception of near-threshold stimuli. Here, we studied the influence of prestimulus alpha power fluctuations on temporal perceptual discrimination of suprathreshold tactile stimuli and subjects' confidence regarding their perceptual decisions. We investigated how prestimulus alpha-band power influences poststimulus decision-making variables. We presented electrical stimuli with different stimulus onset asynchronies (SOAs) to human subjects, and determined the SOA for which temporal perceptual discrimination varied on a trial-by-trial basis between perceiving 1 or 2 stimuli, prior to recording brain activity with magnetoencephalography. We found that low prestimulus alpha power in contralateral somatosensory and occipital areas predicts the veridical temporal perceptual discrimination of 2 stimuli. Additionally, prestimulus alpha power was negatively correlated with confidence ratings in correctly perceived trials, but positively correlated for incorrectly perceived trials. Finally, poststimulus event-related fields (ERFs) were modulated by prestimulus alpha power and reflect the result of a decisional process rather than physical stimulus parameters around ~150 ms. These findings provide new insights into the link between spontaneous prestimulus alpha power fluctuations, temporal perceptual discrimination, decision making, and decisional confidence. The results suggest that prestimulus alpha power modulates perception and decisions on a continuous scale, as reflected in confidence ratings.

Key words: alpha oscillations, MEG, perceptual decision making, prestimulus fluctuations, tactile stimulation

Introduction

Decision making can be understood as a process in which sensory evidence is accumulated in a decision variable. If sensory evidence is sufficiently strong and available for a sufficiently long time, the decision variable accumulates until a decision bound for either decision is reached (see [Gold and Shadlen 2007](#) for a review). In some situations, however, sensory evidence is ambiguous, providing equal sensory evidence for each decisional option. In other situations, sensory evidence is weak or presented insufficiently long for the decision variable to reach a decision bound. Consequently, decisions have to be made based on incomplete or equivocal sensory evidence, frequently causing incorrect decisions and low confidence in the decision. In addition, decision making is not only determined by sensory evidence,

but also by trial-to-trial fluctuations of neuronal activity, usually interpreted as internal noise ([Ratcliff and McKoon 2007](#); [O'Connell et al. 2012](#)).

Recent studies, however, demonstrated that fluctuations of neuronal activity can have a functional role for the perception of weak and ambiguous stimuli. Specifically neuronal oscillatory activity in the alpha band (~8–12 Hz) has drawn much attention. Prestimulus alpha power is modulated by attention (e.g., [Foxe et al. 1998](#); [Worden et al. 2000](#)) and prestimulus power and phase in early sensory areas are correlated with perception ([Linkenkaer-Hansen et al. 2004](#); [van Dijk et al. 2008](#); [Mazaheri et al. 2009](#); [Wyart and Tallon-Baudry 2009](#); [Jensen and Mazaheri 2010](#); [Romei et al. 2010](#); [Keil et al. 2014](#)). Furthermore, it has been shown that prestimulus oscillatory activity can influence

poststimulus evoked responses (Başar et al. 1984; Brandt and Jansen 1991; Mazaheri and Jensen 2008; Jones et al. 2009, 2010; Anderson and Ding 2011; Lange et al. 2012). The influence of prestimulus oscillatory activity on decision variables remains largely unknown. In addition, the influence of prestimulus oscillatory activity on subjective confidence in perceptual decisions is unknown. Subjective confidence represents a measure of the degree to which a decision maker believes in the correctness of his decisions and thus provides an insight into decisional processes on a fine-grained scale (Kiani and Shadlen 2009). Moreover, it remains unexplained how the brain forms decisions when sensory evidence is insufficient to reach a decision bound, for example, due to sensory ambiguity.

To test how prestimulus alpha-band power biases perceptual decisions and the underlying neuronal decision variable in humans, we presented electrical stimuli with different stimulus onset asynchronies (SOAs) and compared 2 subjectively ambiguous experimental conditions in which physically identical tactile stimuli were perceived differently on a trial-by-trial basis. We used magnetoencephalography (MEG) and a forced-choice temporal perceptual discrimination task to investigate whether fluctuations of prestimulus neuronal oscillatory activity are related to the trial-to-trial variability of decisions and how prestimulus oscillatory activity influences the decision variable. We hypothesized that prestimulus alpha power correlates with temporal perceptual discrimination rate, with lower alpha power levels related to increased veridical temporal perceptual discrimination. Further, we expected that characteristics of the decision-making process would be evident in neural activity in the form of poststimulus event-related fields (ERFs). This should result in differences of neuronal activity for trials with different decisional outcomes, despite identical physical stimulation. Additionally, we hypothesized that prestimulus alpha power would influence this decision-related neuronal activity.

Materials and Methods

Subjects

Sixteen, right-handed subjects (7 males, age: 26.1 ± 4.7 years [mean \pm SD]) participated in the study after providing written informed consent in accordance with the Declaration of Helsinki. All participants had normal or corrected-to-normal vision and

reported no somatosensory deficits or known history of neurological disorders.

Experimental Design and Paradigm

The experimental task was designed to compare 2 conditions with identical physical stimuli, differing only in the participant's perception. Each trial started with the presentation of a start cue (500 ms; Fig. 1). Next, the cue decreased in luminance, indicating the prestimulus period (900–1100 ms), after which the subjects received either 1 or 2 short (0.3 ms) electrical pulses, applied by 2 electrodes placed between the 2 distal joints of the left index finger. The amplitude of the pulses was determined individually to a level clearly above subjective perception threshold, but below pain threshold (4.1 ± 1.2 mA [mean \pm SD]). Note that all comparisons of conditions were performed at the within-subject level. Therefore, only conditions with identical stimulation parameters were compared (for details, see MEG Data Acquisition and Analysis). The electrical pulses were applied with varying SOAs: short (0 ms, i.e., only one stimulus was applied), long (100 ms), and 3 SOAs individually determined in a premeasurement. These 3 individual SOAs included a SOA for which subjects reported to perceive one electrical pulse in $\sim 50\%$ of the trials, whereas in the other $\sim 50\%$ of the trials 2 pulses were perceived (SOA: 25.9 ± 1.9 ms (mean \pm standard error of the mean [SEM])). Subsequently, this condition will be labeled the intermediate SOA. The remaining 2 SOAs encompassed the intermediate SOA by ± 10 ms and were included to minimize learning effects and response biases. A training phase of ~ 5 min containing all possible SOAs preceded the experiment to familiarize subjects with the paradigm. The electrical stimulation was followed by a jittered poststimulus period of 500–1200 ms to minimize motor preparation effects, during which the fixation dot remained visible. Next, a written instruction indicated the start of the first response window. Subjects first reported whether they perceived the stimulation as 1 single or 2 temporally separate sensations. Responses were given by button-presses with the index or middle finger of the right hand, while button configurations were randomized from trial to trial to minimize motor preparation effects. Subjects were instructed to report within 3000 ms after presentation of response instructions. Due to the jittered poststimulus epoch (500–1200 ms) which determined the beginning of the subsequent response window, response speed was not taken into

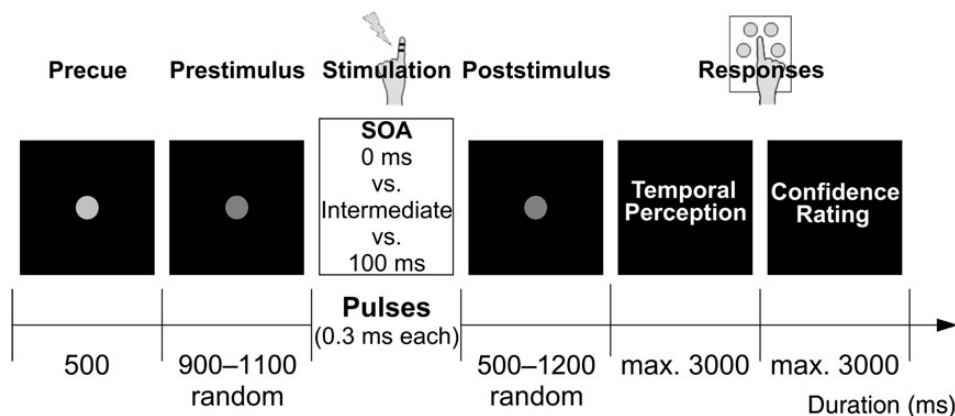


Figure 1. Experimental task. Sequence of events: A central fixation dot serves as start cue, after 500 ms a decrease in luminance signals the start of the prestimulus epoch, consisting of a jittered period of 900–1100 ms. Tactile stimulation is applied to the left index finger with varying SOAs (0 ms, intermediate – 10 ms, intermediate, intermediate + 10 ms, 100 ms). After a jittered poststimulus period (500–1200 ms), written instructions indicate the first response window and subjects report their perception of the stimulation by button-press. Subsequently, written instructions indicate the second response window and subjects report their decisional confidence by button-press.

account. If no response was given after 3000 ms or the subject responded before the presentation of the instructions, a warning was presented visually. The respective trial was discarded from analysis and repeated at the end of the block. After reporting their subjective perception, written instructions indicated a second response window. Here, subjects rated their subjective confidence level regarding their first response. The confidence level was assessed via a 4-point rating scale, ranging from “very sure” to “very unsure.” Once both responses were given, the next trial started. With the exception of the aforementioned warning signal, no further feedback was given. All visual stimuli were projected on the backside of a translucent screen (60 Hz refresh rate) positioned 60 cm in front of the subjects.

Each SOA was presented in 50 trials. To increase statistical power, the intermediate SOA was presented 4 times as often as the other SOAs (i.e., 200 trials). 80 trials constituted one block with each block containing 10 repetitions (40 for the intermediate condition) of each SOA presented in pseudorandom order. Blocks were repeated 5 times, interrupted by self-paced breaks of ~2 min, resulting in an overall 400 trials. The approximate total duration of the MEG measurement was ~45–50 min (400 trials with a trial length of ~6 s on average [4–8.6 s], interrupted by up to 4 self-paced breaks of ~2 min).

Stimulus presentation was controlled using Presentation software (Neurobehavioral Systems, Albany, NY, USA). Before MEG recording, each subject received instructions of the task but remained naïve to the purpose of the experiment and the different SOAs used.

Behavioral Data Analysis

Behavioral data were analyzed with regard to correct responses and compared across conditions by means of a paired sample *t*-test. Prior to this, a Kolmogorov–Smirnov test was applied to ensure that the respective distributions did not differ from a Gaussian distribution. Further, we investigated learning/fatigue trends in the perceptual responses and confidence ratings by dividing experimental trials in 12 bins and computing the average temporal perceptual discrimination rate (i.e., perceived 2 stimuli or 1 stimulus) as well as the average confidence rating over subjects for each bin. Subsequently, we fitted a linear regression to the data in order to determine a linear trend.

MEG Data Acquisition and Analysis

Data Recording and Preprocessing

Ongoing neuromagnetic brain activity was continuously recorded at a sampling rate of 1000 Hz using a 306-channel whole head MEG system (Neuromag Elekta Oy, Helsinki, Finland), including 204 planar gradiometers (102 pairs of orthogonal gradiometers) and 102 magnetometers. Data analysis in the present study was restricted to the planar gradiometers. Additionally, electro-oculograms were recorded for offline artifact rejection by applying electrodes above and below the left eye as well as on the outer sides of each eye. Subjects' head position within the MEG helmet was registered by a head position indication system (HPI) built up of 4 coils placed at subjects' forehead and behind both ears. A 3-T MRI scanner (Siemens, Erlangen, Germany) was used to obtain individual full-brain high-resolution standard T_1 -weighted structural magnetic resonance images (MRIs). The MRIs were offline aligned with the MEG coordinate system using the HPI coils and anatomical landmarks (nasion, left and right preauricular points).

Data were offline analyzed using custom-made Matlab (The Mathworks, Natick, MA, USA) scripts, the Matlab-based open source toolbox FieldTrip (<http://fieldtrip.fcdonders.nl>; Oostenveld et al. 2011), and SPM8 (Litvak et al. 2011). Continuously recorded data were segmented into trials, starting with the appearance of the first fixation dot and ending with the second response of the subject. All trials were semiautomatically and visually inspected for artifacts, whereas artifacts caused by muscle activity, eye movements, or SQUID jumps were removed semiautomatically using a *z*-score-based algorithm implemented in FieldTrip. Excessively noisy channels were removed as well and reconstructed by an interpolation of neighboring channels. In addition, power line noise was removed from the segmented data by using a band-stop filter encompassing the 50, 100, and 150 Hz components. Further preprocessing steps were applied according to the respective analyses.

Time–Frequency Analysis

For exploratory reasons, we first performed a time–frequency analysis on all frequencies between 2 and 40 Hz for all time points (–900 to 500 ms, Fig. 2A). We focused our analysis on the effects of alpha power (8–12 Hz) in the prestimulus epoch (–900 to 0 ms) on perceptual decisions, that is, the responses to the

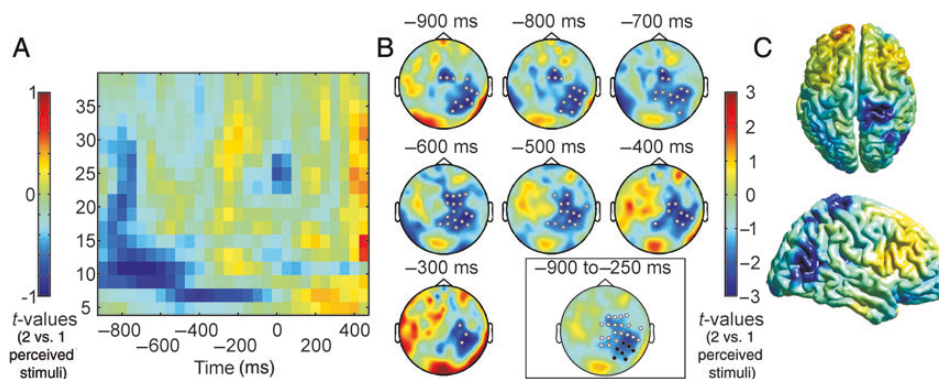


Figure 2. Results of the statistical comparison of correctly (perceived 2 stimuli) versus incorrectly (perceived 1 stimulus) perceived trials with intermediate SOA. (A) Time–frequency representation on sensor level averaged over all sensors. $t = 0$ indicates onset of sensory stimulation. (B) Time series of topographical representations on sensor level averaged over the alpha band (8–12 Hz). Significant sensors ($P < 0.05$) are marked by white circles. The lower right inset illustrates alpha power differences averaged across the whole time window (–900 to –250 ms; white dots represent channels of the anterior/somatosensory sensor-cluster; black crosses represent channels of the parieto-occipital sensor-cluster used for following analyses. See text for details on the separation of the clusters). (C) Source reconstruction projected on the MNI template brain for the significant effect in the alpha band (see B) viewed from the top (top row) and the right (bottom row). Source plots are masked to highlight significant clusters ($P < 0.05$). *P*-values in B and C are cluster corrected to account for multiple comparison corrections. The left color bar applies to A, the right color bar applies to B and C. For both color bars, blue colors indicate lower spectral power in correctly perceived trials compared with incorrectly perceived trials.

temporal perceptual discrimination task. First, the linear trend and mean of every epoch were removed from each trial. Time-frequency representations for each trial were computed by applying a Fourier transformation on adaptive sliding time windows containing 7 full cycles of the respective frequency f ($\Delta t = 7/f$), moved in steps of 50 ms and 2 Hz (van Dijk et al. 2008; Mazaheri et al. 2009; Lange et al. 2012). Data segments were tapered with a single Hanning taper, resulting in a spectral smoothing of $1/\Delta t$. Spectral power was averaged over the alpha band separately for each trial. Alpha power was estimated independently for each of the 204 gradiometers. Subsequently, gradiometer pairs were combined by summing spectral power across the 2 orthogonal channels, resulting in 102 pairs of gradiometers. We sorted the trials with respect to the SOA for each subject separately. For all trials with intermediate SOA, we separated and compared trials with reports of 1 perceived stimulus to trials with 2 perceived stimuli. With this approach, we were able to compare 2 sets of decisional outcomes, which differed only in the subjects' temporal perceptual discrimination of the stimuli, though not regarding their physical properties. Due to the fact that, only for the intermediate condition, a sufficiently high number of trials for both decisional outcomes (perceived 1 stimulus or 2 stimuli) were available, only trials with intermediate SOA entered the analysis. In the following, trials in which stimulation was perceived as 2 temporally separate stimuli will be labeled correctly perceived trials, whereas trials in which stimulation was perceived as 1 single stimulus will be labeled incorrectly perceived trials. To test for statistically significant power differences between sets, we used a cluster-based nonparametric randomization approach (Maris and Oostenveld 2007). In a first step, we compared averaged alpha power between both sets of decisional outcomes (correct and incorrect, i.e., perceived 2 stimuli or 1 stimulus) for each subject independently in all channels and all time points in the prestimulus time window (-900 to 0 ms). Comparison between sets was performed by subtracting the power of both sets and dividing the difference by the variance (equivalent to an independent sample t -test). This step serves as a normalization of interindividual differences (Hoogenboom et al. 2010; Lange et al. 2011, 2013). The comparison was done independently for each time sample and channel, resulting in a time-channel map of pseudo- t -values for each subject. For group-level statistics, we analyzed the consistency of pseudo- t -values over subjects by means of a nonparametric randomization test identifying clusters in time-channel space showing the same effect. Neighboring channels were defined on the basis of spatial adjacency, with spatial clusters requiring a minimum amount of 2 neighboring channels. Spatially and temporally adjacent pseudo- t -values exceeding an a priori-defined threshold ($P < 0.05$) were combined to a cluster. t -values within a cluster were summed up and used as input for the second-level cluster statistic. Next, we computed a reference distribution by randomly permuting the data, assuming no differences between statistical conditions and exchangeability of the data. This process of random assignment was repeated 1000 times, resulting in a summed cluster t -value for each repetition. The proportion of elements in the reference distribution exceeding the observed maximum cluster-level test statistic was used to estimate a P -value for each cluster. This statistical approach effectively controls for the Type I error rate due to multiple comparisons across time points and channels (Maris and Oostenveld 2007).

Source Reconstruction

To identify the cortical sources of the statistically significant effects displayed on sensor level, we calculated source-level

power estimates by means of an adaptive spatial filtering technique (DICS, Gross et al. 2001). To this end, a regular 3D grid with 1 cm resolution was applied to the Montreal Neurological Institute (MNI) template brain. Individual grids for each subject were computed by linearly warping the structural MRI of each subject onto the MNI template brain and applying the inverse of the warp to the MNI template grid. For one subject, no individual structural MRI was available; hence, we used the MNI template brain instead. A lead-field matrix was computed for each grid point employing a realistically shaped single-shell volume conduction model (Nolte 2003). Subsequently, the cross-spectral density (CSD) matrix between all MEG gradiometer sensor pairs was computed for the alpha band by applying a Fourier transformation on time windows of interest. Time windows of interest were based on the significant clusters of the group analysis on sensor level (Fig. 2B). Using the CSD and lead-field matrix, common spatial filters were constructed for each individual grid point. To this end, we pooled trials with intermediate SOA over both sets of decisional outcomes and computed a common spatial filter for each subject. CSD matrices of single trials were projected through those filters, resulting in single-trial estimates of source power (Hoogenboom et al. 2010; Lange et al. 2012), and further sorted according to decisional outcome. In line with the analysis on sensor level, power was contrasted between both sets of decisional outcomes. Similarly to the sensor-level analysis, the resulting individual source parameters were statistically compared across subjects by means of a nonparametric randomization test (Maris and Oostenveld 2007) which effectively controls for the Type I error rate. Group results were displayed on the MNI template brain in form of t -values. Finally, cortical sources were identified using the AFNI atlas (<http://afni.nimh.nih.gov/afni>), integrated into FieldTrip.

Since the time-frequency analysis and the source reconstruction demonstrated 2 spatiotemporally different activation clusters (see Results and Fig. 2B,C), we performed the subsequent analyses on 2 different sensor sets. First, we based the analyses on all channels showing a significant alpha power difference between correctly (perceived 2 stimuli) versus incorrectly (perceived 1 stimulus) perceived trials with intermediate SOA (as shown in Fig. 2B). Second, we based the analyses on 2 spatiotemporally separated sensor-clusters (see inset in Fig. 2B), 1 anterior/somatosensory sensor-cluster (MEG-sensors: MEG0712 + 13, MEG0722 + 23, MEG1042 + 43, MEG1112 + 13, MEG1122 + 23, MEG1132 + 33, MEG1142 + 43, MEG1312 + 13, MEG1342 + 43, MEG1832 + 33, MEG2012 + 13, MEG2022 + 23, MEG2212 + 13, MEG2222 + 23, MEG2232 + 33, MEG2242 + 43, MEG2412 + 13, MEG2422 + 23, MEG2612 + 13, MEG2642 + 43), and 1 parieto-occipital sensor-cluster (MEG-sensors: MEG2312 + 13, MEG2322 + 23, MEG2342 + 43, MEG2432 + 33, MEG2442 + 43, MEG2512 + 13, MEG2522 + 23).

Correlation of Prestimulus Power, Perceptual Decisions, and Confidence Ratings

To examine the relationship between prestimulus power and perceptual decisions, we averaged spectral power over time, frequency, and sensors and correlated averaged power values with perceptual decisions. To this end, we selected the sensors and time points showing a significant difference between decisional outcomes (see above, Fig. 2B). Note that this approach resembles a post hoc statistical analysis in the sense that sensor selection was based on those sensors showing a significant difference in the alpha band (see above, Fig. 2B). Averaging was done separately for each subject and trial, using a fixed time-frequency-sensor triplet resulting from the significant time-channel clusters

derived from group-level statistics and the predetermined alpha frequency (8–12 Hz). Trials of each subject were sorted from low to high alpha power and divided into 5 bins (Linkenkaer-Hansen et al. 2004; Jones et al. 2010; Lange et al. 2012, 2013). For each bin and subject, we calculated the average temporal perceptual discrimination rate and normalized the resulting value for each bin to the individual average temporal perceptual discrimination rate across all bins by first subtracting and then dividing by the individual averaged temporal perceptual discrimination rate across all trials. This resulted in a percentage change relative to the normalized mean across all bins for each subject (Linkenkaer-Hansen et al. 2004; Lange et al. 2012, 2013). For each bin, average power and SEM were computed over all subjects. Linear and quadratic functions were fitted to the data to determine the best fit (Linkenkaer-Hansen et al. 2004; van Dijk et al. 2008; Jones et al. 2010; Lange et al. 2012, 2013). Average temporal perceptual discrimination rates in the respective bins were statistically compared by applying a one-way repeated-measures ANOVA and post hoc t-tests.

Additionally, we investigated the correlation of prestimulus power and confidence ratings. The analysis was conducted as stated above, with the following exceptions. To separately determine the relation between prestimulus power and confidence rating for correctly and incorrectly perceived trials, we divided the trials with intermediate SOA regarding their decisional outcome, that is, correctly and incorrectly perceived trials were analyzed separately. For each bin, we calculated the average confidence rating and normalized the result in each bin to the average confidence rating across all trials with the respective decisional outcome. Finally, the average confidence ratings were averaged over subjects. Likewise, linear and quadratic functions were fitted to the data.

Further, we separated the significant channels in 2 clusters (anterior/somatosensory vs. parieto-occipital; see above and inset of Fig. 2B) based on their spatiotemporal characteristics and performed the correlation analysis with power values averaged over the channels of these separated sensor-clusters.

Relation Between Decision Variable, Prestimulus Power, and Poststimulus ERFs

To examine the neural dynamics of perceptual decision making under conditions with suboptimal evidence accumulation and ambiguous stimulus perception, we studied the relation of poststimulus ERFs, prestimulus alpha power and decisional outcome. Perceptual decisions can be conceptualized as a process in which sensory evidence for a decision accumulates over time in a decision variable until a decision bound is reached, followed by a particular response selection (Gold and Shadlen 2007; Ratcliff and McKoon 2007; Kiani and Shadlen 2009). Recent works in human electrophysiology suggest that such decision variables are reflected in poststimulus event-related potentials (e.g., VanRullen and Thorpe 2001; Philiastides and Sajda 2006; Philiastides et al. 2006; O'Connell et al. 2012). Since event-related potentials/fields resemble a population-based measure of neuronal activity (Hari and Kaukoranta 1985), this is further supported by studies that identify signals from multiple neurons as basis of behavioral decisions (Britten et al. 1996). We hypothesized that, in trials with intermediate SOA, the total accumulation of sensory evidence would remain below any decisional bound due to insufficient sensory information in favor of any decision, therefore requiring forced-choice decisions. We aimed to assess these decision variables in poststimulus ERFs. Additionally, confidence levels should be a function of the distance of the decision variable to

the decision bounds, with closer proximity of the decision variable to the respective decision bound resulting in higher confidence. Moreover, we hypothesized that prestimulus alpha power modulates the distance of the decision variable to the respective decision bounds.

To compute ERFs, preprocessed data were filtered between 2 and 40 Hz, the mean of each epoch was removed from each trial, and these data were averaged across trials. For each subject, ERFs were computed for all sensors that showed a significant difference between decisional outcomes (as shown in Fig. 2B). Additionally, we separated the significant channels in 2 spatial clusters (anterior/somatosensory vs. parieto-occipital, see inset of Fig. 2B) based on their spatiotemporal characteristics and calculated ERFs for all sensors of the respective sensor-cluster separately. To avoid cancellation effects when averaging across sensors and subjects, the signals of the 2 orthogonal sensors of each gradiometer pair were combined by taking the root mean square of the signals in the time domain (e.g., van Dijk et al. 2008; Lange et al. 2012), resulting in 102 gradiometer pairs. Poststimulus ERFs were baseline corrected by subtracting the mean of the prestimulus period (–900 to 0 ms). First, we determined potential poststimulus decision boundaries in the poststimulus ERFs. To this end, we computed ERFs for the 2 conditions with 0 and 100 ms SOA as they provided the most unambiguous perception of 1 and 2 stimuli. Only trials with correct responses (i.e., perceived 1 stimulus for trials with SOA 0 ms and perceived 2 stimuli for trials with SOA 100 ms) were included in this analysis, with conditions subsequently labeled as 0ms-1 and 100ms-2. We statistically compared the ERFs in the poststimulus period (0–300 ms) to identify time periods that maximally discriminated between these 2 reference conditions with 0 and 100 ms SOA. We used a nonparametric statistical test which effectively controls for the Type I error rate due to multiple comparisons across time points in line with the procedure described above (for details, see Time-Frequency Analysis). In brief, we calculated the difference between both ERFs for each subject, followed by a group-level statistic testing the consistency of the differences across subjects against a reference null distribution based on 1000 random sets of permutations regarding the 2 experimental conditions.

Next, we examined whether the ERFs reflect a decision variable that is independent of sensory input, but differing according to subject's decisional outcome. To this end, we sorted trials with intermediate SOA in trials with correct and incorrect responses. We hypothesized that due to their ambiguity and insufficient accumulation of sensory evidence, the decision bounds (i.e., ERFs of conditions 0ms-1 and 100ms-2) will not be reached in trials with intermediate SOA. Nonetheless, because of the implemented forced-choice task, subjects are forced to make the decision with a particular level of uncertainty. We hypothesized that confidence levels should be a function of the distance of the decision variable to the decision bounds, with closer proximity of the decision variable to the respective decision bound resulting in higher confidence. Moreover, we hypothesized that prestimulus alpha power has a distinguishable effect on the decision variable. Since prestimulus alpha power significantly influenced temporal perceptual discrimination and confidence ratings (Fig. 3A,B), an effect of prestimulus alpha power should be visible in the poststimulus decision variable. We hypothesized that prestimulus alpha power modulates the distance of the decision variable to the respective decision bounds (Fig. 4B). To this end, we averaged prestimulus alpha power across those time points and sensors that showed a significant difference between decisional outcomes (see above, Fig. 2B) and grouped the trials with intermediate SOA

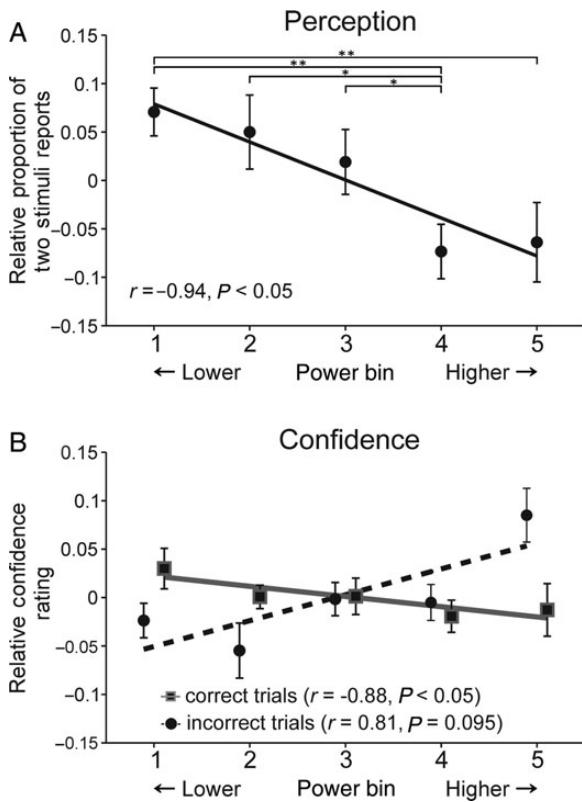


Figure 3. Results of the post hoc correlation analyses of averaged prestimulus alpha power (8–12 Hz) for significant sensors (as shown in Fig. 2B) and (A) normalized average temporal perceptual discrimination rate or (B) normalized confidence ratings, separated for correctly and incorrectly perceived trials. Insets show results of the linear regression analyses (black and gray lines). Higher number bins indicate higher spectral power. Error bars represent SEM. ** $P < 0.01$, * $P < 0.05$.

into correct and incorrect trials with either high and low prestimulus alpha power. This resulted in 4 different conditions: low prestimulus alpha power and perceived 2 stimuli (subsequently labeled low α -2), high prestimulus alpha power and perceived 2 stimuli (high α -2), low prestimulus alpha power and perceived 1 stimulus (low α -1), high prestimulus alpha power and perceived 1 stimulus (high α -1). We then computed poststimulus ERFs for each of these conditions.

To quantify the relation between these conditions, we chose 2 parallel approaches to determine a time window of interest. In the first approach, we averaged ERF amplitudes for each condition over those time points showing a significant difference between the conditions 0ms-1 and 100ms-2 (i.e., 145–171 ms; see above and Fig. 4A; see Supplementary Fig. 1 for the complete ERF time courses of all conditions). In the second approach, we determined the time point of maximum amplitude difference between the conditions 0ms-1 and 100ms-2 within those time points showing a significant difference between the conditions (150 ms). Please see the Discussion section for a further discussion on the selection criteria for the time window of interest. We averaged ERF amplitudes for each condition over the 10 ms that precede this time point of maximal difference (i.e., 140–150 ms). The rationale of this approach was that decision variables are thought to increase until a decision bound is reached and decline again afterwards to baseline (Kiani and Shadlen 2009; O’Connell et al. 2012). Thus, the time point of maximal difference between the reference conditions and the preceding time

window should be the best predictor of the decision process (see model in Fig. 4B).

For the additional analyses based on separated sensor-clusters, significant differences between the conditions 0ms-1 and 100ms-2 could be demonstrated from 139 to 172 ms (see Fig. 4D) and the point of maximum amplitude difference was located at 151 ms for the anterior/somatosensory sensor-cluster. For the parieto-occipital cluster, no significant differences between the conditions 0ms-1 and 100ms-2 could be demonstrated (see Fig. 4F). To ensure that the absence of significant differences for the parieto-occipital cluster did not result from low statistical power due to a lower number of channels in this cluster (parieto-occipital cluster: 7 channel pairs, anterior/somatosensory sensor-cluster: 20 channel pairs), we further compared the conditions 0ms-1 and 100ms-2 for a random selection of 7 channel pairs from the anterior/somatosensory sensor-cluster. The results of this analysis reproduced the significant differences between the conditions 0ms-1 and 100ms-2 (139–169 ms; data not shown) as well as a significant negative linear correlation for the ordered averaged ERFs (i.e., 100ms-2, low α -2, high α -2, low α -1, high α -1, 0ms-1; $r = -0.96$, $P < 0.01$ for time window 139–169 ms; $r = -0.87$, $P < 0.05$ for time window 139–149 ms; data not shown). Based on these results, we conclude that the absent significant difference between the conditions 0ms-1 and 100ms-2 for the parieto-occipital cluster cannot be generally explained by the smaller number of channels in this cluster, but instead must be mainly attributed to the absence of decision-related ERF components in the parieto-occipital sensor-cluster.

For both sensor sets (all significant sensors and the anterior/somatosensory sensor-cluster), we subsequently ordered the conditions regarding the expected averaged ERF amplitudes (100ms-2, low α -2, high α -2, low α -1, high α -1, 0ms-1) and fitted a linear regression to the data to determine a linear trend (Fig. 5). Due to the a priori difference of the conditions 100ms-2 and 0ms-1, we performed an additional analysis in which we excluded these conditions from the regression analysis. Hence, the regression analysis was additionally calculated for the ordered intermediate conditions (low α -2, high α -2, low α -1, high α -1) only. Averaged ERF amplitudes were statistically compared by applying a one-way repeated-measures ANOVA. Because no time window showing a significant difference between the conditions 0ms-1 and 100ms-2 was found for the parieto-occipital sensor-cluster, we refrained from performing this analysis for the parieto-occipital sensor-cluster.

Finally, we calculated the average confidence ratings per subject for each condition and averaged the mean confidence levels per condition over all subjects. Since confidence levels should be a function of the distance of the decision variable to the respective decision bounds (i.e., low α -2 and high α -2 to 100ms-2; low α -1 and high α -1 to 0ms-1, see Fig. 4B), we calculated the mean power difference of each intermediate condition (i.e., low α -2, high α -2, low α -1, high α -1) from the respective decision bounds averaged over the time window showing a significant difference between the conditions 0ms-1 and 100ms-2 (i.e., 145–171 ms) and the time window preceding the point of maximum amplitude difference between the conditions 0ms-1 and 100ms-2 (i.e., 140–150 ms, Fig. 5C). We plotted the distance of the decision variables to the respective decision bounds and related it to the mean confidence levels per condition over all subjects. Subsequently, we fitted a linear regression to the data to determine a linear trend. Additionally, we performed this analysis with amplitude values calculated for the time windows based on the anterior/somatosensory sensor-cluster (i.e., 139–172 ms; 141–151 ms, Fig. 5F). Due to the fact that, for the parieto-occipital sensor-cluster, no

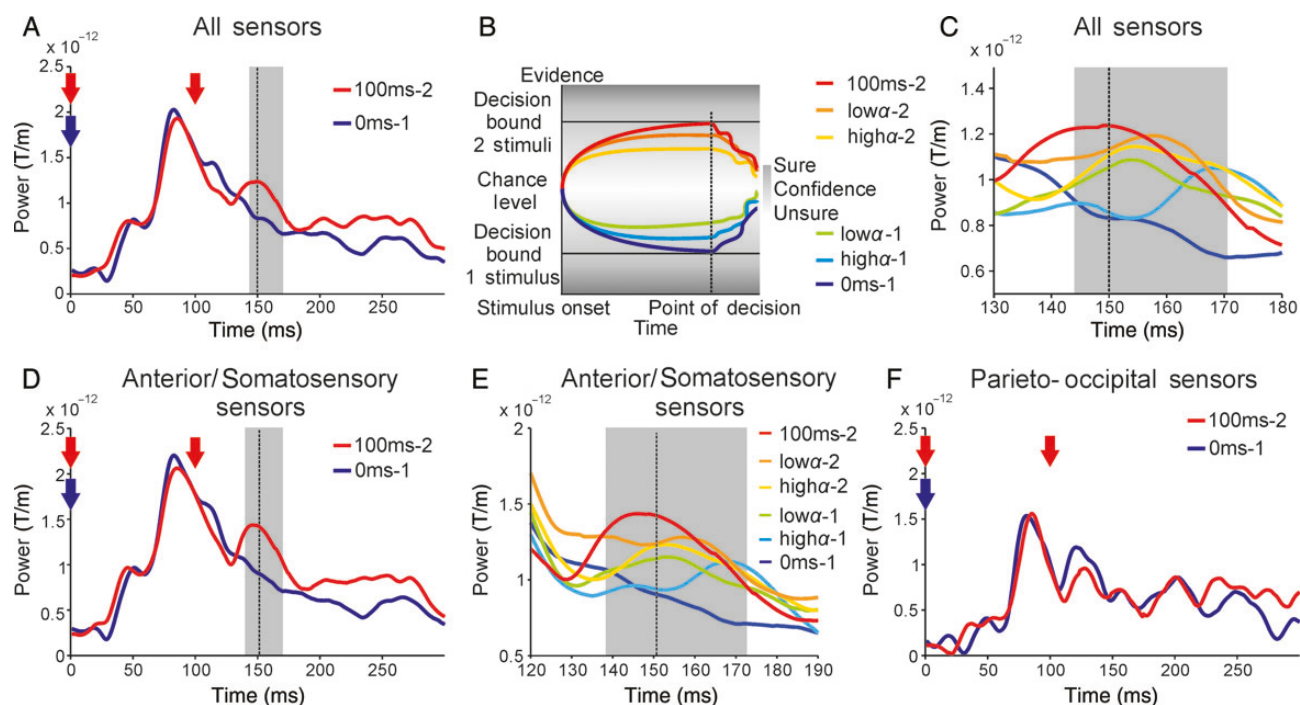


Figure 4. Results of the analysis of poststimulus ERFs. (A) Statistical comparison of poststimulus ERF amplitudes (averaged over all significant sensors, as shown in Fig. 2B) of correctly perceived trials with 0 ms (0ms-1) and 100 ms (100ms-2) SOA. Significant differences are indicated by shaded area (145–171 ms). The dashed line represents the point of maximum amplitude difference between the reference conditions 0ms-1 and 100ms-2 (150 ms). The blue arrow highlights the time point of stimulation for the 0ms-1 condition, while the red arrows highlight the time points of stimulation for the 100ms-2 condition. (B) Predicted poststimulus ERFs. Decision model illustrating the hypothesized order of poststimulus ERFs. Conditions 0ms-1 and 100ms-2 reflect the decision bounds for perceiving 1 and 2 stimuli, respectively. The other conditions are predicted to be between these bounds in the presented order. Distance to the bound is hypothesized to reflect confidence in the decision (indicated by gray-shaded background). The dashed line represents the point of maximum amplitude difference between the reference conditions 0ms-1 and 100ms-2. Beyond this point, the decision variables are thought to decline again to baseline. (C) MEG data of poststimulus ERFs. Close-up on the time window of significant difference (145–171 ms; shaded area) between poststimulus ERF amplitudes of 0ms-1 and 100ms-2 (averaged over all significant sensors, as shown in Fig. 2B). Shaded area and dashed line as in A. Color scheme as in B. (D) Same as A, but now for amplitude values averaged over the anterior/somatosensory sensor-cluster (as shown in Fig. 2B; time window: 139–172 ms; time point of maximum amplitude difference: 151 ms). Blue and red arrows as in A. (E) Same as C, but now for amplitude values averaged over the anterior/somatosensory sensor-cluster (as shown in Fig. 2B; time window: 139–172 ms; time point of maximum amplitude difference: 151 ms). Shaded area and dashed line as in D. (F) Same as A, but now for amplitude values averaged over the parieto-occipital sensor-cluster (as shown in Fig. 2B). Blue and red arrows as in A. No statistically significant difference was found. Significance values in A–F are cluster corrected to account for multiple comparison corrections. $t = 0$ indicates onset of sensory stimulation, that is, the first stimulus of every stimulation.

time window showing a significant difference between the conditions 0ms-1 and 100ms-2 was found, we refrained from performing this analysis for the parieto-occipital sensor-cluster.

Results

Behavioral Results

Subjects performed a forced-choice temporal perceptual discrimination task (Fig. 1) and had to report how many electrical stimulations applied to their left index finger they perceived. For SOAs of 0 and 100 ms, subjects made only negligible errors (SOA 0 ms: $92.3 \pm 1.8\%$ [mean \pm SD] correct reports; SOA of 100 ms: $93.8 \pm 2.7\%$ correct reports). For intermediate SOAs, subjects correctly perceived stimulation in approximately half of the trials ($56.7 \pm 3.2\%$ correct reports). The response distribution of each condition did not significantly differ from a Gaussian distribution ($P > 0.05$). Statistical testing revealed highly significant differences regarding temporal perceptual discrimination rates between the intermediate condition and the 0 ms ($t_{(15)} = 10.086$, $P < 0.0001$) as well as the 100 ms condition ($t_{(15)} = 11.811$, $P < 0.0001$). Overall, the absolute influence of learning/fatigue is negligible. No significant linear trends indicating learning or fatigue effects could be determined for average temporal perceptual discrimination

rate ($r = 0.49$, $P > 0.05$, Supplementary Fig. 2A) or confidence ratings ($r = 0.55$, $P > 0.05$, Supplementary Fig. 2B).

Time-Frequency Analysis

We studied the role of prestimulus alpha-band oscillations (8–12 Hz) on temporal perceptual discrimination. We focused on trials with intermediate SOA and compared alpha power in the prestimulus period (–900 to 0 ms) between correctly and incorrectly perceived trials. The exploratory time-frequency analysis confirmed a prominent alpha effect in the prestimulus period (Fig. 2A). Prestimulus alpha power was found to be statistically significantly decreased if subjects correctly perceived the stimulation as 2 stimuli compared with incorrectly perceived trials ($P < 0.05$, Fig. 2B). Significant differences were most evident for anterior/somatosensory and parieto-occipital sensors contralateral to stimulation site between –900 and –250 ms. Particularly, the topographical location of the effect shifted over time, with significant decreases in both contralateral anterior/somatosensory and parieto-occipital sensors at the beginning of the prestimulus epoch (–900 to –500 ms), compared with a decrease of power in more posterior sensors in the later prestimulus epoch (–400 to –250 ms). Note that, although both sensor-clusters show a

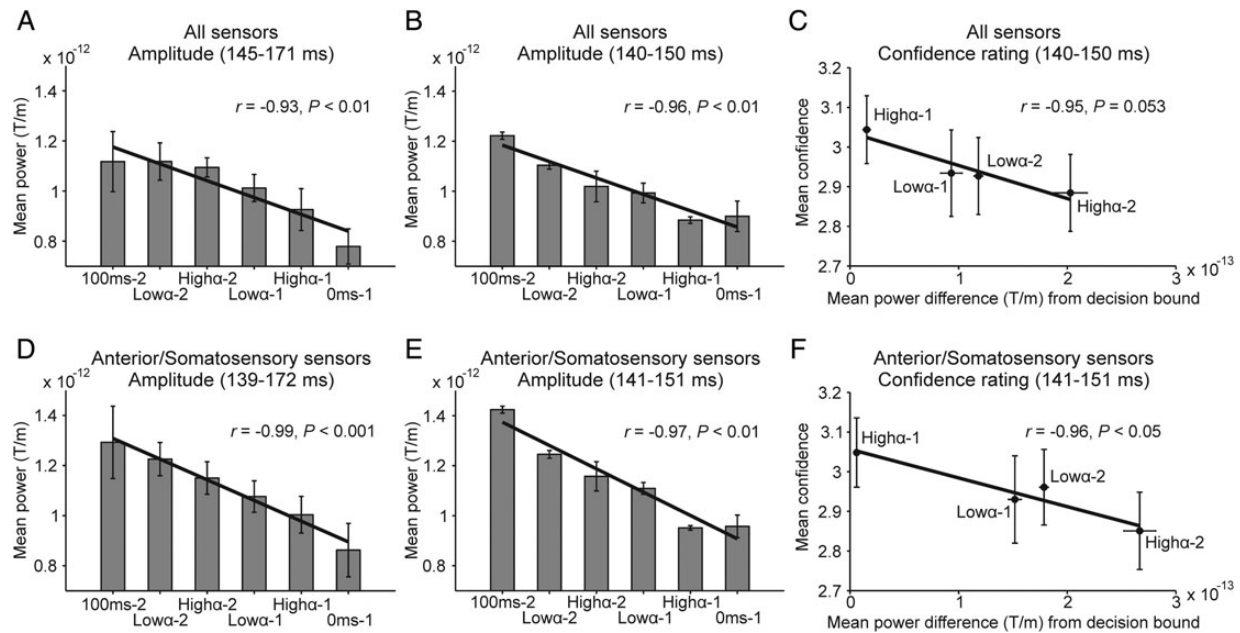


Figure 5. Averaged amplitude values and confidence ratings of poststimulus ERFs. (A) Amplitude values (based on all significant sensors, as shown in Fig. 2B) averaged over the time window showing a significant difference between poststimulus ERF amplitudes of 0ms-1 and 100ms-2 (145–171 ms, see Fig. 4A,C). (B) Amplitude values (based on all significant sensors, as shown in Fig. 2B) averaged over the time window preceding the point of maximal amplitude difference (150 ms) between poststimulus ERF amplitudes of 0ms-1 and 100ms-2 (140–150 ms, see Fig. 4A,C). (C) Average confidence ratings per condition in relation to mean power difference to the respective decision bound (based on all significant sensors, as shown in Fig. 2B) for the time window 140 to 150 ms (see Fig. 4A,C). (D) Same as A, but now for amplitude values based on the anterior/somatosensory sensor-cluster (as shown in Fig. 2B; time window: 139–172 ms, Fig. 4D,E). (E) Same as B, but now for amplitude values based on the anterior/somatosensory sensor-cluster (as shown in Fig. 2B; time window: 141–151 ms, Fig. 4D,E). (F) Same as C, but now for mean power difference based on the anterior/somatosensory sensor-cluster (as shown in Fig. 2B; time window 141–151 ms, Fig. 4D,E). In A, B, D, and E conditions are ordered according to the hypothesized decision model (Fig. 4B). Insets in A, B, D, and E show results of the linear regression analyses (black lines) based on all 6 conditions (i.e., 100ms-2, low α -2, high α -2, low α -1, high α -1, 0ms-1). Note that the additional regression analyses excluding the 100ms-2 and 0ms-1 conditions similarly demonstrate a significant negative linear correlation ($P < 0.05$; regression lines not shown) for the ordered intermediate ERFs (i.e., low α -2, high α -2, low α -1, high α -1) for all 4 time windows (145–171, 140–150, 139–172, 141–151 ms). Insets in C and F show results of the linear regression analyses (black lines).

significant alpha power decrease in the prestimulus epoch, the decision-related effects of alpha power visible in the poststimulus ERFs could only be demonstrated for the anterior/somatosensory sensor-cluster (see Relation between Decision Variable, Prestimulus Power, and Poststimulus ERFs and Fig. 4).

Source Reconstruction

To identify the underlying cortical sources of the aforementioned significant effect, we applied a beamforming approach. We identified one source mainly located in contralateral postcentral gyrus (Brodmann area 3, Fig. 2C). A second cluster was found in the contralateral middle occipital region, encompassing Brodmann areas 19, 21, and 39.

Correlation of Prestimulus Power, Perceptual Decisions, and Confidence Ratings

To determine more precisely the relation of prestimulus alpha power and subjective perception, we performed a correlation analysis. We computed single-trial power averaged over alpha frequencies and significant sensor-time points (time window: –900 to –250 ms, see Fig. 2B). Trials were sorted from low to high power and divided into 5 bins. Response probabilities for each bin were calculated as the percentage change in temporal perceptual discrimination rate from the mean, normalized per subject to the individual mean temporal perceptual discrimination rate over all bins.

We found a significant negative linear relationship between prestimulus alpha power averaged over all sensors showing a significant alpha power difference between correctly (perceived 2 stimuli) versus incorrectly (perceived 1 stimulus) perceived trials with intermediate SOA and subjects' perceptual decisions ($r = -0.94$, $P < 0.05$, Fig. 3A). In other words, probability of correctly perceiving the stimulation as 2 temporally separate stimuli was greater during trials with lower prestimulus alpha power. A one-way repeated-measures ANOVA revealed a significant main effect ($P < 0.05$). Post hoc t -tests revealed significant differences between bin1 versus bin4 ($t_{(15)} = 3.049$, $P < 0.01$), bin1 versus bin5 ($t_{(15)} = 3.096$, $P < 0.01$), bin2 versus bin4 ($t_{(15)} = 2.545$, $P < 0.05$), and bin3 versus bin4 ($t_{(15)} = 2.142$, $P < 0.05$). No significant quadratic relationship between prestimulus alpha power and subject's perceptual decisions was found ($r = 0.94$, $P = 0.11$). In addition, we performed the same analysis with power values averaged over the sensors of the spatiotemporally separated sensor-clusters (anterior/somatosensory vs. parieto-occipital). For the anterior/somatosensory sensor-cluster, both linear ($r = -0.97$, $P < 0.01$) and quadratic ($r = 0.99$, $P < 0.05$) fits for the relationship between prestimulus alpha power and subjects' perceptual decisions were significant. A one-way repeated-measures ANOVA revealed an effect on trend level ($P = 0.1$). Post hoc t -tests revealed significant differences between bin1 versus bin4 ($t_{(15)} = 2.74$, $P < 0.05$), bin1 versus bin5 ($t_{(15)} = 2.14$, $P < 0.05$), and bin2 versus bin4 ($t_{(15)} = 2.32$, $P < 0.05$). Similarly for the parieto-occipital sensor-cluster, both linear ($r = -0.96$, $P < 0.05$) and quadratic ($r = 0.99$, $P < 0.05$) fits for the relationship between prestimulus alpha power and

subjects' perceptual decisions were significant. No significant effect was found by a one-way repeated-measures ANOVA ($P = 0.15$). Post hoc t -tests revealed significant differences between bin1 versus bin4 ($t_{(15)} = 2.47, P < 0.05$).

In a similar analysis, we investigated the correlation between prestimulus alpha power and subjects' level of confidence regarding their perceptual decisions. We found a significant negative linear relationship between prestimulus alpha power averaged over all sensors showing a significant alpha power difference between correctly (perceived 1 stimuli) versus incorrectly (perceived 2 stimuli) perceived trials with intermediate SOA and confidence ratings for correctly perceived trials ($r = -0.88, P < 0.05$, Fig. 3B) and a strong trend toward a significant positive linear correlation for incorrectly perceived trials ($r = 0.81, P = 0.095$). No significant quadratic relationship between prestimulus alpha power and subjects' confidence ratings was found (correct trials: $r = 0.95, P = 0.1$; incorrect trials: $r = 0.94, P = 0.11$). For the anterior/somatosensory sensor-cluster, a significant negative linear relationship between prestimulus alpha power and confidence ratings for correctly perceived trials ($r = -0.92, P < 0.05$) could be demonstrated, while no significant effect was found for incorrect trials ($r = 0.6, P = 0.28$). For quadratic relationships between prestimulus alpha power and subjects' confidence ratings, no significant fit was found (correct trials: $r = 0.92, P = 0.14$; incorrect trials: $r = 0.8, P = 0.35$). Finally, no significant linear or quadratic relationship between prestimulus alpha power and confidence ratings could be demonstrated for the parieto-occipital cluster, neither for correct (linear: $r = -0.49, P = 0.41$; quadratic: $r = 0.59, P = 0.65$) or incorrect trials (linear: $r = 0.73, P = 0.17$; quadratic: $r = 0.94, P = 0.11$).

Relation Between Decision Variable, Prestimulus Power, and Poststimulus ERFs

We investigated if poststimulus ERFs show characteristics of a decision variable and the influence of prestimulus alpha power on these variables. We analyzed poststimulus ERFs by applying a boundary-crossing decision-making model (Philiastides et al. 2006; O'Connell et al. 2012). To this end, we estimated decision bounds for the unambiguous perception of 1 and 2 stimuli by calculating poststimulus ERFs from all correct trials of the 0 and 100 ms SOA conditions, subsequently labeled 0ms-1 and 100ms-2. Statistical comparison revealed a significant difference between both ERF amplitudes between 145 and 171 ms ($P < 0.05$), indicating that the 2 signals significantly diverge during this time window (Fig. 4A). The spatial distribution of the stimuli-evoked ERFs for those time points showing a significant difference between the conditions 0ms-1 and 100ms-2 (i.e., 145–171 ms) revealed highly similar patterns of activity over conditions (Supplementary Fig. 3).

According to our hypothesis, these ERFs should reflect the lower and upper boundaries for decisions toward 1 and 2 stimuli, respectively. ERFs of trials with intermediate SOA should be located in between these boundaries and the distance toward the respective boundary should reflect the perceptual decision as well as the confidence in the decision (Fig. 4B). The results demonstrate that, despite physically identical stimulation, the ERFs of trials with intermediate SOA differ with respect to subjects' perception and prestimulus alpha power (Fig. 4C). In line with our hypothesis, we found a significant negative linear correlation for the ordered averaged ERFs (i.e., 100ms-2, low α -2, high α -2, low α -1, high α -1, 0ms-1), indicating a monotonic decrease in amplitude from the 100ms-2 condition to the 0ms-1 condition ($r = -0.93, P < 0.01$ for time window 145–171 ms, Fig. 5A; $r = -0.96,$

$P < 0.01$ for time window 140–150 ms, Fig. 5B). An additional regression analysis which excluded the 100ms-2 and 0ms-1 conditions also revealed a significant negative linear correlation for the ordered averaged intermediate ERFs (i.e., low α -2, high α -2, low α -1, high α -1), indicating a monotonic decrease in amplitude from the low α -2 condition to the high α -1 condition ($r = -0.97, P < 0.05$ for time window 145–171 ms, see also captions Fig. 5; $r = -0.98, P < 0.05$ for time window 140–150 ms, see also captions Fig. 5). A one-way repeated-measures ANOVA revealed a strong trend toward a significant main effect ($P = 0.065$) for the analysis of the time window 145–171 ms. No significant effect was found for the time window 140–150 ms.

For the additional regression analysis performed on the anterior/somatosensory sensor-cluster (Fig. 4D,E), a significant negative linear correlation for the ordered averaged ERFs (i.e., 100ms-2, low α -2, high α -2, low α -1, high α -1, 0ms-1) could be demonstrated ($r = -0.99, P < 0.001$ for time window 139–172 ms, Fig. 5D; $r = -0.97, P < 0.01$ for time window 141–151 ms, Fig. 5E). The negative linear correlations remained significant under exclusion of the 100ms-2 and 0ms-1 conditions ($r = -0.99, P < 0.001$ for time window 139–172 ms, see also captions Fig. 5; $r = -0.97, P < 0.05$ for time window 141–151 ms, see also captions Fig. 5). A one-way repeated-measures ANOVA revealed a significant main effect for both time windows ($P < 0.05$ for time window 139–172 ms; $P < 0.05$ for time window 141–151 ms). Because no time window showing a significant difference between the conditions 0ms-1 and 100ms-2 was found for the parieto-occipital sensor-cluster (see Fig. 4F), we refrained from performing the regression analysis for the parieto-occipital sensor-cluster.

We further related the average confidence ratings per condition to the distance of the decision variables to the respective decision bounds. According to our hypothesis, the average confidence ratings per condition should increase with closer proximity of the decision variables to the respective decision bounds (see Fig. 4B). While for the time window from 145 to 171 ms, no significant linear relation between confidence ratings and distance of the decision variables to the respective decision bounds could be demonstrated ($r = 0.43, P = 0.57$), a strong trend toward a significant negative linear relation ($r = -0.95, P = 0.053$) was evident for the time window from 140 to 150 ms (Fig. 5C). For the critical time windows based on the anterior/somatosensory sensor-cluster, a significant negative linear relation could only be demonstrated for the time window from 141 to 151 ms ($r = -0.96, P < 0.05$, Fig. 5F). For the time window from 139 to 172 ms, no significant linear fit was found ($r = -0.24, P = 0.84$). Regarding the time windows before the point of maximum amplitude difference (140–150 ms for all significant sensors, 141–151 ms for the anterior/somatosensory sensor-cluster), in agreement with our hypothesis a closer distance to the reference conditions resulted in higher confidence ratings. Because no time window showing a significant difference between the conditions 0ms-1 and 100ms-2 was found for the parieto-occipital sensor-cluster, we refrained from performing this analysis for the parieto-occipital sensor-cluster.

Discussion

We investigated the influence of prestimulus alpha activity on the temporal perceptual discrimination of suprathreshold tactile stimuli, the confidence in perceptual decisions and the underlying neuronal decision variable. Subjects received 1 or 2 tactile stimuli with different SOAs. In a forced-choice task, subjects reported their perceptual decision and their confidence in this decision.

Subjects frequently misperceived stimulation as 1 stimulus for trials with intermediate SOA, indicating perceptual ambiguity despite physically identical stimulation. For these trials with intermediate SOA, correct perception of 2 separate stimuli was correlated with a decrease of alpha power (8–12 Hz) relative to incorrectly perceived trials. This effect was evident before onset of stimulation (–900 to –250 ms) mainly in the contralateral postcentral gyrus (presumably primary somatosensory cortex) and the contralateral middle occipital region. Additionally, prestimulus alpha power correlated with subjects' confidence ratings. For correctly perceived trials, high confidence ratings correlated with low prestimulus alpha power. Contrarily, for incorrectly perceived trials, high confidence ratings correlated with high prestimulus alpha power. Finally, poststimulus ERFs at ~150 ms revealed characteristics of a decision variable. In summary, we found: 1) Poststimulus ERFs at ~150 ms reflect perceptual decisions and subjects' confidence in their decisions rather than pure sensory evidence. 2) ERFs for all conditions were in line with an accumulation-to-bound model in which sensory evidence is accumulated in a decision variable (Gold and Shadlen 2007). In trials with ambiguous, intermediate SOA, ERFs of correctly perceived trials were closer to the putative categorical decision bound for perceiving 2 stimuli while incorrectly perceived trials were closer to the categorical decision bound for perceiving 1 stimulus. 3) Due to their perceptual ambiguity, stimuli with intermediate SOA provided only incomplete sensory evidence, resulting in incomplete evidence accumulation and hence ERFs did not cross the decision bound. 4) Incomplete evidence accumulation resulted in lower confidence as reflected in the ERFs. 5) The variability of ERFs, decisions, and confidence ratings is biased by fluctuations of prestimulus alpha power. 6) Finally, the above-mentioned results could be replicated only for the anterior/somatosensory sensor-cluster after separating the sensors of interest. Therefore, it appears that mainly the somatosensory cortex areas account for the decision-related components visible at ~150 ms.

We estimated the poststimulus categorical decision boundaries by calculating significant differences between ERFs of the reference conditions 0ms-1 and 100ms-2. One might argue that these conditions differ not only by subjects' decisions but also by sensory evidence (1 stimulus vs. 2 stimuli), and thus, our putative decision variable might reflect sensory input rather than decisional processes. However, we demonstrate that ERFs around ~150 ms for trials with intermediate SOA, that is, with constant stimulation, correlate with perceptual decisions rather than sensory input.

Several studies have reported an inverted U-shaped relationship between prestimulus alpha power and perceptual performance, with intermediate alpha levels resulting in best performance levels (Linkenkaer-Hansen et al. 2004; Zhang and Ding 2009; Lange et al. 2012). On the contrary, other studies emphasize a linear relationship, with lower power levels being related to better performance (Thut et al. 2006; Hanslmayr et al. 2007; Schubert et al. 2008; van Dijk et al. 2008; Mathewson et al. 2009; Jones et al. 2010). In the present study, linear as well as quadratic fits were applied to the data. For most analyses, both linear and quadratic fits were significant for the correlation of prestimulus alpha power and perceptual decisions for the anterior/somatosensory and the parieto-occipital sensor-cluster. This demonstration of both linear and quadratic dependencies hinders a final conclusion on this matter. It remains to be seen if future studies can clarify the relevant factors in terms of neuroanatomical region or experimental conditions favoring one dependency over the other.

Notably, the majority of previous studies used near-threshold stimuli and relied on conditions where stimuli are either perceived or not perceived. Thus, subjects had to report whether or not stimulation is perceived, irrespective of its content. Here, we contrasted 2 different perceptual qualities with suprathreshold intensities, since subjects had to report whether they perceived 1 stimulus or 2 stimuli. Our paradigm therefore focuses on temporal discrimination and employs temporal ambiguity, with identical suprathreshold stimulation resulting in varying perceptual decisions. Hence, the present study provides critical extensions to the aforementioned studies.

Our results are in line with several studies reporting a correlation of prestimulus alpha power and detection or discrimination of near-threshold stimuli (e.g., Linkenkaer-Hansen et al. 2004; Zhang and Ding 2009; Jones et al. 2010). We critically extend these studies by demonstrating that alpha power influences also the temporal resolution of perception. Although formerly interpreted as correlate of cortical idling (Pfurtscheller et al. 1996), alpha activity has recently been suggested to gate neuronal processing by functional inhibition of task-irrelevant areas (Jensen and Mazaheri 2010; Jensen et al. 2012) and/or by modulating cortical excitability (Thut et al. 2006; Romei, Brodbeck et al. 2008; Romei, Rihms et al. 2008; Lange et al. 2013), resulting in more efficient neuronal stimulus processing in task-related neuronal groups. By using 2 clearly suprathreshold stimuli, we demonstrate that prestimulus alpha power extends the role of a simple binary switch between inhibition and processing. Rather, it modulates the quantity (1 stimulus or 2 stimuli, e.g., Lange et al. 2013; Keil et al. 2014) and the subjective quality (i.e., confidence) of perception continuously. This continuous modulation is reflected in confidence ratings, providing a more fine-grained scale of the decision process.

Prestimulus alpha power can be modulated by attention or expectation (Foxe et al. 1998; Worden et al. 2000; Jones et al. 2010; Anderson and Ding 2011; Haegens et al. 2012). In line with these results, recent studies demonstrated that prestimulus alpha power is predictive of perceptual performance in attention-based tasks (Kelly et al. 2009; O'Connell et al. 2009). While we did not explicitly modulate attention in our study, we suggest that spontaneous fluctuations of attention or arousal modulate prestimulus alpha power and thus influence perception and confidence. Further, it seems that such fluctuations are distinguishable from general training effects, since we did not find significant learning/fatigue trends for either perception or confidence.

We found alpha power to differ significantly in the prestimulus period in the contralateral postcentral gyrus and contralateral middle occipital region. Differential alpha-band activity in the postcentral gyrus (presumably primary somatosensory areas) has been found for other tactile tasks (e.g., Zhang and Ding 2009; Jones et al. 2010; Lange et al. 2012). Here, we extend the role of the postcentral gyrus to temporal perceptual discrimination of 2 subsequently presented stimuli. Since we applied only tactile stimuli and a tactile decision task, the significant alpha-band effect in visual areas might seem surprising. However, our results are in line with findings from a tactile spatial attention task, showing that in the absence of visual stimulation, attention to tactile stimulation resulted in suppression of alpha-band power in occipital areas (Bauer et al. 2006). Similarly, a recent study indicates that task-relevant spatial attention in one sensory domain affects oscillatory activity in other domains (Bauer et al. 2012). In accordance to these findings, a recent study demonstrated that parieto-occipital activation in the alpha band is linked to spatial attention across modalities (Banerjee et al. 2011).

In line with these results, the power differences in the contralateral middle occipital region can also be interpreted as correlate of global attention, thus not restricted to the somatosensory domain. This is supported by classical findings which localize the central generator of alpha rhythms in parieto-occipital areas (e.g., Salmelin and Hari 1994; Manshanden et al. 2002), independent of task requirements. The explanation is further strengthened by our findings that the decision-related ERF components could only be found for the anterior/somatosensory sensor-cluster, but not in the parieto-occipital cluster. This indicates that the parieto-occipital sensor-cluster, although showing significant power differences between perceptual conditions, is not central for decision-related processes. The influence of prestimulus alpha on decision variables is also in line with a recent EEG study (Lou et al. 2014). In this study, the influence of prestimulus activity is seen as top-down attention-based modulation, indicating that the sensory evidence is comprised of stimulus information and attentional state.

We demonstrate that prestimulus alpha power does not only correlate with perceptual decisions, but also with the subjective quality of such decisions. If alpha power was low, subjects were more confident with their decisions, but notably only for correctly perceived stimuli. Contrarily, if stimulation was perceived incorrectly, low alpha power correlated with low confidence. This seemingly contradictory result can be explained by a decision model. It has been proposed that sensory evidence is accumulated over time in a decision variable until a decision bound is reached (e.g., Shadlen and Newsome 2001). Here, we used such a decision-to-bound model to examine poststimulus decision variables. We hypothesized that due to the ambiguity of sensory evidence the decision variable does not cross a decision bound. Further, fluctuations of prestimulus alpha power should influence the decision variable and the confidence in perceptual decisions, if sensory evidence was insufficient to reach a decision bound. We identified this proposed pattern of a decision variable in poststimulus ERFs at ~ 150 ms. Despite identical stimulation, poststimulus ERFs of trials with intermediate SOA differed according to the decisional outcome. While neither condition reached the categorical decision bound, the distance of the decision variable to the respective decision bounds determined the decisional outcome.

We identified perceptual decision-related components in the somatosensory domain, that is, differences in ERF amplitudes for conditions with physically similar stimulation parameters that discriminated between perceptual reports, as early as ~ 150 ms. Other recent studies addressing perceptual decision making in the visual domain report decision-related neural activity at later time points (~ 300 ms) and relate earlier components to low-level stimulus processing mechanisms (Philiastides et al. 2006; Lou et al. 2014). Such stimulus processing mechanisms can hardly fully explain our results, since our stimulation parameters remained constant for trials with intermediate SOA. An early decision-related component is further supported by studies where early components around ~ 75 – 80 ms were shown to discriminate between high-level properties such as semantic category and components around ~ 150 ms discriminate between target and nontarget conditions (and hence task-specific decision-related demands), independent of visual category (VanRullen and Thorpe 2001). In line with these results, the present components around ~ 150 ms can be interpreted as a correlate of the subjects' perceptual recognition and subsequent decision, not merely as stimulus-related bottom-up processing. However, it is important to keep in mind that somatosensory processing presumably does not end after

the aforementioned component, but it appears that at this time point sufficient information for a perceptual decision is accumulated.

Kiani and Shadlen (2009) recorded neuronal activity in monkey lateral intraparietal cortex during a decision-making task. If the monkey chose to opt out, that is, at low confidence levels, neural activity was at an intermediate level between decision bounds. We used a more detailed confidence rating and found that subjects' confidence correlated with the distance to a decision bound. This suggests that categorical decision making and confidence estimation can be a simple and fast inherent property of the same process (e.g., Kepecs et al. 2008; Kiani and Shadlen 2009), rather than a serial process requiring additional steps or higher (meta) cognitive functions (e.g., Grinband et al. 2006; Yeung and Summerfield 2012).

Additionally, we found poststimulus ERFs to interact with prestimulus alpha levels. Low prestimulus alpha levels shifted the decision variable towards the decision bound for 2 perceived stimuli, independent of decisional outcome. For correctly perceived intermediate SOA trials, low prestimulus alpha power increased confidence, because the distance between the decision variable and the decision bound for 2 perceived stimuli decreased. Contrarily, for incorrectly perceived intermediate SOA trials, low prestimulus alpha power decreased confidence, because the distance between the decision variable and the decision boundary for 1 perceived stimulus increased. The influence of prestimulus alpha power on poststimulus ERFs is in line with recent studies (Jones et al. 2009, 2010; Anderson and Ding 2011; Lange et al. 2012). The influence of prestimulus activity on decisions and the underlying decision variable is also in line with a recent study demonstrating that prestimulus firing rates bias decisions (Carnevale et al. 2012). While this study considers prestimulus activity as noise fluctuations, we argue that prestimulus alpha power is a functionally relevant marker of cortical excitability that can fluctuate over time or that can be endogenously or exogenously modulated by, for example, attention, arousal, or expectation (e.g., Foxe et al. 1998; Worden et al. 2000; Thut et al. 2006; Jones et al. 2010; Anderson and Ding 2011; de Lange et al. 2011).

In line with a recent study (de Lange et al. 2013), we suggest that prestimulus alpha power biases the starting point of the decision variable. Thus, the decision variable is the combination of the internal brain state (prestimulus activity) and the sensory evidence provided by the stimulus. If sensory evidence is weak or ambiguous, prestimulus activity can effectively bias decisions and confidence ratings by shifting the decision variable closer to either decision bound. The fact that prestimulus activity influences the decisional process implies that the decision-making process starts before stimulus presentation (Carnevale et al. 2012; de Lange et al. 2013). Such prestimulus fluctuations can also explain why decisions, confidence ratings, or response times can vary despite physically identical stimulation.

In conclusion, our results demonstrate that the brain state, characterized by alpha power, substantially modulates temporal perceptual discrimination of tactile stimuli despite identical physical stimulation, as well as confidence in perceptual decisions. Moreover, these fluctuations in prestimulus alpha power are visible in poststimulus ERFs mainly determined by somatosensory areas, reflecting the physiological correlate of evidence accumulation in a decision variable for perceptual decisions based on insufficient and suboptimal evidence. We conclude that alpha-band activity continuously modulates the quality of processing underlying perceptual decisions, resulting in differences in temporal perceptual discrimination.

Supplementary Material

Supplementary material can be found at: <http://www.cercor.oxfordjournals.org/>.

Funding

J.L. was supported by the German Research Foundation (LA 2400/4-1).

Notes

We thank Erika Rädisch for help with the MRI recordings. *Conflict of Interest*: None declared.

References

- Anderson KL, Ding M. 2011. Attentional modulation of the somatosensory mu rhythm. *Neuroscience*. 180:165–180.
- Banerjee S, Snyder AC, Molholm S, Foxe JJ. 2011. Oscillatory alpha-band mechanisms and the deployment of spatial attention to anticipated auditory and visual target locations: supramodal or sensory-specific control mechanisms? *J Neurosci*. 31:9923–9932.
- Başar E, Başar-Eroglu C, Rosen B, Schütt A. 1984. A new approach to endogenous event-related potentials in man: relation between EEG and P300-Wave. *Int J Neurosci*. 24:1–21.
- Bauer M, Kennett S, Driver J. 2012. Attentional selection of location and modality in vision and touch modulates low-frequency activity in associated sensory cortices. *J Neurophysiol*. 107:2342–2351.
- Bauer M, Oostenveld R, Peeters M, Fries P. 2006. Tactile spatial attention enhances gamma-band activity in somatosensory cortex and reduces low-frequency activity in parieto-occipital areas. *J Neurosci*. 26:490–501.
- Brandt ME, Jansen BH. 1991. The relationship between prestimulus alpha amplitude and visual evoked potential amplitude. *Int J Neurosci*. 61:261–268.
- Britten KH, Newsome WT, Shadlen MN, Celebrini S, Movshon JA. 1996. A relationship between behavioral choice and the visual responses of neurons in macaque MT. *Vis Neurosci*. 13:87–100.
- Carnevale F, de Lafuente V, Romo R, Parga N. 2012. Internal signal correlates neural populations and biases perceptual decision reports. *Proc Nat Acad Sci USA*. 109:18938–18943.
- de Lange FP, Rahnev DA, Donner TH, Lau H. 2013. Prestimulus oscillatory activity over motor cortex reflects perceptual expectations. *J Neurosci*. 33:1400–1410.
- de Lange FP, van Gaal S, Lamme VAF, Dehaene S. 2011. How awareness changes the relative weights of evidence during human decision-making. *PLoS Biol*. 9:e1001203.
- Foxe JJ, Simpson GV, Ahlfors SP. 1998. Parieto-occipital ~10 Hz activity reflects anticipatory state of visual attention mechanisms. *Neuroreport*. 9:3929–3933.
- Gold JJ, Shadlen MN. 2007. The neural basis of decision making. *Annu Rev Neurosci*. 30:535–574.
- Grinband J, Hirsch J, Ferrera VP. 2006. A neural representation of categorization uncertainty in the human brain. *Neuron*. 49:757–763.
- Gross J, Kujala J, Hamalainen M, Timmermann L, Schnitzler A, Salmelin R. 2001. Dynamic imaging of coherent sources: studying neural interactions in the human brain. *Proc Nat Acad Sci USA*. 98:694–699.
- Haegens S, Luther L, Jensen O. 2012. Somatosensory anticipatory alpha activity increases to suppress distracting input. *J Cogn Neurosci*. 24:677–685.
- Hanslmayr S, Aslan A, Staudigl T, Klimesch W, Herrmann CS, Bäuml K. 2007. Prestimulus oscillations predict visual perception performance between and within subjects. *Neuroimage*. 37:1465–1473.
- Hari R, Kaukoranta E. 1985. Neuromagnetic studies of somatosensory system: principles and examples. *Prog Neurobiol*. 24:233–256.
- Hoogenboom N, Schoffelen J, Oostenveld R, Fries P. 2010. Visually induced gamma-band activity predicts speed of change detection in humans. *Neuroimage*. 51:1162–1167.
- Jensen O, Bonnefond M, VanRullen R. 2012. An oscillatory mechanism for prioritizing salient unattended stimuli. *Trends Cogn Sci*. 16:200–206.
- Jensen O, Mazaheri A. 2010. Shaping functional architecture by oscillatory alpha activity: gating by inhibition. *Front Hum Neurosci*. 4:186.
- Jones SR, Pritchett DL, Sikora MA, Stufflebeam SM, Hämäläinen M, Moore CI. 2009. Quantitative analysis and biophysically realistic neural modeling of the MEG mu rhythm: rhythmogenesis and modulation of sensory-evoked responses. *J Neurophysiol*. 102:3554–3572.
- Jones SR, Kerr CE, Wan Q, Pritchett DL, Hamalainen M, Moore CI. 2010. Cued spatial attention drives functionally relevant modulation of the mu rhythm in primary somatosensory cortex. *J Neurosci*. 30:13760–13765.
- Keil J, Müller N, Hartmann T, Weisz N. 2014. Prestimulus beta power and phase synchrony influence the sound-induced flash illusion. *Cereb Cortex*. 24:1278–1288.
- Kelly SP, Gomez-Ramirez M, Foxe JJ. 2009. The strength of anticipatory spatial biasing predicts target discrimination at attended locations: a high-density EEG study. *Eur J Neurosci*. 30:2224–2234.
- Kepecs A, Uchida N, Zariwala HA, Mainen ZF. 2008. Neural correlates, computation and behavioural impact of decision confidence. *Nature*. 455:227–231.
- Kiani R, Shadlen MN. 2009. Representation of confidence associated with a decision by neurons in the parietal cortex. *Science*. 324:759–764.
- Lange J, Halacz J, van Dijk H, Kahlbrock N, Schnitzler A. 2012. Fluctuations of prestimulus oscillatory power predict subjective perception of tactile simultaneity. *Cereb Cortex*. 22:2564–2574.
- Lange J, Oostenveld R, Fries P. 2011. Perception of the touch-induced visual double-flash illusion correlates with changes of rhythmic neuronal activity in human visual and somatosensory areas. *Neuroimage*. 54:1395–1405.
- Lange J, Oostenveld R, Fries P. 2013. Reduced occipital alpha power indexes enhanced excitability rather than improved visual perception. *J Neurosci*. 33:3212–3220.
- Linkenkaer-Hansen K, Nikulin VV, Palva S, Ilmoniemi RJ, Palva JM. 2004. Prestimulus oscillations enhance psychophysical performance in humans. *J Neurosci*. 24:10186–10190.
- Litvak V, Mattout J, Kiebel S, Phillips C, Henson R, Kilner J, Barnes G, Oostenveld R, Daunizeau J, Flandin G, et al. 2011. EEG and MEG data analysis in SPM8. *Comput Intell Neurosci*. 2011:852961.
- Lou B, Li Y, Philiastides MG, Sajda P. 2014. Prestimulus alpha power predicts fidelity of sensory encoding in perceptual decision making. *Neuroimage*. 87:242–251.
- Manshanden I, de Munck JC, Simon NR, Lopes da Silva FH. 2002. Source localization of MEG sleep spindles and the relation to

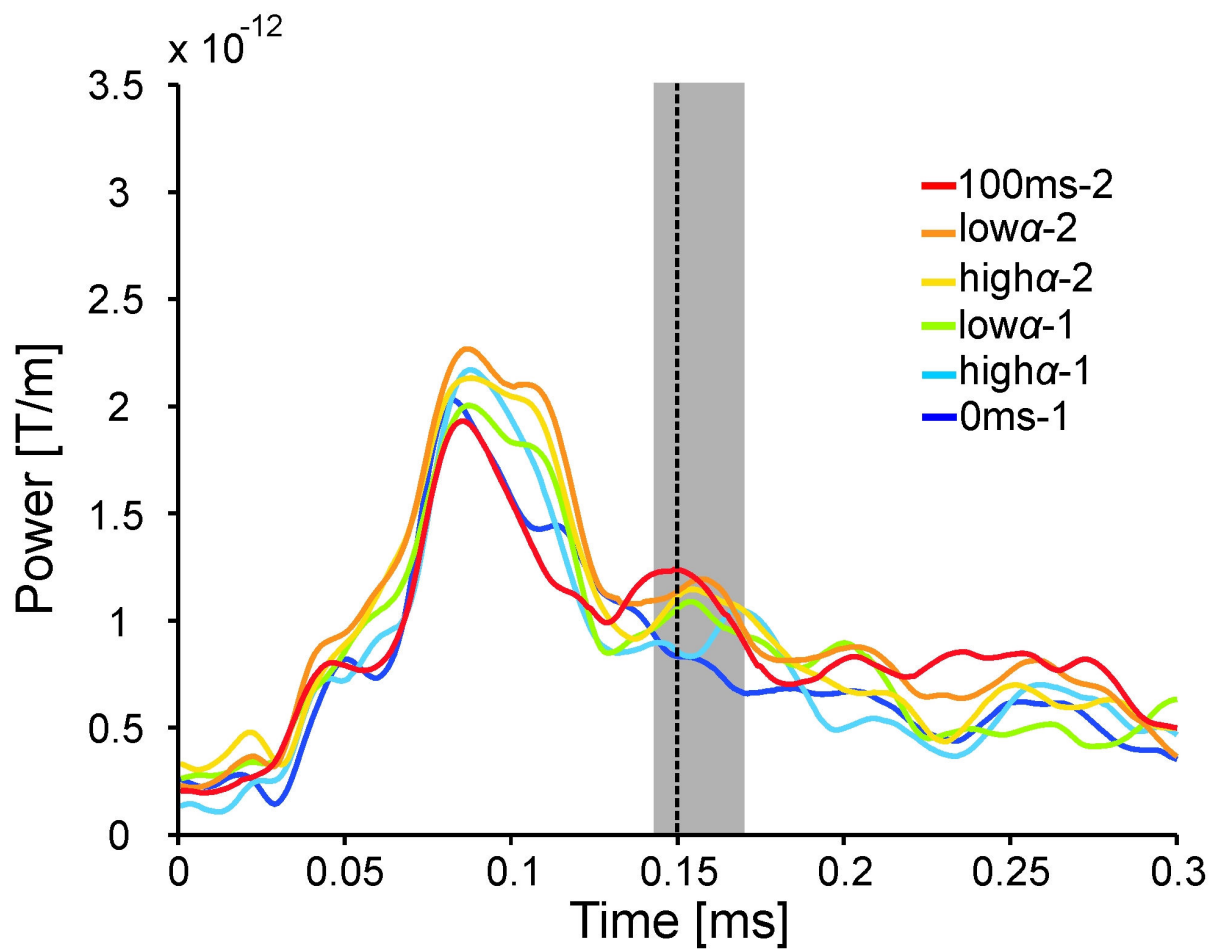
- sources of alpha band rhythms. *Clin Neurophysiol.* 113: 1937–1947.
- Maris E, Oostenveld R. 2007. Nonparametric statistical testing of EEG- and MEG-data. *J Neurosci Methods.* 164:177–190.
- Mathewson KE, Gratton G, Fabiani M, Beck DM, Ro T. 2009. To see or not to see: prestimulus α phase predicts visual awareness. *J Neurosci.* 29:2725–2732.
- Mazaheri A, Jensen O. 2008. Asymmetric amplitude modulations of brain oscillations generate slow evoked responses. *J Neurosci.* 28:7781–7787.
- Mazaheri A, Nieuwenhuis IL, van Dijk H, Jensen O. 2009. Prestimulus alpha and mu activity predicts failure to inhibit motor responses. *Hum Brain Mapp.* 30:1791–1800.
- Nolte G. 2003. The magnetic lead field theorem in the quasi-static approximation and its use for magnetoencephalography forward calculation in realistic volume conductors. *Phys Med Biol.* 48:3637–3652.
- O’Connell RG, Dockree PM, Kelly SP. 2012. A supramodal accumulation-to-bound signal that determines perceptual decisions in humans. *Nat Neurosci.* 15:1729–1735.
- O’Connell RG, Dockree PM, Robertson IH, Bellgrove MA, Foxe JJ, Kelly SP. 2009. Uncovering the neural signature of lapsing attention: electrophysiological signals predict errors up to 20 s before they occur. *J Neurosci.* 29:8604–8611.
- Oostenveld R, Fries P, Maris E, Schoffelen J. 2011. FieldTrip: open source software for advanced analysis of MEG, EEG, and invasive electrophysiological data. *Comput Intell Neurosci.* 2011:156869.
- Pfurtscheller G, Stancák A Jr, Neuper C. 1996. Event-related synchronization (ERS) in the alpha band—an electrophysiological correlate of cortical idling: a review. *Int J Psychophysiol.* 24:39–46.
- Philiastides MG, Ratcliff R, Sajda P. 2006. Neural representation of task difficulty and decision making during perceptual categorization: a timing diagram. *J Neurosci.* 26: 8965–8975.
- Philiastides MG, Sajda P. 2006. Temporal characterization of the neural correlates of perceptual decision making in the human brain. *Cereb Cortex.* 16:509–518.
- Ratcliff R, McKoon G. 2007. The diffusion decision model: theory and data for two-choice decision tasks. *Neural Comput.* 20:873–922.
- Romei V, Brodbeck V, Michel C, Amedi A, Pascual-Leone A, Thut G. 2008. Spontaneous fluctuations in posterior α -band EEG activity reflect variability in excitability of human visual areas. *Cereb Cortex.* 18:2010–2018.
- Romei V, Gross J, Thut G. 2010. On the role of prestimulus alpha rhythms over occipito-parietal areas in visual input regulation: correlation or causation? *J Neurosci.* 30:8692–8697.
- Romei V, Rihs T, Brodbeck V, Thut G. 2008. Resting electroencephalogram alpha-power over posterior sites indexes baseline visual cortex excitability. *Neuroreport.* 19:203–208.
- Salmelin R, Hari R. 1994. Characterization of spontaneous MEG rhythms in healthy adults. *Electroencephalogr Clin Neurophysiol.* 91:237–248.
- Schubert R, Haufe S, Blankenburg F, Villringer A, Curio G. 2008. Now you’ll feel it, now you won’t: EEG rhythms predict the effectiveness of perceptual masking. *J Neurosci.* 21:2407–2419.
- Shadlen MN, Newsome WT. 2001. Neural basis of a perceptual decision in the parietal cortex (Area LIP) of the rhesus monkey. *J Neurophysiol.* 86:1916–1936.
- Thut G, Nietzel A, Brandt SA, Pascual-Leone A. 2006. α -band electroencephalographic activity over occipital cortex indexes visuospatial attention bias and predicts visual target detection. *J Cogn Neurosci.* 26:9494–9502.
- van Dijk H, Schoffelen J, Oostenveld R, Jensen O. 2008. Prestimulus oscillatory activity in the alpha band predicts visual discrimination ability. *J Neurosci.* 28:1816–1823.
- VanRullen R, Thorpe SJ. 2001. The time course of visual processing: from early perception to decision-making. *J Cogn Neurosci.* 13:454–461.
- Worden MS, Foxe JJ, Wang N, Simpson GV. 2000. Anticipatory biasing of visuospatial attention indexed by retinotopically specific α -band electroencephalography increases over occipital cortex. *J Neurosci.* 20:RC63.
- Wyart V, Tallon-Baudry C. 2009. How ongoing fluctuations in human visual cortex predict perceptual awareness: baseline shift versus decision bias. *J Neurosci.* 29:8715–8725.
- Yeung N, Summerfield C. 2012. Metacognition in human decision-making: confidence and error monitoring. *Philos Trans R Soc Lond B Biol Sci.* 367:1310–1321.
- Zhang Y, Ding M. 2009. Detection of a weak somatosensory stimulus: role of the prestimulus mu rhythm and its top-down modulation. *J Cogn Neurosci.* 22:307–322.

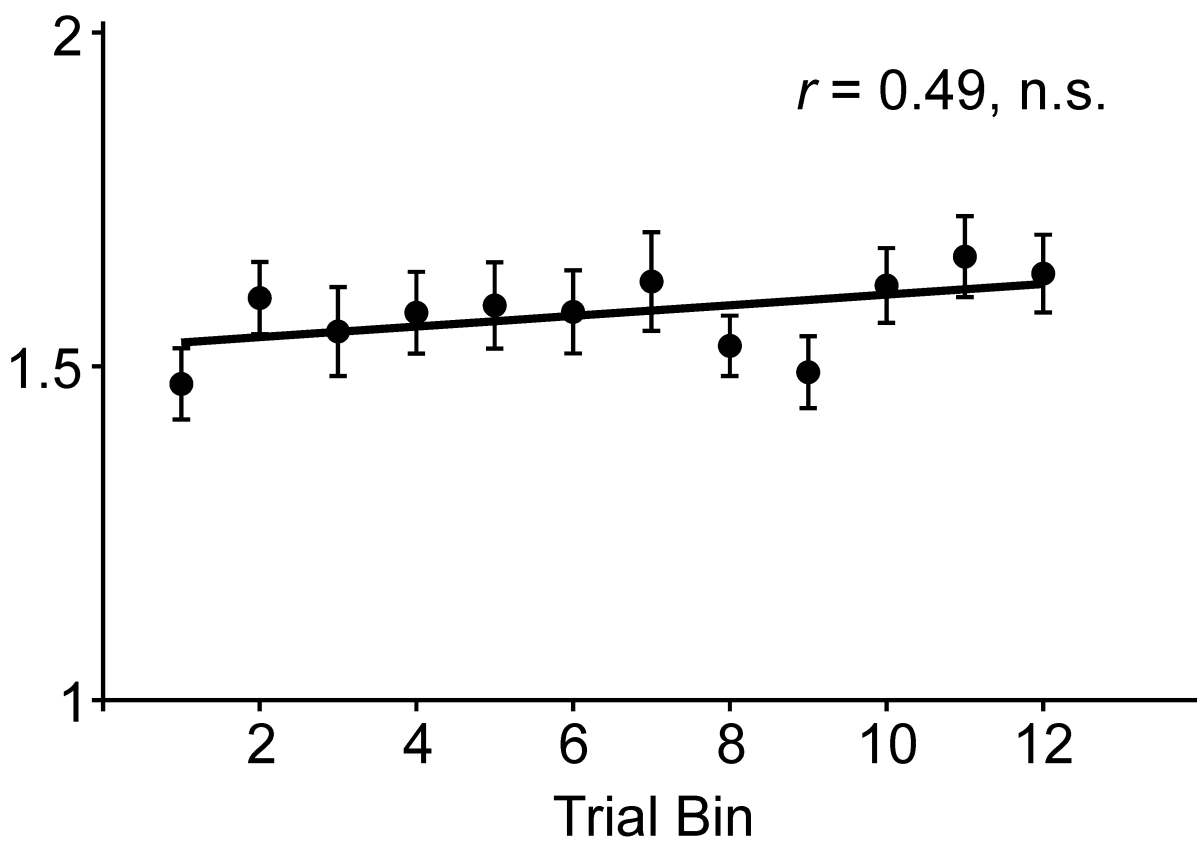
Supplementary Figures

Figure S1. Results of the analysis of poststimulus ERFs. Statistical comparison of poststimulus ERF amplitudes (averaged over all significant sensors, as shown in Fig. 2B) of correctly perceived trials with 0 ms (0ms-1) and 100 ms (100ms-2) SOA. Significant differences are indicated by shaded area (145 to 171 ms). Significance values were cluster corrected to account for multiple comparisons corrections. $t = 0$ indicates onset of sensory stimulation, i.e. the first stimulus of stimulation.

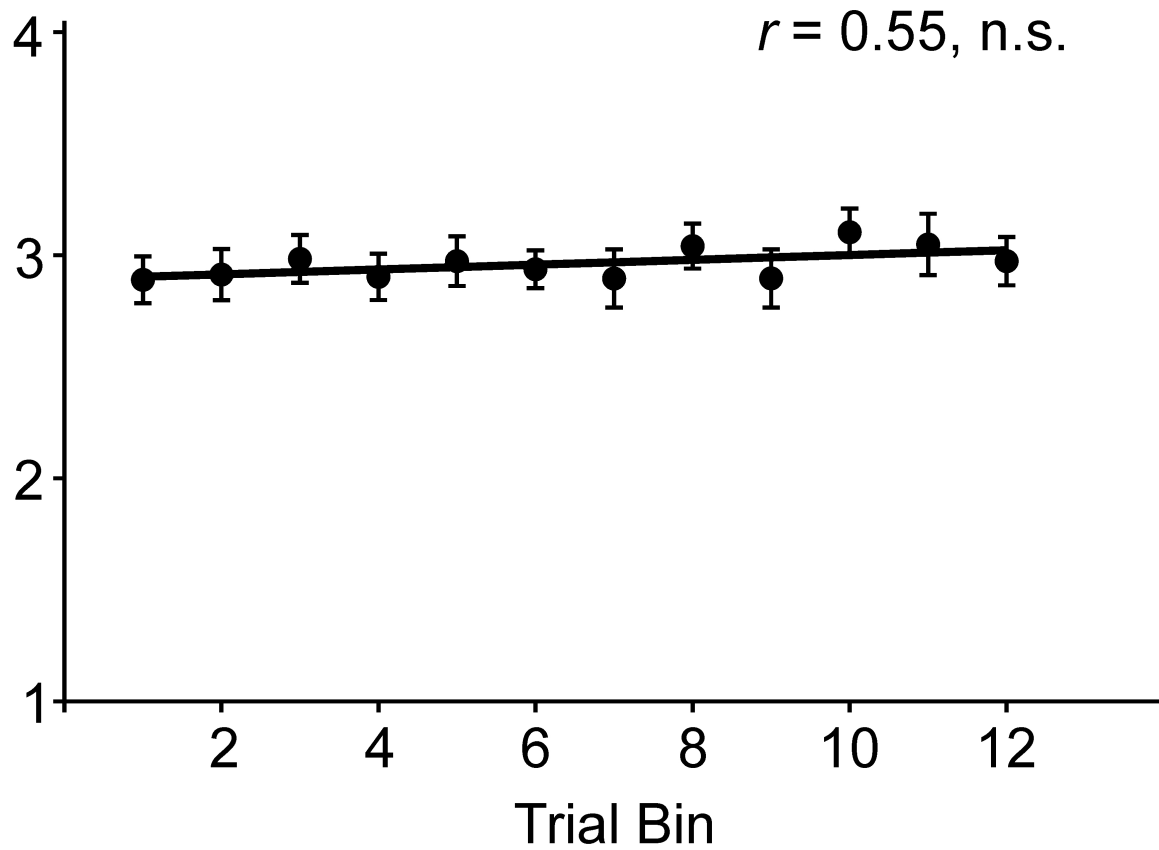
Figure S2. Analysis of behavioral parameters across the experiment. **A)** Average temporal perceptual discrimination rate (1 = incorrectly (perceived one stimulus) vs. 2 = correctly (perceived two stimuli) perceived trial) per bin for all trials with intermediate SOA. **B)** Average confidence rating (4 = very high confidence, 3 = rather high confidence, 2 = rather low confidence, 1 = very low confidence) per bin for all trials with intermediate SOA. Insets show results of the linear regression analyses (black lines). Error bars represent SEM.

Figure S3. Topographical representation of poststimulus ERFs for different conditions (100ms-2, 0ms-1, low α -2, high α -2, low α -1, high α -1, intermediate trials hits, intermediate trials misses) averaged over the time window of significant difference (145 to 171 ms) between poststimulus ERF amplitudes of correctly perceived trials with 0ms and 100ms SOA (averaged over all significant sensors, as shown in Fig. 2B).

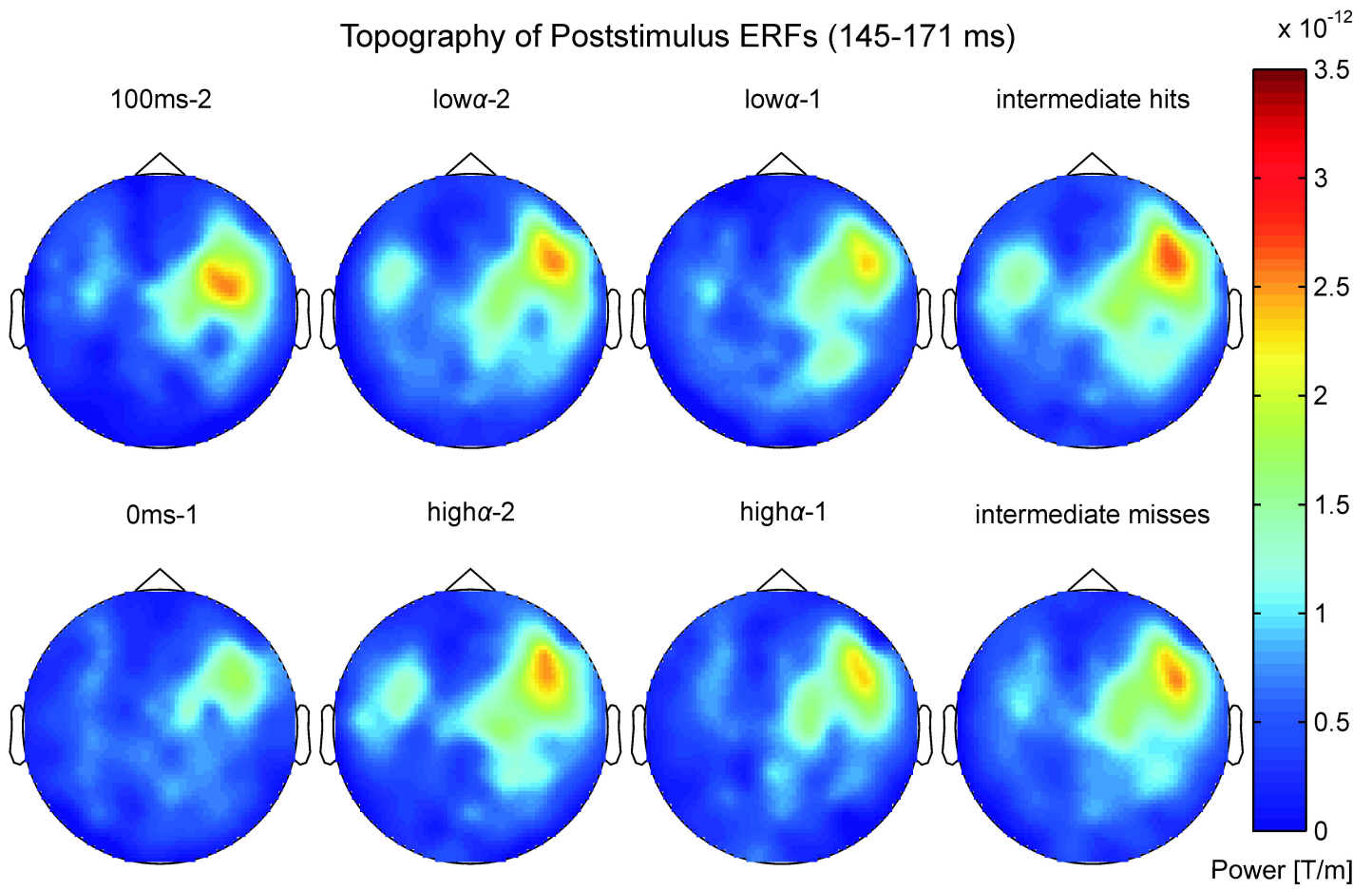


AAverage Temporal Perceptual
Discrimination Rate**B**

Average Confidence Rating



Topography of Poststimulus ERFs (145-171 ms)



Beta oscillations define discrete perceptual cycles in the somatosensory domain

Thomas J. Baumgarten¹, Alfons Schnitzler, and Joachim Lange

Institute of Clinical Neuroscience and Medical Psychology, Medical Faculty, Heinrich-Heine-University Düsseldorf, 40225 Düsseldorf, Germany

Edited by Ranulfo Romo, Universidad Nacional Autónoma de México, Mexico City, D.F., Mexico, and approved July 31, 2015 (received for review January 22, 2015)

Whether seeing a movie, listening to a song, or feeling a breeze on the skin, we coherently experience these stimuli as continuous, seamless percepts. However, there are rare perceptual phenomena that argue against continuous perception but, instead, suggest discrete processing of sensory input. Empirical evidence supporting such a discrete mechanism, however, remains scarce and comes entirely from the visual domain. Here, we demonstrate compelling evidence for discrete perceptual sampling in the somatosensory domain. Using magnetoencephalography (MEG) and a tactile temporal discrimination task in humans, we find that oscillatory alpha and low beta-band (8–20 Hz) cycles in primary somatosensory cortex represent neurophysiological correlates of discrete perceptual cycles. Our results agree with several theoretical concepts of discrete perceptual sampling and empirical evidence of perceptual cycles in the visual domain. Critically, these results show that discrete perceptual cycles are not domain-specific, and thus restricted to the visual domain, but extend to the somatosensory domain.

somatosensory perception | beta oscillations | MEG | oscillatory phase

The sensory system continuously receives and processes numerous stimuli. Subjective experience implies that conscious perception, and thus cortical processing, of this stimulation is also continuous. This view of continuous cortical processing, however, has been challenged by several studies proposing that the brain operates discontinuously within a framework of discretely sampled “perceptual cycles” (1–4). This process of perceptual cycles is thought to create a temporally defined window, with discrete stimuli falling inside this window being consciously perceived as a single event (4). Discrete sampling of sensory information allows for the possibility of transforming perceptual input into temporal code (5, 6), metabolic efficiency (7), and the efficient organization of information, thereby preventing information overload (6). Over the past decades, however, there has been an ongoing discussion about the nature of perception. Several studies have argued against the theory of discontinuous perceptual cycles (8, 9). In recent years, the hypothesis of a discontinuous cyclic perception received new support by electroencephalography (EEG) and magnetoencephalography (MEG) studies investigating neuronal oscillations. This novel support is attributable to the theory that serial perceptual sampling is thought to depend on the temporal relationship between external stimuli and some ongoing internal neurophysiological process (4) providing a temporal reference frame (5), with neuronal oscillations representing a probable candidate measure for this underlying process.

There is growing evidence that oscillatory power and phase influence cortical processing (10, 11) and perception (3, 12–14). Most of these studies investigated perception of single near-threshold stimuli. Although these studies demonstrate that neuronal oscillations play a critical role in defining neuronal states, which, in turn, influence perception and neuronal processing (5, 15, 16), these studies do not provide direct evidence for or against the theory of perceptual cycles. Recent studies, however, argued that parietooccipital alpha oscillations (~8–12 Hz) might define cycles of perception (6, 15, 17–19). However, they only provide evidence for discrete perceptual sampling in the visual domain. To claim that discrete perception is not domain-specific, it

is critical to demonstrate discrete and cyclic perception also for other sensory modalities and whether different modalities work via the same mechanism (e.g., whether alpha cycles generally define critical perceptual cycles for all modalities). Because sensory modalities work on different time scales, there is some indication that the mechanisms might differ.

We investigated whether discrete perceptual cycles exist in the somatosensory domain. Contrary to most studies in the visual domain, we used discrete rather than continuous stimuli, which differed only in perceptual impact, yet not in physical stimulation parameters. By this method, we could study whether two successively presented stimuli are perceived as either one single or two separate sensory events, depending on their temporal relationship to discrete perceptual cycles defined by the ongoing neuronal oscillatory phase. This setup allowed us to test the theory of discrete perceptual sampling critically in the somatosensory domain, and thus whether cycles of perception represent a mechanism of conscious perception that exists beyond the visual domain.

Results

Behavioral Results. Subjects received one or two electrical pulses separated by a specific stimulus onset asynchrony (SOA; nomenclature is provided in *Materials and Methods*) and had to perform a forced-choice temporal discrimination task (Fig. 1), wherein they had to report whether they perceived one or two stimuli. Subjects made negligible errors for the conditions 0 ms and 100 ms [SOA 0 ms: $97.7 \pm 0.4\%$ (mean \pm SEM) reports of correctly perceiving one stimulus, SOA 100 ms: $94.6 \pm 2.3\%$ reports of correctly perceiving two stimuli]. Individually determined, intermediate SOAs yielded correct perception of two stimuli in ~50% of the trials ($58.0 \pm 3.1\%$ reports). For the condition intermediate – 10 ms, subjects perceived two stimuli in $25.6 \pm 4.7\%$ reports, and for intermediate + 10 ms, subjects perceived two stimuli in $79.1 \pm 4.7\%$ reports. A one-way repeated

Significance

Our sensory system constantly receives multiple inputs, which are usually perceived as a seamless stream. Thus, perception is commonly regarded as a continuous process. Alternatively, a few phenomena and recent studies suggest that perception might work in a discrete and periodic sampling mode. In a human magnetoencephalography study, we challenged the common view of continuous perception. We demonstrate that neuronal oscillations in the alpha band and low beta band determine discrete perceptual sampling windows in primary somatosensory cortex. The current results elucidate how ongoing neuronal oscillations shape discrete perceptual cycles, which constitute the basis for a discontinuous and periodic nature of somatosensory perception.

Author contributions: J.L. designed research; T.J.B. performed research; T.J.B. and J.L. analyzed data; and T.J.B., A.S., and J.L. wrote the paper.

The authors declare no conflict of interest.

This article is a PNAS Direct Submission.

¹To whom correspondence should be addressed. Email: thomas.baumgarten@med.uni-duesseldorf.de.

This article contains supporting information online at www.pnas.org/lookup/suppl/doi:10.1073/pnas.1501438112/-DCSupplemental.

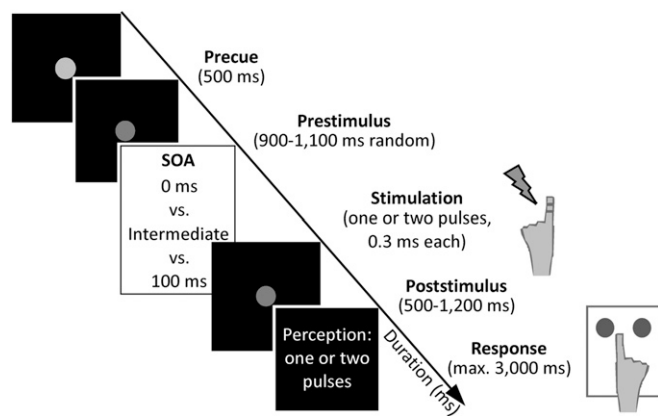


Fig. 1. Experimental paradigm. The sequence of events begins with presentation of a central fixation dot (500 ms). Luminance decrease signals start at the prestimulus epoch (900–1,100 ms), after which tactile stimulation is applied to the left index finger with varying SOAs (0 ms, intermediate – 10 ms, intermediate, intermediate + 10 ms, 100 ms). Stimulation is followed by a jittered poststimulus period (500–1,200 ms), after which written instructions signal subjects to report their respective perception of the stimulation by pressing a button.

measures ANOVA comparing average hit rates between conditions demonstrated a highly significant difference [$F(4,60) = 141.25, P < 0.001$]. Post hoc t tests revealed significant differences between the condition 0 ms vs. intermediate – 10 ms [$t(15) = 5.14, P < 0.01$], 0 ms vs. intermediate [$t(15) = 18.34, P < 0.001$], 0 ms vs. intermediate + 10 ms [$t(15) = 15.79, P < 0.001$], 0 ms vs. 100 ms [$t(15) = -37.15, P < 0.001$], intermediate – 10 ms vs. intermediate [$t(15) = 7.36, P < 0.001$], intermediate – 10 ms vs. intermediate + 10 ms [$t(15) = -7.15, P < 0.001$], intermediate – 10 ms vs. 100 ms [$t(15) = -13.1, P < 0.001$], intermediate vs. intermediate + 10 ms [$t(15) = -5.35, P < 0.001$], intermediate vs. 100 ms [$t(15) = -12.54, P < 0.001$], and intermediate + 10 ms vs. 100 ms [$t(15) = -3.79, P < 0.01$].

Phase Angle Contrast. To study the influence of oscillatory phase angles on perception, we sorted trials with intermediate SOA according to perceptual response (perceived one or two stimuli), resulting in two perceptual conditions (intermediate1 vs. intermediate2). We computed phase angles for each condition in source space by means of a virtual channel in the primary somatosensory cortex (S1) (Fig. 2A) and contrasted the phases of intermediate2 with intermediate1 (Fig. S1). The analysis revealed a significant positive cluster ($P < 0.05$; Fig. 2B) in the prestimulus epoch (–0.53 to –0.09 s) for frequencies in the alpha band and

lower beta band (8–20 Hz). Notably, the effect was more prominent and temporally extended in the beta band (14–20 Hz, –0.53 to –0.09 s) compared with the alpha band (8–12 Hz, –0.39 to –0.24 s). That is, the phase difference between perceptual conditions differed significantly more in this time-frequency range compared with randomly distributed phases. For frequencies in the lower beta band, phase difference fluctuated around maximum (i.e., π) in the prestimulus period (Fig. 2C). To exclude any bias due to power differences, we analyzed power differences between perceptual conditions for those time-frequency elements exhibiting significant phase differences (analysis parameters are provided in ref. 14). The results did not reveal any significant power differences ($P > 0.05$, uncorrected). Regarding phase angle differences, we found an additional significant negative cluster ($P < 0.05$; Fig. 2B) between 2 and 28 Hz and between –0.1 and 0.24 s. Here, phase differences were significantly smaller compared with randomly distributed phases. This effect presumably resembles the phase resetting after stimulus presentation (18, 20).

Phase Angles and Perception. To analyze the extent by which perception was influenced by phase, we computed for each subject the momentary phase for each single trial for both perceptual conditions at the time point showing the largest statistical phase difference effect (*Materials and Methods*). Trials were placed in one of six different phase bins and aligned for each subject so that the highest probability for perceiving two stimuli corresponded to a zero phase angle. For each subject, we calculated the normalized perceptual response rate per bin, and we then averaged normalized response rates across subjects (Fig. 2D). Although this analysis resembles a post hoc test (because it is based on the time-frequency points of maximal phase difference determined in the previous analysis), it quantifies the magnitude by which phase influences perception, as well as the grade by which performance varies over different phase bins. A one-way repeated measures ANOVA comparing normalized perceptual response rates between bins demonstrated a highly significant difference [$F(4,60) = 6.53, P < 0.001$]. Post hoc t tests revealed significant differences between bin 1 vs. bin 3 [$t(5) = -4.17, P < 0.01$], bin 1 vs. bin 5 [$t(5) = -4.21, P < 0.01$], bin 1 vs. bin 6 [$t(5) = -4.13, P < 0.01$], bin 2 vs. bin 3 [$t(5) = -2.77, P < 0.05$], and bin 2 vs. bin 5 [$t(5) = -3.16, P < 0.01$]. The results indicate a monotonic decrease of mean response rate from zero phase angle to π , with the response rates differing by 13% points between the lowest ($-\pi$, 38%) and highest ($1/3 \pi$, 51%) phase bins (with exclusion of the zero phase bin).

Beta-Band Cycles Determine Perceptual Cycles. Fig. 3 illustrates a model derived from the analysis of phase angle contrasts and the theory of temporal framing (3, 19, 21). The model proposes that

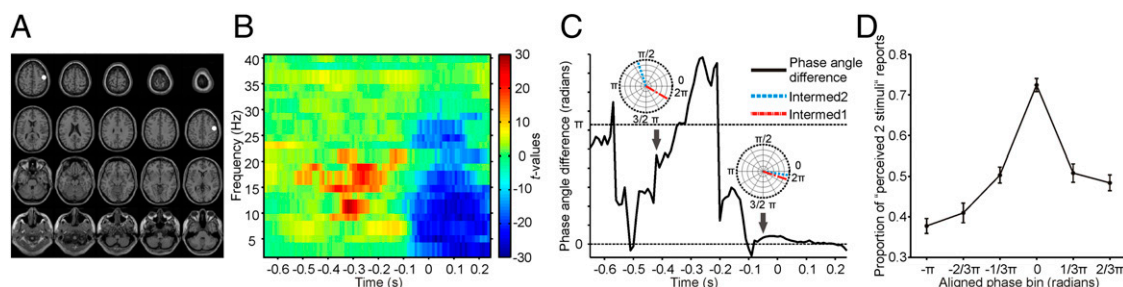


Fig. 2. Virtual sensor location and phase angle differences. (A) Virtual sensor location based on the voxel of maximum activity of the contrast M50 vs. prestimulus baseline. The voxel is highlighted on a slice plot of the Montreal Neurological Institute (MNI) template brain (MNI coordinates: 50 –10 50). (B) Time-frequency plot showing the results of the statistical analysis of phase angle differences between intermediate2 vs. intermediate1. Significant clusters ($P < 0.05$, corrected) are highlighted. Red colors indicate higher phase differences compared with randomly distributed phases. $t = 0$ indicates onset of the first stimulus. (C) Phase angle difference (black solid line) between intermediate2 (Intermed2) and intermediate1 (Intermed1) for an exemplary 14-Hz band. The upper dashed line indicates the maximum phase angle difference (π). (Insets) Phase angles for intermediate2 (blue lines) and intermediate1 (red lines) for exemplary time points (Left, $t = -420$ ms; Right, $t = -50$ ms). (D) Relationship between the momentary phase (*Materials and Methods*) and the normalized perceptual response rate. The probability of perceiving two stimuli significantly depends on the phase angle and differs maximally between opposite phase angles (ANOVA, $P < 0.001$).

the temporal resolution of perception is defined by one cycle of a specific frequency. If presented within one cycle, the two stimuli are merged into one perceptual event and perceived as one single stimulus (Fig. 3A, white rectangles). If presented within two separate cycles, they will be perceived as two temporally separate perceptual events (Fig. 3A, black rectangles). Although the neural representation of the first stimulus can arrive at any point in the oscillatory cycle (21) for ongoing oscillations, the arrival of the second stimulus is determined by the SOA. For a cycle length twice as long as the respective SOA, a stimulus arriving in the first half of the cycle determines the arrival of the second stimulus in the same cycle (one perceived stimulus). Vice versa, a stimulus arriving in the second half of the cycle determines the arrival of the second stimulus in a subsequent cycle (two perceived stimuli). From the results of the phase angle contrast analysis, we derive that this critical frequency band lies in the alpha band and, particularly, the lower beta band between 8 and 20 Hz (Fig. 2B). Given these model preconditions, we can make two predictions. First, if the SOA between two stimuli equals half the length of the cycle of the critical frequency (e.g., 25 ms for a 20-Hz oscillation), mean phases for the perception of one stimulus (range: 0 to π for the example in Fig. 3A) and two stimuli (range: π to 2π) should differ maximally ($\sim\pi$). More precisely, perception rates should critically depend on the phase at which the first stimulus arrives (Fig. 3B–D). That is, if the stimulus arrives at a given phase ϕ , perception rates should differ significantly from $\phi + \pi$. Second, if the critical frequency is known, we can predict behavioral response rates for different SOAs. The first prediction is confirmed by the analysis of phase angle contrast (Fig. 2B and C). Based on these results, the post hoc phase binning analysis shows a monotonic decrease in perception over bins, and, thus, the dependence of perception rates on phase (Fig. 2D). The second prediction will be tested and presented below.

Prediction of Perception. Based on the model (Fig. 3), we predicted response rates for the different SOAs and computed linear regressions between predicted and behaviorally measured response rates. We computed predictions based on (i) group-level effect frequencies determined from MEG experimental data (8–20 Hz; Fig. 2B), (ii) based on single subject-level individual frequencies determined from MEG experimental data (Fig. S2 and Table S1), and (iii) based on frequencies determined from behavioral experimental data (i.e., the intermediate SOAs):

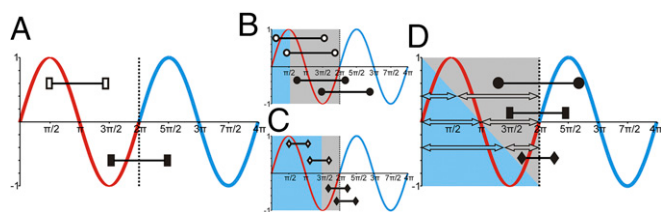


Fig. 3. Model for perceptual cycles. (A) Red and blue lines illustrate two perceptual cycles. Two stimuli can occur within one (white rectangles, one stimulus perceived) or two (black rectangles, two separate stimuli perceived) perceptual cycles. (B) Same as in A, but for stimulus pairs with a longer SOA. The blue background illustrates the time frame in which the occurrence of the first stimulus results in one perceived stimulus (○), and the gray background illustrates the time frame in which the occurrence of the first stimulus results in two perceived stimuli (●). (C) Same as in B, but for stimuli with a shorter SOA. Note different lengths of blue and gray time frames. (D) Same as in B, but for examples of three different SOAs. Intermediate SOAs (rectangles) result in time frames for one (blue arrows) or two (gray arrows) perceived stimuli of approximately equal length. For longer SOAs (●), the time frame for two perceived stimuli (gray arrows) is bigger than for one perceived stimulus (blue arrows). For shorter SOAs (○), the time frame for two perceived stimuli (gray arrows) is smaller than for one perceived stimulus (blue arrows).

- i) Based on group-level effect frequencies (8–20 Hz; Fig. 2B), the linear regression analysis for behavioral response rates and predicted response rates (Fig. 4) resulted in a highly significant correlation coefficient ($r = 0.93$, $P < 0.01$). The resulting slope estimate (0.83 ± 0.1) did not differ significantly from 1 [$t(4) = -1.8$, $P > 0.05$].
- ii) Linear regression analysis of the individual behavioral and predicted individual response rates resulted in a significant correlation coefficient in all 16 subjects (r ranging from 0.69 to 0.96, $P < 0.05$). For 12 of 16 subjects, the resulting slope estimate did not differ significantly from 1 [$t(4)$ ranging from -2.6 to 2.4 , $P > 0.05$; Fig. S2 and Table S1]. We additionally predicted group-level response rates by averaging the individual response rates over subjects. The resulting predictions were virtually similar to the predictions based on the averaging over group-level effect frequencies (i) (Fig. 4). The resulting slope estimate (0.78 ± 0.1) did not differ significantly from 1 [$t(4) = -2.23$, $P > 0.05$].
- iii) Predictions based on frequencies determined from behavioral experimental data yielded results highly similar to those results determined from MEG experimental data (details are provided in SI Results).

Discussion

We investigated the neuronal mechanisms of varying conscious perception in the somatosensory domain. The results argue against a continuous perceptual mechanism and provide evidence that somatosensory perception operates in a discrete mode, with sensory input being sampled by discrete perceptual cycles in the alpha band and, in particular, the lower beta band (8–20 Hz).

Beta-Band Cycles Determine Discrete Perceptual Sampling. We found that phase angles in S1 in the alpha band and lower beta band (8–20 Hz) before stimulus onset predicted whether subjects perceived two constant electrical stimuli with an SOA of ~ 25 ms as one or two stimuli (Fig. 2B). Notably, this effect was most prominent in the lower beta band (14–18 Hz). We put forward a model proposing that somatosensory stimulation is discretely sampled and that the underlying perceptual cycles are determined by ongoing oscillatory alpha and beta cycles (Fig. 3). If multiple discrete stimuli fall within one perceptual cycle, the temporally fine-grained information is lost and the distinct stimuli are fused to a single percept, a phenomenon that has been labeled perceptual or temporal framing in the visual domain (3, 19, 21). The model was confirmed by two theoretical predictions. First, beta oscillations were found to be antiphasic (phase difference of π) for perception of one vs. two stimuli for intermediate SOAs (~ 25 ms; Fig. 2B–D). Based on these results, response rates were shown to depend on the specific phase at which the first stimulus arrives (Fig. 2D). Second, the model predicts behavioral performance on group (Fig. 4) and single-subject (Fig. S2) levels.

Based on behavioral response rates, the model predicted a theoretical critical sampling frequency of ~ 23 Hz. The experimentally observed frequency range based on statistical analysis of phase angles revealed a significant effect between 8 and 20 Hz. Whereas the upper end of the experimental frequency range is close to the theoretically assumed frequency, the experimental frequency band also includes lower frequencies. A potential reason for this underestimation of the critical sampling frequency might be a decreased signal-to-noise ratio for higher frequencies. Noninvasive measurement (e.g., via EEG/MEG) of phase has been assumed to be especially susceptible to various interferences (e.g., delays in synaptic transmission) at higher frequencies (5). Likewise, phase differences in lower frequency bands could also resemble processes different than perceptual sampling (e.g., attentional processes) (22). This idea is in line with the different temporal distributions of phase angle differences for alpha- and beta-band frequencies. Finally, the presented model does not claim to cover all portions of the decision process determining the final response but, instead, focuses on early perceptual components. For example, the present data are derived

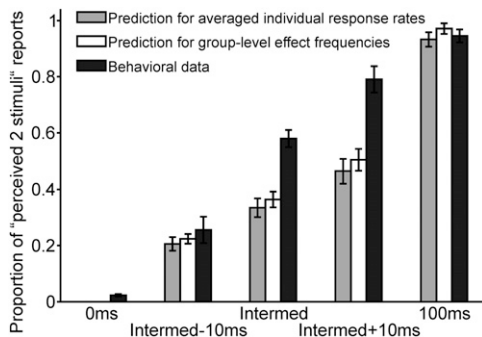


Fig. 4. Model prediction of response rates. Proportion of “perceived two stimuli” reports for conditions with different SOAs for model predictions based on averaged individual response rates (gray bars), significant group-level frequencies (8–20 Hz, white bars), and behavioral data (black bars). Predicted responses based on frequencies were calculated per frequency bin and then averaged over all respective frequencies. Hit rates are presented as mean \pm SEM.

from S1, thus not taking into account other cortical areas involved in the decisional process.

Discrete Perceptual Sampling Is Not a Domain-Specific Mechanism.

The theory of discrete perceptual cycles was introduced decades ago (1, 2). However, it has been controversially discussed (8, 9). Recently, the discussion on discrete perceptual cycles has gained new momentum by studies using EEG, which allows one to study potential neuronal mechanisms of discrete perceptual cycles noninvasively (5, 17, 22). Nonetheless, empirical evidence to support the theory of discrete perceptual cycles remains scarce and focuses mainly on the visual domain (3, 17), whereas evidence for discrete cycles in other domains is largely missing (19). The present study is thus, to our knowledge, the first to demonstrate the existence of perceptual cycles in the somatosensory domain, indicating that the cyclic characteristic of perception is not a domain-specific visual mechanism (19).

Modality-Specific Differences. For the visual domain, EEG studies propose discrete cycles in perception and attentional updating defined by the alpha cycle (3, 17, 22). Our model agrees with these studies, albeit we propose perceptual cycles to be defined by alpha-band and, decisively, beta-band frequencies in the somatosensory domain. Although the significant group-level phase angle differences cover a rather broad band between 8 and 20 Hz, the major effect can be found in a narrower band between 14 and 18 Hz (Fig. 2B). Because subjects exhibit different individual intermediate SOAs, different individual frequencies for the discrete perceptual cycles are also to be expected (thereby blurring the group-level effect). In fact, the analyses based on individually determined frequencies confirmed that the individual narrow-band frequencies represent an appropriate predictor for individual response rates (Fig. S2). These domain-specific differences agree with a more prominent role of alpha oscillations in the visual domain for perception and neuronal processing (23, 24), whereas there is experimental evidence for a specific role of beta oscillations in the somatosensory domain (10, 13, 25–27). The present findings are in line with studies investigating steady-state somatosensory evoked potentials (SSSEPs). These studies found that the largest SSSEP amplitudes can be achieved by a stimulation frequency of \sim 18–26 Hz (i.e., in the beta band) (27–29). Stimulation at this frequency would place every stimulus in a separate beta cycle, therefore enhancing SSSEPs and, consequently, facilitating perceptual detection (26). Finally, the proportion perceiving two stimuli differed by 13% between the lowest ($-\pi$) and the highest ($1/3\pi$) phase bins (with exclusion of the zero phase bin). This difference agrees with ranges reported for visual stimuli (5, 15). Thus, both visual and somatosensory

perception seems to be influenced by phase with a comparable magnitude.

What About Absolute Phase Angles? Varela et al. (3) reported that the phase of occipital alpha oscillations determines whether subjects perceive two sequential visual stimuli as one or two stimuli. The respective phase for perceiving one vs. two stimuli was anticyclic (i.e., the phase difference was π). Although later studies failed to replicate this result (19, 30), our results support the finding by Varela et al. (3), because we find a phase difference of π between phases for perceiving one vs. two tactile stimuli. In contrast to Varela et al. (3), however, we do not claim that the specific phase (the peak or trough) is important for perception but, rather, whether two stimuli fall within a single cycle or separate cycles. The majority of studies investigating the influence of oscillatory phase on perception analyzed absolute phase angles within an oscillatory cycle at a specific moment, which are either favorable or unfavorable for subsequent perception (5, 11, 12, 15, 31). Thus, a potential concern might be that our results could be explained by favorable or unfavorable phases within one cycle. In such a framework, one stimulus might be presented at a favorable phase and the other stimulus might be presented at an unfavorable phase, thus leading to the erroneous perception of only one stimulus. The above-mentioned studies, however, used near-threshold stimuli. We presented stimuli with clearly suprathreshold intensities that are presumably perceived independent of the specific phase. Although a hypothesis proposing an influence of (un)favorable phases would predict that \sim 50% of the stimuli with SOA 0 ms would be missed, subjects correctly perceived almost all stimuli. Similarly, such a framework would predict a higher percentage of trials with SOA 100 ms to be perceived as one stimulus than found in our behavioral data. Therefore, the present results cannot be explained by favorable or unfavorable phases within one oscillatory cycle.

Differentiating Effects of Phase and Power. Recent studies demonstrated an influence of oscillatory power for perception of single (near-threshold) tactile stimuli, as well as for the temporal discrimination of two tactile stimuli (10, 25). The majority of these studies [including a previous study by our group on the dataset presented in this study (14)] found prestimulus power differences in the alpha band (8–12 Hz), whereas the present phase angles differed mostly in the lower beta band (14–18 Hz). Further, we found no significant power differences in those time-frequency elements showing significant phase angle differences between perceptual conditions. It is thus unlikely that the presented phase effect was biased by power differences. Indeed, there is experimental evidence for an influence of both oscillatory power (10) and phase (12, 31) for neuronal processing and perception, and recent studies could demonstrate that these measures act largely independently (5, 22). This differentiation is further supported by results showing that phase is able to transport more units of information per time than power changes (32) or spike counts (33), and represents a suitable candidate measure to encode fast-changing stimulus features (21).

Contradicting Subjective Experience. There is accumulating evidence that our brain processes incoming stimulus information in a phasic mode (3, 17). However, personal experience does not intuitively match with a discrete sequencing approach but, rather, resembles a seamlessly updated percept. This divergence might explain why relatively few studies address this topic, although the concept of discrete perceptual sampling has been put forward at least since the middle of the 20th century (1, 2). It remains an open question how the brain transforms discretely sampled sensory information into a subjectively seamless impression. Although the mechanisms for such perceptual “smoothing” are unknown, there are, at least for the visual domain, several reports where the mechanisms fail to work (34). For example, in akinetopsia, subjects report perceiving a sequence of snapshots rather than a continuous motion (35, 36). Similarly, the ingestion of lysergic acid diethylamide often results in a perceptual disturbance

wherein visual motion is perceived as a sequence of discrete stationary images (37, 38).

Conclusions

The present study demonstrates an influence of oscillatory phase on the temporal perception of two stimuli. We propose the existence of discrete perceptual cycles for the conscious perception of subsequently presented tactile stimuli. The perceptual cycles are determined particularly by frequencies in the beta band acting as the specific physiological correlate for perceptual cycles for the somatosensory modality. In combination with previous studies investigating similar paradigms in the visual domain (3, 30), the present results support the theory of temporal framing (1–3, 19, 21) and indicate that perceptual cycles are no domain-specific visual phenomenon, albeit modality-specific frequencies that define perceptual cycles seem to be present.

Materials and Methods

Subjects. The subjects, stimuli, paradigm, and MEG recording of the present study were previously reported in detail (14). Here, we present a comprehensive overview. Sixteen right-handed volunteers [seven males, age: 26.1 ± 4.7 y (mean \pm SD)] participated in the study. Subjects provided written informed consent before the experiment in accordance with the Declaration of Helsinki and approved by the Ethical Committee of the Medical Faculty, Heinrich-Heine-University Düsseldorf.

Experimental Paradigm. Details on the paradigm can be found in the study by Baumgarten et al. (14). A comprehensive overview is provided in Fig. 1 and *SI Materials and Methods*.

MEG Data Recording and Preprocessing. Electromagnetic brain activity was continuously recorded using a 306-channel, whole-head MEG system (Neuromag Elekta Oy). Analysis was restricted to the gradiometers. Individual structural MRI scans were acquired using a 3-T MRI scanner (Siemens). Offline analysis of the data was carried out using custom-made MATLAB (MathWorks) scripts and the MATLAB-based open-source toolboxes FieldTrip (fieldtriptoolbox.org) (39), CircStat (40), and SPM8 (41). Continuously recorded data were segmented into trials. All trials were semiautomatically and visually inspected for artifacts, whereas artifacts caused by muscle activity, eye movements, or technical artifacts were removed semiautomatically using a z-score-based algorithm implemented in FieldTrip.

Virtual Channel Construction. To focus on S1, we analyzed oscillatory activity in a predefined region of interest in source space (“virtual sensor”). Details regarding the construction of the virtual sensor are provided in *SI Materials and Methods*.

Phase Angle Contrast. Oscillatory phase was calculated for the virtual sensor. We sorted trials with respect to the SOA for each subject separately, resulting in five different conditions defined by the length of the SOA (0 ms, intermediate – 10 ms, intermediate, intermediate + 10 ms, and 100 ms). Subsequently, we separated intermediate trials by perceptual response (perceived one vs. two stimuli, subsequently labeled intermediate1 vs. intermediate2). Because trial numbers are known to influence phase measures crucially (42), trial numbers were equated across conditions in each analysis by determining the condition with the lowest number of trials per subject and randomly selecting the same number of trials from the remaining conditions. To exclude potential effects due to a specific trial selection, we performed trial selection by means of random subsampling 100 times, and subsequently computed the median of the resulting phase parameters over these 100 repetitions (because F values were not normally distributed). The time point $t = 0$ was defined as the onset of the first stimulus. The oscillatory phase was calculated for each time-frequency element (–650 to 240 ms, 2–40 Hz) of each single trial by applying a discrete Fourier transform (DFT) on fixed sliding time windows with a length of 500 ms, moved in steps of 10 ms. Data segments were tapered with a single Hanning taper, resulting in a spectral smoothing of 2 Hz. For each subject s , trial r , frequency f , and time point t , we normalized the complex outcome $F_{s,r,f,t}$ of the DFT by dividing it by its absolute (abs) value, thus normalizing the signal by its amplitude:

$$F_{s,r,f,t}^{norm} = \frac{F_{s,r,f,t}}{\text{abs}(F_{s,r,f,t})} \quad [1]$$

From these normalized values, we computed for each subject s , trial r , frequency f , and time point t , the normalized phase:

$$\Phi_{s,r,f,t}^{norm} = \text{atan} \left(\frac{\text{Im} \left(F_{s,r,f,t}^{norm} \right)}{\text{Re} \left(F_{s,r,f,t}^{norm} \right)} \right) \quad [2]$$

where Im and Re are the imaginary part and real part, respectively, of the DFT.

To analyze statistically whether phase angles differed between perceptual conditions, we compared phase angles between the intermediate1 and intermediate2 conditions for each time-frequency element at the within-subject level by means of the Watson–Williams multisample test for equal means [CircStat toolbox (40)]. This test for circular data is equivalent to a two-sample t test for equal angular means. For each randomized trial selection, we compared phase angles for each subject independently for each time-frequency element, resulting in 100 F values for each time-frequency element. We took for each time-frequency element the median of all 100 F values, resulting in a time-channel map of F values for each subject, which constitutes the test distribution. To assess the consistency of phase angle differences over subjects, we performed a nonparametric randomization test identifying clusters in time-frequency space demonstrating a similarly directed phase angle difference relative to a null distribution (43). We computed this null distribution under the null hypothesis that phases are randomly and uniformly distributed, showing no difference between conditions. That is, for each subject, we assigned to each condition random phases (equaling the number of trials for each subject) and then repeated the above-mentioned statistical analysis. We compared (random) phase angles between both conditions for each time-frequency element at the within-subject level by applying the Watson–Williams test. This procedure was repeated 100 times (each time with new, randomly chosen phases), resulting in 100 F values for each time-frequency element. Subsequently, we took the median of all 100 F values for each time-frequency element, resulting in a time-channel map of F values for each subject, which constitutes the null distribution. We then statistically compared the F values of the test distribution with the F values of the null distribution for each time-frequency element by means of a dependent-samples t test, resulting in a time-frequency map of t values. Positive t values for a specific time-frequency element demonstrate a larger phase angle difference compared with randomly distributed phase angles, and vice versa for negative t values (44). To investigate whether the phase angle differences between perceptual conditions were significantly different from randomly distributed phases, we applied a cluster-based randomization approach (14). This statistical approach effectively controls for the type I error rate due to multiple comparisons across time points and channels (43).

To ensure that phase angle differences are not biased by power, we analyzed power differences between perceptual conditions for those time-frequency elements exhibiting significant phase differences. The respective analysis parameters are discussed in ref. 14. To visualize phase angle differences on the group level, we computed phase angle differences for each time-frequency element. We computed the circular distance between the over-trial averages of the intermediate2 and intermediate1 conditions for each subsampling run, and subsequently averaged circular distances over all subsampling runs on the single-subject level and over subjects (Fig. 2C).

Phase Angles and Perception. To determine to what extent perception of one or two stimuli is associated with different phase angles, we selected for each subject the time-frequency point showing the largest statistical phase angle effect (maximum Watson–Williams test F value) within the time-frequency range of the aforementioned phase contrast effect (8–20 Hz, -0.53 to -0.09 s; Fig. 2B). This analysis resembles a post hoc test based on previous results. For each subject, the momentary phase for the respective time-frequency point was computed for each single trial for both perceptual conditions. Subsequently, the trial was placed in one of six different, equally spaced phase bins (bin width = $1/3 \pi$), ranging from $-\pi$ to $+\pi$. For each subject, we calculated the normalized perceptual response rate per bin. We adjusted phase distributions for each subject so that the bin showing maximum perception of two distinct stimuli was aligned to a phase angle of zero (a similar procedure is described in refs. 5 and 11). This process was repeated for each of the 100 specific randomized trial selections. Subsequently, we computed the median of the normalized perceptual response rates for each bin across the 100 repetitions for random trial selection and averaged response rates over subjects (Fig. 2D). To assess an effect of phase angle on perceptual response rates, a one-way repeated measures ANOVA and post hoc paired sample t tests were conducted. Due to the realignment, we excluded the bin centered on zero from the statistical analyses.

Prediction of Perception. Based on the model (Fig. 3), we predicted response rates for the different SOAs and computed linear regressions between predicted and behaviorally measured response rates. We used different approaches to predict response rates, with each approach based on a slightly different method to determine the critical frequency: (i) based on group-level effect frequencies determined from MEG experimental data (Fig. 2B), (ii) based on single-subject individual frequencies determined from MEG

experimental data (Fig. S2 and Table S1), and (iii) based on frequencies determined from behavioral experimental data (i.e., the intermediate SOAs). The approaches are described in detail in *SI Materials and Methods*.

ACKNOWLEDGMENTS. We thank Erika Rädtsch for help with the MRI recordings. J.L. was supported by the German Research Foundation (Grant LA 2400/4-1). T.J.B. was supported by the German Research Foundation (SFB 974, B07).

1. Stroud JM (1956) *Information Theory in Psychology*, ed Quastler H (Free Press, Chicago), pp 174–205.
2. Harter MR (1967) Excitability cycles and cortical scanning: A review of two hypotheses of central intermittency in perception. *Psychol Bull* 68(1):47–58.
3. Varela FJ, Toro A, John ER, Schwartz EL (1981) Perceptual framing and cortical alpha rhythm. *Neuropsychologia* 19(5):675–686.
4. VanRullen R, Koch C (2003) Is perception discrete or continuous? *Trends Cogn Sci* 7(5):207–213.
5. Busch NA, Dubois J, VanRullen R (2009) The phase of ongoing EEG oscillations predicts visual perception. *J Neurosci* 29(24):7869–7876.
6. Jensen O, Gips B, Bergmann TO, Bonnefond M (2014) Temporal coding organized by coupled alpha and gamma oscillations prioritize visual processing. *Trends Neurosci* 37(7):357–369.
7. Schroeder CE, Lakatos P (2009) Low-frequency neuronal oscillations as instruments of sensory selection. *Trends Neurosci* 32(1):9–18.
8. Allport DA (1968) Phenomenal simultaneity and the perceptual moment hypothesis. *Br J Psychol* 59(4):395–406.
9. Kline KA, Eagleman DM (2008) Evidence against the temporal subsampling account of illusory motion reversal. *J Vis* 8(4):1–5.
10. Lange J, Halacz J, van Dijk H, Kahlbrock N, Schnitzler A (2012) Fluctuations of prestimulus oscillatory power predict subjective perception of tactile simultaneity. *Cereb Cortex* 22(11):2564–2574.
11. Ng BS, Schroeder T, Kayser C (2012) A precluding but not ensuring role of entrained low-frequency oscillations for auditory perception. *J Neurosci* 32(35):12268–12276.
12. Mathewson KE, Gratton G, Fabiani M, Beck DM, Ro T (2009) To see or not to see: Prestimulus alpha phase predicts visual awareness. *J Neurosci* 29(9):2725–2732.
13. Jones SR, et al. (2010) Cued spatial attention drives functionally relevant modulation of the mu rhythm in primary somatosensory cortex. *J Neurosci* 30(41):13760–13765.
14. Baumgarten TJ, Schnitzler A, Lange J (2014) Prestimulus alpha power influences tactile temporal perceptual discrimination and confidence in decisions. *Cereb Cortex*, 10.1093/cercor/bhu247.
15. Dugué L, Marque P, VanRullen R (2011) The phase of ongoing oscillations mediates the causal relation between brain excitation and visual perception. *J Neurosci* 31(33):11889–11893.
16. Lange J, Keil J, Schnitzler A, van Dijk H, Weisz N (2014) The role of alpha oscillations for illusory perception. *Behav Brain Res* 271:294–301.
17. Chakravarthi R, Vanrullen R (2012) Conscious updating is a rhythmic process. *Proc Natl Acad Sci USA* 109(26):10599–10604.
18. Romei V, Gross J, Thut G (2012) Sounds reset rhythms of visual cortex and corresponding human visual perception. *Curr Biol* 22(9):807–813.
19. VanRullen R, Zoefel B, Ilhan B (2014) On the cyclic nature of perception in vision versus audition. *Philos Trans R Soc Lond B Biol Sci* 369(1641):20130214.
20. Lakatos P, Chen CM, O'Connell MN, Mills A, Schroeder CE (2007) Neuronal oscillations and multisensory interaction in primary auditory cortex. *Neuron* 53(2):279–292.
21. Vanrullen R, Busch NA, Drewes J, Dubois J (2011) Ongoing EEG phase as a trial-by-trial predictor of perceptual and attentional variability. *Front Psychol* 2:60.
22. Busch NA, VanRullen R (2010) Spontaneous EEG oscillations reveal periodic sampling of visual attention. *Proc Natl Acad Sci USA* 107(37):16048–16053.
23. Romei V, et al. (2008) Spontaneous fluctuations in posterior α -band EEG activity reflect variability in excitability of human visual areas. *Cereb Cortex* 18(9):2010–2018.
24. Wyart V, Tallon-Baudry C (2009) How ongoing fluctuations in human visual cortex predict perceptual awareness: Baseline shift versus decision bias. *J Neurosci* 29(27):8715–8725.
25. Linkenkaer-Hansen K, Nikulin VV, Palva S, Ilmoniemi RJ, Palva JM (2004) Prestimulus oscillations enhance psychophysical performance in humans. *J Neurosci* 24(45):10186–10190.
26. Jones SR, Pritchett DL, Stufflebeam SM, Hämäläinen M, Moore CI (2007) Neural correlates of tactile detection: A combined magnetoencephalography and biophysically based computational modeling study. *J Neurosci* 27(40):10751–10764.
27. Haegens S, et al. (2011) Beta oscillations in the monkey sensorimotor network reflect somatosensory decision making. *Proc Natl Acad Sci USA* 108(26):10708–10713.
28. Snyder AZ (1992) Steady-state vibration evoked potentials: Descriptions of technique and characterization of responses. *Electroencephalogr Clin Neurophysiol* 84(3):257–268.
29. Tobimatsu S, Zhang YM, Kato M (1999) Steady-state vibration somatosensory evoked potentials: Physiological characteristics and tuning function. *Clin Neurophysiol* 110(11):1953–1958.
30. Gho M, Varela FJ (1988–1989) A quantitative assessment of the dependency of the visual temporal frame upon the cortical rhythm. *J Physiol (Paris)* 83(2):95–101.
31. Neuling T, Rach S, Wagner S, Wolters CH, Herrmann CS (2012) Good vibrations: Oscillatory phase shapes perception. *Neuroimage* 63(2):771–778.
32. Schyns PG, Thut G, Gross J (2011) Cracking the code of oscillatory activity. *PLoS Biol* 9(5):e1001064.
33. Montemurro MA, Rasch MJ, Murayama Y, Logothetis NK, Panzeri S (2008) Phase-of-firing coding of natural visual stimuli in primary visual cortex. *Curr Biol* 18(5):375–380.
34. Dubois J, Vanrullen R (2011) Visual trails: Do the doors of perception open periodically? *PLoS Biol* 9(5):e1001056.
35. Horton JC, Trobe JD (1999) Akinetopsia from nefazodone toxicity. *Am J Ophthalmol* 128(4):530–531.
36. Tsai PH, Mendez MF (2009) Akinetopsia in the posterior cortical variant of Alzheimer disease. *Neurology* 73(9):731–732.
37. Abraham HD (1983) Visual phenomenology of the LSD flashback. *Arch Gen Psychiatry* 40(8):884–889.
38. Kawasaki A, Purvin V (1996) Persistent palinopsia following ingestion of lysergic acid diethylamide (LSD). *Arch Ophthalmol* 114(1):47–50.
39. Oostenveld R, Fries P, Maris E, Schoffelen JM (2011) FieldTrip: Open source software for advanced analysis of MEG, EEG, and invasive electrophysiological data. *Comput Intell Neurosci* 2011:156869.
40. Berens P (2009) CircStat: A MATLAB toolbox for circular statistics. *J Stat Softw* 31(10):1–21.
41. Litvak V, et al. (2011) EEG and MEG data analysis in SPM8. *Comput Intell Neurosci* 2011:852961.
42. Hanslmayr S, Volberg G, Wimber M, Dalal SS, Greenlee MW (2013) Prestimulus oscillatory phase at 7 Hz gates cortical information flow and visual perception. *Curr Biol* 23(22):2273–2278.
43. Maris E, Oostenveld R (2007) Nonparametric statistical testing of EEG- and MEG-data. *J Neurosci Methods* 164(1):177–190.
44. Keil J, Müller N, Hartmann T, Weisz N (2014) Prestimulus beta power and phase synchrony influence the sound-induced flash illusion. *Cereb Cortex* 24(5):1278–1288.
45. Suk J, Ribary U, Cappel J, Yamamoto T, Llinás R (1991) Anatomical localization revealed by MEG recordings of the human somatosensory system. *Electroencephalogr Clin Neurophysiol* 78(3):185–196.
46. Iguchi Y, Hoshi Y, Tanosaki M, Taira M, Hashimoto I (2005) Attention induces reciprocal activity in the human somatosensory cortex enhancing relevant- and suppressing irrelevant inputs from fingers. *Clin Neurophysiol* 116(5):1077–1087.
47. Van Veen BD, van Drongelen W, Yuchtman M, Suzuki A (1997) Localization of brain electrical activity via linearly constrained minimum variance spatial filtering. *IEEE Trans Biomed Eng* 44(9):867–880.
48. Nolte G (2003) The magnetic lead field theorem in the quasi-static approximation and its use for magnetoencephalography forward calculation in realistic volume conductors. *Phys Med Biol* 48(22):3637–3652.
49. Schoffelen JM, Poort J, Oostenveld R, Fries P (2011) Selective movement preparation is subserved by selective increases in corticomuscular gamma-band coherence. *J Neurosci* 31(18):6750–6758.

Supporting Information

Baumgarten et al. 10.1073/pnas.1501438112

SI Results

To compare the predictions of perception based on MEG experimental data (*Results* and Fig. 4) with a model based on the behavioral experimental data, we computed the critical frequency determined by the average intermediate SOA of 25.9 ms (22.4 Hz) and predicted response rates for this frequency. The linear regression analysis between predicted and behavioral response rates resulted in a highly significant correlation coefficient ($r = 0.99$, $P < 0.01$). The resulting slope (1.05 ± 0.04) did not differ significantly from 1 [$t(4) = 1.29$, $P > 0.05$]. Finally, we computed critical frequencies determined from behavioral experimental data on the single-subject level (i.e., based on individual intermediate SOAs and behavioral response rates) and averaged the resulting critical frequencies over subjects (23.9 ± 2.0 Hz). Linear regression analysis resulted in a highly significant correlation coefficient ($r = 0.99$, $P < 0.01$). The resulting slope estimate (1.08 ± 0.04) did not differ significantly from 1 [$t(4) = 2.12$, $P > 0.05$]. Thus, theoretically and experimentally determined frequencies yielded highly similar results: Both reveal significant correlation values and slopes not significantly different from 1.

SI Materials and Methods

Experimental Paradigm. Each trial began with a precue period (500 ms; Fig. 1). After 900–1,100 ms, either one or two electrical pulses (0.3 ms) were applied to the subject's left index finger, with the pulse amplitude determined individually to a level above the subjective perception threshold [4.1 ± 1.2 mA (mean \pm SD)]. SOAs between the electrical pulses varied from short (0 ms) to long (100 ms), and comprised an individually determined SOA for which subjects reported the perception of one electrical pulse in ~50% of the trials, whereas two pulses were perceived [SOA: 25.9 ± 1.9 ms (mean \pm SEM)] in the other ~50% of the trials, subsequently labeled intermediate SOA. Two additional SOAs encompassed the intermediate SOA ± 10 ms (subsequently labeled intermediate + 10 ms and intermediate – 10 ms, respectively). After a jittered poststimulus period (500–1,200 ms), a response window indicated that subjects should report their perception (one or two stimuli) by pressing a button with the right hand. No feedback was given.

Virtual Channel Construction. To focus the analysis on S1, we analyzed oscillatory brain activity in a predefined region of interest in source space. This “virtual channel” was determined by localizing the individual sources of the evoked responses (M50 component) to left index finger stimulation, because this component is known to originate from S1 (45, 46). To determine the virtual channel, all trials on the sensor level were filtered between 2 and 40 Hz and the mean of every epoch was removed from each trial. We then pooled all trials (irrespective of SOA) for each subject and computed the individual event-related fields. Next, we identified the individual M50 component by focusing on the time window of 20–70 ms after stimulation onset. Source localization was performed by means of a linearly constrained minimum variance beam former (47) on 3D grids with a resolution of 1 cm. Individual subject grids were computed by linearly warping the structural MRI of each subject onto the Montreal Neurological Institute (MNI) template brain and applying the inverse of the warp to the regular MNI template grid. For one subject, the MNI template brain was used instead of the individual structural MRI, because no individual MRI was available. A lead-field matrix was computed for each grid point using a realistically shaped single-shell volume conduction model (48). Covariance matrices across all MEG sensors were calculated based on the average across all trials to

determine the source of evoked responses. Using the covariance matrices and lead field matrices, separate individual spatial filters for both prestimulus and poststimulus activity were constructed for each grid point. We calculated for each subject the ratio of M50 activity (20–70 ms) relative to baseline activity (–400 to –350 ms) for each grid point. Next, we averaged the source activity for each grid point over subjects and determined the grid point with maximum M50 activity. This grid point was selected as the location of the virtual sensor (Fig. 2A). The corresponding label was identified with the help of the Analysis of Functional NeuroImages atlas (afni.nimh.nih.gov/afni).

Single-trial time courses for this virtual channel were computed from MEG sensor data. We computed covariance matrices across all MEG sensors, based on averaged nonoverlapping trials, from –900 to 500 ms after trials were filtered between 2 and 40 Hz, and the mean of every epoch was removed from each trial. Covariance matrices were used to construct a spatial filter for the selected grid point of maximum M50 activity. The largest of the three dipole directions per spatial filter was used for further analysis (49). We applied this spatial filter on the MEG sensor data to reconstruct the single-trial time series in the virtual channel:

$$\text{source}TS_{s,r} = sf_s * \text{sensor}TS_{s,r,c}, \quad [\text{S1}]$$

with $\text{sensor}TS_{s,r,c}$ defining the time series data on the sensor level for each subject s , trial r , and channels c projected through the spatial filter sf_s to obtain the time series data on source level ($\text{source}TS_{s,r}$) for each subject s and trial r . MEG sensor data were first segmented to trials with a length of 1,400 ms (–900 to 500 ms) and then detrended, demeaned, and filtered (2–250 Hz). The resulting source-based time signal was then used as input for the oscillatory phase estimation.

Prediction of Perception. Predictions of response rates and linear regressions between predicted and behaviorally measured response rates were based on three different approaches: (i) group-level effect frequencies determined from MEG experimental data (8–20 Hz; Fig. 2B), (ii) single subject-level individual frequencies determined from MEG experimental data (Fig. S2 and Table S1), and (iii) frequencies determined from behavioral experimental data (i.e., the intermediate SOAs). These approaches are in detail:

- i) As the critical frequency of the model, we chose the frequencies showing a significant group-level phase angle difference between the conditions intermediate2 and intermediate1 (8–20 Hz; Fig. 2B). We calculated the cycle length for each frequency and then divided the length of the respective SOA by the cycle length, thus calculating for each cycle the ratio of time points for which the two stimuli would fall into one cycle (one perceived stimulus) or into two cycles (two perceived stimuli) (Fig. 3). Thereby, we calculated the predicted response rate per frequency bin, and subsequently averaged predicted response rates over all frequencies showing a significant group-level phase angle difference between perceptual conditions (8–20 Hz). Finally, we computed the mean response rate and SEM across all frequencies. We statistically compared these predicted response rates with the group-level average of the measured behavioral response rates (Fig. 4) by first computing the correlation coefficients of the linear regression for the predicted and behavioral response rates under the premise of a y -axis intercept at (0,0). The correlation coefficient assesses the goodness of correlation

between the predicted response rates and the behavioral response rates. Next, we compared the resulting slope estimate with the slope resulting from an ideal fit (i.e., 1) by means of a one-sample, two-tailed t test. By this approach, we were able to test if the predicted response rate linearly agrees with the behavioral response rate over the different SOAs or if a systematic over- or underestimation is present (which would lead to a significant difference between slope estimate and ideal slope).

ii) Additionally, we predicted response rates on a single-subject level. According to our model, subjects with different intermediate SOAs should exhibit different critical frequencies, which, in turn, determine their respective perceptual cycles and predict individual response rates. To determine individual critical frequencies, individual F values resulting from the Watson–Williams test were summed up over all time points of the significant group-level effect (-0.53 to -0.09 s) separately for each frequency of the significant group-level effect (8–20 Hz). For each subject, the frequency showing the maximum F values was selected as the individual critical frequency, for which we calculated predicted individual response rates according to the analysis on the group level (discussed above). Similarly, we computed and

compared the slopes of the linear regressions for the individual predicted and individual behavioral response rates. To compare the individual response rate predictions with the group-level predictions based on the frequencies showing significant group-level phase angle differences (discussed above in *i*), we averaged predicted individual response rates over subjects and compared the slope of the linear regression for the predicted and behavioral response rates according to the aforementioned analysis.

iii) To compare the predictions based on the critical frequencies determined from MEG experimental data with a model based on the behavioral experimental data, we calculated the critical frequency based on the average intermediate SOA length and group-level behavioral response rates ($F_{\text{crit}} = \text{ratio of perceived two stimuli reports}/\text{mean length intermediate SOA} * 1,000$). We then predicted response rates and computed the resulting slope (discussed above). Likewise, we computed individual critical frequencies determined from behavioral experimental data (based on individual intermediate SOAs and individual response rates). We averaged the resulting individual critical frequencies over subjects, and likewise predicted response rates and computed the resulting slope.

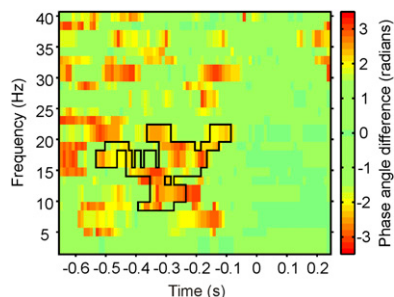


Fig. S1. Time-frequency plot showing the phase angle differences between intermediate2 vs. intermediate1. Red colors indicate a higher angular difference. Black outlines represent the extent of the significant group-level phase angle difference effect. $t = 0$ indicates the onset of the first stimulus.

Table S1. Predicted individual response rates based on individual frequencies determined from MEG experimental data and individual behavioral response rates

Subject no.	Individual critical frequency (Hz)	PRR, SOA 0 ms		PRR, SOA -10 ms		BRR, SOA -10 ms		PRR, SOA intermediate		BRR, SOA intermediate +10 ms		PRR, SOA intermediate +10 ms		BRR, SOA intermediate +10 ms		PRR, SOA 100 ms		BRR, SOA 100 ms		r value correlation coefficient	P value correlation coefficient	Slope estimate (±SEM)	t value slope comparison	P value comparison, two-tailed one-sample t test
		PRR	SOA	PRR	SOA	BRR	SOA	PRR	SOA	BRR	SOA	PRR	SOA	BRR	SOA	PRR	SOA	BRR	SOA					
1	8	0	0	0.0393	0.1178	0.1364	0.1178	0.6645	0.1963	0.1963	0.9118	0.7852	0.9737	0.6864	0.0447	0.4337 (±0.15)	-3.7692	0.0196						
2	8	0	0.0256	0.1178	0.1963	0.2973	0.1963	0.5828	0.2748	0.2748	0.9118	0.7852	1	0.8154	0.0108	0.5244 (±0.12)	-4.0786	0.0151						
3	16	0	0.0244	0.2355	0.3926	0.2857	0.3926	0.7692	0.5496	0.5496	0.9722	1	1	0.8789	0.0028	0.7268 (±0.11)	-2.4705	0.0689						
4	8	0	0.037	0.0785	0.157	0.2857	0.157	0.6214	0.2355	0.2355	0.7812	0.7852	0.913	0.7694	0.0206	0.5336 (±0.14)	-3.2458	0.0315						
5	14	0	0	0.2141	0.3569	0.303	0.3569	0.5508	0.4996	0.4996	0.9355	1	1	0.8648	0.0039	0.7665 (±0.13)	-1.8267	0.1418						
6	16	0	0	0.2355	0.3926	0.0789	0.3926	0.5294	0.5496	0.5496	0.875	1	1	0.9155	0.0014	0.832 (±0.11)	-1.5941	0.1861						
7	20	0	0.0278	0.2998	0.4996	0.6216	0.4996	0.5664	0.6995	0.6995	0.4474	1	0.9487	0.839	0.0034	0.9573 (±0.15)	-0.2771	0.7954						
8	20	0	0.0345	0.2998	0.4996	0.129	0.4996	0.6797	0.6995	0.6995	0.871	1	1	0.9432	0.0005	0.8879 (±0.09)	-1.3252	0.2557						
9	8	0	0	0.0393	0.1178	0.1111	0.1178	0.3866	0.1963	0.1963	0.9189	0.7852	0.8966	0.7363	0.0329	0.5161 (±0.16)	-3.0007	0.0399						
10	12	0	0.0465	0.182	0.3034	0.5909	0.3034	0.7637	0.4247	0.4247	0.9767	1	1	0.7511	0.0149	0.6088 (±0.15)	-2.635	0.0579						
11	18	0	0.0312	0.3569	0.5353	0.2703	0.5353	0.3852	0.7138	0.7138	0.4571	1	1	0.9364	0.0005	1.138 (±0.11)	1.2516	0.2789						
12	10	0	0.0323	0.1499	0.2498	0.1724	0.2498	0.5932	0.3498	0.3498	0.7333	0.9993	0.9655	0.8599	0.0065	0.7532 (±0.15)	-1.7075	0.1629						
13	16	0	0.0278	0.2355	0.3926	0.1333	0.3926	0.413	0.5496	0.5496	0.5	1	0.7097	0.9641	0.0003	1.2495 (±0.1)	2.432	0.0718						
14	10	0	0	0.2998	0.3997	0.5122	0.3997	0.7237	0.4996	0.4996	0.8095	1	1	0.8997	0.0018	0.7564 (±0.1)	-2.3936	0.0749						
15	8	0	0.0526	0.2748	0.3533	0.3846	0.3533	0.5259	0.4318	0.4318	0.6216	0.7852	0.7419	0.9251	0.0008	0.8375 (±0.09)	-1.7608	0.1531						
16	16	0	0.027	0.2355	0.3926	0.0541	0.3926	0.5177	0.5496	0.5496	0.8378	1	1	0.9189	0.0013	0.8494 (±0.11)	-1.4292	0.2262						

BRR, behavioral response rate; PRR, predicted response rate.

1 Beta peak frequencies at rest correlate with endogenous
2 GABA/Cr concentrations in the left sensorimotor cortex

3 Thomas J. Baumgarten^{1*}, Georg Oeltzschner^{1,2}, Nienke Hoogenboom¹, Hans-Jörg Wittsack²,
4 Alfons Schnitzler¹, Joachim Lange¹

5 ¹ Institute of Clinical Neuroscience and Medical Psychology, Medical Faculty, Heinrich-Heine-
6 University Düsseldorf, 40225 Düsseldorf, Germany

7 ² Department of Diagnostic and Interventional Radiology, Medical Faculty, Heinrich-Heine-
8 University Düsseldorf, 40225 Düsseldorf, Germany

9

10 * Corresponding author. Institute of Clinical Neuroscience and Medical Psychology, Medical Faculty,
11 Heinrich-Heine-University, Universitätsstraße 1, 40225 Düsseldorf, Germany

12 Phone: 0049 (0) 211 81-13016, E-mail: Thomas.Baumgarten@med.uni-duesseldorf.de

13

14 **Number of figures:** 3

15 **Number of tables:** 2

16 **Number of words:** Abstract: 225, Introduction: 585, Materials & Methods: 1421, Results: 609,

17 Discussion: 1493

18 Abstract

19 Neuronal oscillatory activity in the beta band (15-30 Hz) is a prominent signal within the human
20 sensorimotor cortex. Computational modeling and pharmacological modulation studies suggest
21 an influence of GABAergic interneurons on the generation of beta band oscillations.
22 Accordingly, studies in humans have demonstrated a correlation between GABA concentrations
23 and power of beta band oscillations. It remains unclear, however, if GABA concentrations also
24 influence beta peak frequencies and whether this influence is present in the sensorimotor
25 cortex at rest and without pharmacological modulation. In the present study, we investigated
26 the relation between endogenous GABA concentration (measured by magnetic resonance
27 spectroscopy) and beta oscillations (measured by magnetoencephalography) at rest in humans.
28 GABA concentrations and beta band oscillations were measured for the left and right
29 sensorimotor and occipital cortex. A significant positive linear correlation between GABA
30 concentration and beta peak frequency was found for the left sensorimotor cortex, whereas no
31 significant correlations were found for the right sensorimotor and the occipital cortex. The
32 results show a novel connection between endogenous GABA concentration and beta peak
33 frequency at rest. This finding supports previous results that demonstrated a connection
34 between oscillatory beta activity and pharmacologically modulated GABA concentration in the
35 sensorimotor cortex. Furthermore, the results demonstrate that for a predominantly right-
36 handed sample, the correlation between beta band oscillations and endogenous GABA
37 concentrations is evident only in the left sensorimotor cortex.

38 Introduction

39 Oscillatory activity in the beta (15-30 Hz) frequency range is a prominent signal in the human
40 sensorimotor cortex, both at rest and during motor activity [1–4]. Beta band activity differs
41 across areas and depends on motor output (see [5] for a review). For example, beta band power
42 in sensorimotor cortex decreases during movement, whereas beta band power increases
43 following movement [6].

44 The majority of studies on beta band activity investigated the role of power (e.g., [7,8]). In
45 addition to power, there is increasing evidence that beta peak frequency (i.e., the frequency
46 within the beta band with the highest power) is an important and functionally relevant
47 parameter of oscillatory activity [9]. Beta peak frequency differs across distinct recording sites
48 within the sensorimotor cortex [1]. Furthermore, beta peak frequency differs during movement
49 and stimulation of lower and upper limbs, thereby distinguishing between different
50 somatotopic representations [10]. Finally, beta peak frequency seems to be an important factor
51 for the communication between cortical areas and muscles during movement. For example,
52 neuronal activity in the motor cortex and electromyographic activity during movement is
53 coherently coupled at ~20 Hz [11]. This 20 Hz motor cortical activity is thought to optimize
54 motor output by maximal recruitment of motor neurons at a minimum discharge in the
55 pyramidal tract [11].

56 Animal and modeling studies provide evidence for an essential role of GABAergic interneuronal
57 activity for the generation of beta oscillations in the sensorimotor cortex [12–14]. For example,
58 a study using modeled neuronal networks found increases in the power of beta band

59 oscillations to result from an increase in the synaptic conductance of GABA_A-mediated inhibition
60 [12]. Further, studies demonstrated increases in human beta power [7,8,12,15,16] as well as
61 decreases in beta peak frequency [12] (but see [16,17]) as a result of pharmacological
62 GABAergic modulation. Such modulations of beta power were evident at rest [7,12] as well as
63 after motor output [8,15,17].

64 While the abovementioned studies demonstrated a causal link between GABA administration
65 and changes in beta band power and peak frequencies, the concentration of GABA and its direct
66 modulation in sensorimotor cortex was not measured. Thus the quantitative relation remains
67 unclear. Magnetic resonance spectroscopy (MRS) offers a non-invasive method for in vivo
68 quantification of endogenous neurotransmitter concentrations in spatially restricted cortical
69 regions [18]. While this approach has initially been applied to estimate GABA concentrations
70 especially in occipital cortical areas (e.g., [19,20]), recent studies also focused on the
71 sensorimotor cortex (e.g., [16,21,22]). These studies demonstrated a linear relationship
72 between sensorimotor GABA concentration and post-movement oscillatory beta power. In
73 contrast, no relationship could be demonstrated between sensorimotor GABA concentration
74 and post-movement oscillatory beta peak frequency [16]. Taken together, there are consistent
75 results supporting a general relationship between GABA concentration and beta band power in
76 sensorimotor cortex areas. Contrarily, the results concerning beta band peak frequency are less
77 consistent. Therefore, the question remains whether beta peak frequency is related to GABA
78 concentrations and if such a potential relation is present at rest (i.e., without movement) and
79 for endogenous (i.e., non-modulated) GABA concentrations.

80 Here, we investigated whether the peak frequency of ongoing beta band oscillations is
81 correlated to endogenous GABA concentration in the sensorimotor cortex at rest. Beta peak
82 frequencies were determined by magnetoencephalography (MEG) and individual GABA
83 concentrations were measured by means of MRS. Peak frequencies were determined for the
84 left and right sensorimotor cortex, as well as for a control region in the occipital cortex. For
85 these three regions of interest (ROIs), we linearly related peak frequencies to GABA
86 concentrations estimated for analogue cortical areas.

87 Materials & Methods

88 **Subjects**

89 15 subjects (7 male, age: 59.9 ± 9 years (mean \pm SD)) participated after providing written
90 informed consent in accordance with the Declaration of Helsinki and the Ethical Committee of
91 the Medical Faculty, Heinrich-Heine-University Düsseldorf. All participants had normal or
92 corrected to normal vision and reported no sensory impairments, known history of neurological
93 disorders or use of neuro-modulatory medication. The subjects were selected from the healthy
94 controls of a sample that was previously reported in [23].

95 **Behavioral data**

96 Individual handedness was assessed by comparing bi-manual performance (hand dominance
97 test (HDT) [24]). Categorization based on the performance measure resulted in 12 clearly right-
98 handed subjects (HDT score: 29.8 ± 8.1 (mean \pm SD)) and 3 subjects with no clear hand
99 preference (HDT score: -6.8 ± 9.7).

100 **Magnetic resonance spectroscopy (MRS) data**

101 **Spectroscopy**

102 MRS data were recorded using a 3T whole-body MRI scanner (Siemens MAGNETOM Trio A TIM
103 System, Siemens Healthcare AG, Erlangen, Germany) in connection with a 12-channel head
104 matrix coil. Subjects were instructed to lie in the scanner, relax and refrain from any further
105 activity. For the determination of neurotransmitter concentrations, MRS voxels ($3 \times 3 \times 3$ cm³) were
106 placed in left and right sensorimotor cortices and occipital cortex (Fig 1A). For both
107 sensorimotor cortices, voxels were centered on the respective 'hand knob' within the *Gyrus*

108 *praecentralis* [25], thus covering both motor and somatosensory cortex. The occipital MRS voxel
109 was medially centered on the occipital lobe with the inferior boundary of the voxel aligned with
110 the *Tentorium cerebelli*. For all subjects, voxel placement was performed with the focus to
111 include a maximum portion of cortical volume, as well as a minimal volume of non-cerebral
112 tissues to avoid any additional lipid contamination of the spectra. MRS voxels will be addressed
113 as MRS ROIs (in contrast to MEG ROIs) subsequently.

114 After the localization of target volumes by means of T_1 -weighted planning sequences, MEGA-
115 PRESS spectra [26] were acquired (number of excitations = 192, TR = 1500 ms, TE = 68 ms, V =
116 $3 \times 3 \times 3$ cm³, bandwidth = 1200 Hz, 1024 data points). Spectral editing was performed by J-
117 refocusing pulses irradiated at 1.9 ppm and 7.5 ppm using Gaussian pulses with a bandwidth of
118 44 Hz. Processing of MEGA-PRESS data was performed with the MATLAB-based tool GANNET
119 2.0 [27], including frequency and phase correction of the single acquisitions as well as Gaussian
120 fitting of the 3 ppm GABA resonance. For subsequent analyses, the GABA-to-creatine ratio
121 (GABA/Cr) was used [28].

122 GABA/Cr estimates were not available for every MRS ROI in each subject (see results section for
123 further details). Therefore, we applied two different statistical tests: 1) GABA/Cr concentrations
124 were compared across the left, right and occipital MRS ROIs by means of a one-factor repeated-
125 measures ANOVA (with listwise deletion of values for all MRS ROIs of a single subject if a value
126 was missing in one MRS ROI). 2) We additionally computed pairwise comparisons between MRS
127 ROIs by means of paired-sample t -tests corrected for multiple comparisons by means of the
128 Holm-Bonferroni procedure (see [29] for a similar procedure). Although this comparison also
129 implemented listwise deletion of missing values, the respective deletions are determined for

130 each comparison separately, resulting in fewer deletions compared to the abovementioned
131 ANOVA. This served to achieve a higher statistical power since more subjects could be included
132 in the respective *t*-test comparisons.

133

134 **MEG data**

135 **Experimental Design**

136 Subjects were seated in the MEG with all visual stimuli projected on the backside of a
137 translucent screen (60 Hz refresh rate) positioned 57 cm in front of the subjects. Resting-state
138 neuromagnetic activity was recorded during two sessions with a respective duration of 5
139 minutes, with subjects being instructed to relax and refrain from any additional activity. In the
140 first session, subjects had to focus a dimmed fixation dot (diameter: 0.5 degree) presented in
141 the middle of the translucent screen (eyes open condition (EO)). After completing the first
142 session, subjects were verbally informed regarding the beginning and the instructions of the
143 second session. In the second session, subjects had to close their eyes (eyes closed condition
144 (EC)) but remain awake during the measurement. Stimulus presentation was controlled using
145 Presentation software (Neurobehavioral Systems, Albany, NY, USA).

146 **Data Recording and Preprocessing**

147 Continuous neuromagnetic brain activity was recorded at a sampling rate of 1000 Hz using a
148 306-channel whole head MEG system (Neuromag Elekta Oy, Helsinki, Finland), including 204
149 planar gradiometers (102 pairs of orthogonal gradiometers) and 102 magnetometers. Data
150 analysis in the present study was restricted to the planar gradiometers. Electro-oculograms
151 (EOGs) were recorded for offline artifact rejection by applying electrodes above and below the

152 left eye as well as on the outer sides of each eye. Further, an electro-cardiogram (ECG) was
153 recorded for offline artifact rejection by means of two electrodes placed on the left collarbone
154 and the lowest left rib.

155 Data were offline analyzed using custom-made Matlab (The Mathworks Inc., Natick/MA, USA)
156 scripts and the Matlab-based open source toolbox FieldTrip (<http://fieldtriptoolbox.org>; [30]).
157 Continuously recorded data were divided into two epochs according to the respective session
158 (EO and EC), starting 3 s after beginning and ending 3 seconds before the end of the respective
159 task. Data were band-pass filtered at 1 Hz to 200 Hz and power line noise was removed by using
160 a band-stop filter encompassing the 50, 100, and 150 Hz components. Data were detrended and
161 the mean of every epoch was subtracted. Continuous data were segmented into trials of 1 s
162 duration with a 0.25 s overlap. Subsequently, trials were semi-automatically and visually
163 inspected for artifacts. Artifacts caused by muscle activity, eye movements or SQUID jumps
164 were removed semi-automatically using a z-score based algorithm implemented in FieldTrip.
165 Excessively noisy channels were removed. To further eliminate cardiac and ocular artifacts, an
166 independent component analysis was computed. Mutual information was calculated between
167 the resulting components and the EOG and ECG channels [31,32]. Components were sorted
168 according to their level of mutual information and subsequently visually examined regarding
169 their topography and time course. Those components showing high mutual information with
170 EOG and ECG channels as well as topographies and time courses typical for cardiac and ocular
171 artifacts were rejected. Afterwards, removed channels were reconstructed by an interpolation
172 of neighboring channels. After artifact rejection, 292 ± 34.5 (mean \pm SD) trials in the EC
173 condition and 304 ± 35.4 trials in the EO condition remained for further analysis. Subsequent

174 analyses were performed separately for the EO and EC condition as well as for a combined data
175 set created by appending the EO and EC condition (EC+EO).

176 **Frequency Analysis and Peak Frequency Determination**

177 To determine individual peak frequencies, we performed a frequency analysis encompassing all
178 frequencies of the beta-band (15 to 30 Hz; [6,33]) by applying a Fourier transformation over the
179 entire trial duration. Trials were tapered with a single Hanning taper, resulting in a spectral
180 resolution of 1 Hz. Within each condition, spectral power was averaged over all trials for each
181 frequency separately. Power was estimated independently for each of the 204 gradiometers.
182 Subsequently, gradiometer pairs were combined by summing spectral power across the two
183 orthogonal channels, resulting in 102 pairs of gradiometers.

184 Since GABA-concentrations were assessed for three different MRS ROIs (left and right
185 sensorimotor cortex, occipital cortex; see Fig 1A and methods section (MRS data, Spectroscopy)
186 for details), we determined corresponding MEG ROIs by selecting 6 sensor pairs in the left and 6
187 sensor pairs in the right hemisphere covering the respective sensorimotor cortices (Fig 2A). The
188 selection of sensors was based on previous studies [34,35]. In addition, we selected 6 posterior
189 sensor pairs covering the occipital cortex [36].

190 Individual beta peak frequencies were determined within each MEG ROI separately for each
191 subject. For each subject, the frequency showing the maximum power within the predefined
192 beta-band (15-30 Hz) was selected as the individual peak frequency. Beta peak frequencies
193 were statistically compared between the three MEG ROIs and the three conditions by means of
194 a two-factor repeated-measures ANOVA (main factors: MEG ROI (left sensorimotor, right

195 sensorimotor, occipital) and condition (EO, EC, EC+EO)). In case of violations of sphericity,
196 Greenhouse-Geisser corrected values were reported.

197 **Correlation of MRS and MEG data**

198 In order to examine the relationship between GABA/Cr concentrations and resting-state
199 neuromagnetic brain activity, we linearly correlated individual GABA/Cr concentrations within
200 the respective MRS ROIs with the beta band peak frequencies determined for the corresponding
201 MEG ROIs. We computed correlations within each ROI (e.g., between left sensorimotor MRS ROI
202 and left sensorimotor MEG ROI), thus resulting in 3 correlations for each condition (EO, EC,
203 EC+EO). In addition, we corrected the respective correlations for the HDT handedness scores by
204 means of partial correlation (Pearson).

205 Results

206 **GABA/Cr concentrations**

207 GABA/Cr values were determined in left sensorimotor, right sensorimotor and occipital MRS
208 ROIs (Fig 1). Due to cancellation of the measurements or distorted spectra, GABA/Cr
209 concentrations could not be estimated for the left sensorimotor, right sensorimotor and
210 occipital MRS ROI in 4, 2, and 1 subjects, respectively (see Table 1 for a summary of GABA/Cr
211 estimates). For the remaining subjects, a one-factor repeated-measures ANOVA yielded no
212 significant difference between GABA/Cr concentrations in the 3 MRS ROIs ($F(2, 16) = 2.06, p =$
213 0.16 ; Fig 1B). Likewise, paired-sample t -tests yielded no significant differences in GABA/Cr
214 concentration between MRS ROIs ($p > 0.017$, after correction for multiple comparisons).

215

216 **MEG data**

217 Beta peak frequencies could be determined in all subjects (Fig 2B; Table 2). A two-factor
218 repeated measures ANOVA comparing beta peak frequencies for the factors MEG ROI (left
219 sensorimotor, right sensorimotor, occipital) and condition (EO, EC, EC+EO) demonstrated a
220 highly significant main effect for the factor MEG ROI ($F(1.43, 19.97) = 7.27, p < 0.01$; Fig 2C).
221 Post hoc t -tests revealed a significant difference between peak frequencies in left sensorimotor
222 MEG ROI vs. occipital MEG ROI ($p < 0.01$) and between peak frequencies in the right
223 sensorimotor MEG ROI vs. the occipital MEG ROI ($p < 0.05$). For the factor condition, no
224 significant main effect was found ($F(2, 28) = 1.17, p > 0.05$). Since no significant results could be
225 found for the factor condition, we chose the combined condition EC+EO for visualization

226 purposes in Fig 2B. Likewise, an ANOVA did not reveal a significant interaction between the
227 factors ROI and condition ($F(2.06, 28.77) = 0.49, p > 0.05$).

228 **Correlation of MRS and MEG data**

229 We computed linear correlations between GABA/Cr concentrations determined in MRS ROIs
230 and beta peak frequencies determined in MEG ROIs, separately for each of the three ROIs (left
231 sensorimotor cortex, right sensorimotor cortex, occipital cortex). Correlation analyses revealed
232 significant linear correlations in the left sensorimotor ROI (EO: $r = 0.62, p < 0.05$, EC: $r = 0.62, p <$
233 0.05 , EC+EO: $r = 0.73, p < 0.05$; Fig 3A). No significant correlations were found in the right
234 sensorimotor ROI (EO: $r = -0.14, p > 0.05$, EC: $r = -0.07, p > 0.05$, EC+EO: $r = -0.13, p > 0.05$; Fig
235 3B). Similarly, no significant correlations were found in the occipital ROI (EO: $r = 0.24, p > 0.05$,
236 EC: $r = 0.09, p > 0.05$, EC+EO: $r = 0.35, p > 0.05$; Fig 3C). Since, within each ROI, correlations were
237 highly similar across conditions, we selected the combined condition EC+EO for visualization
238 purposes in Fig 3. Further, correlations within the respective ROIs statistically remained highly
239 similar when correlations were restricted to those subjects for whom valid MRS spectra could
240 be determined for all 3 MRS ROIs (see section MRS data above).

241 We only found correlations between GABA/Cr concentrations and beta peak frequencies to be
242 significant for the left sensorimotor ROI. Because the majority of the subjects (12/15) were
243 classified as right-handed by means of the HDT performance measure, we additionally
244 investigated the influence of handedness on the relationship between GABA/Cr concentration
245 and beta peak frequency. Therefore, we partialized out the effect of handedness (assessed by
246 the HDT performance measure) on the correlations between GABA/Cr concentration and beta
247 peak frequencies. We found a significant correlation between GABA/Cr concentration and beta

248 peak frequencies for the left sensorimotor cortex for the EO and EC+EO conditions (EO: $r = 0.69$,
249 $p < 0.05$, ECEO: $r = 0.77$, $p < 0.01$), and a strong trend towards significance for the EC condition (r
250 $= 0.6$, $p = 0.07$). No significant correlations were found for the right sensorimotor and occipital
251 cortex.

252 Discussion

253 Using magnetoencephalography (MEG) and magnetic resonance spectroscopy (MRS) in healthy
254 human subjects, we investigated the relationship between beta peak frequencies at rest and
255 endogenous (i.e., non-modulated) GABA/Cr concentrations in the left and right sensorimotor
256 and occipital cortex. The results show significant positive linear correlations between peak
257 frequencies in the beta-band (15-30 Hz) and GABA/Cr concentrations for the left sensorimotor
258 cortex, i.e., higher beta peak frequency was related to a higher GABA/Cr concentration.

259 The present study is one of the first to investigate the connection between beta peak frequency
260 at rest (i.e., without movement or a movement-related task) and non-modulated GABA/Cr
261 values in the sensorimotor cortex. Previous studies that have addressed the general question if
262 sensorimotor beta activity is related to the GABAergic system, applied pharmacological
263 GABAergic modulators [7,8,12,15,17] and/or investigated movement-related sensorimotor beta
264 activity [8,15–17]. By focusing exclusively on non-modulated (i.e., no movement-related and
265 pharmaco-induced manipulation) parameters, the present study was able to show a correlation
266 between GABA/Cr concentrations and beta peak frequency at rest.

267 Beta peak frequencies differed across measurement sites. While left and right sensorimotor
268 cortices showed clear peaks in the beta-band in all subjects (Fig 2B), beta peaks were less
269 prominent in the occipital cortex, with five subjects showing no clear peak. This is in agreement
270 with the specific role of beta band activity for the sensorimotor cortex [1,4], while beta band
271 activity in occipital regions is less common. Less clear peaks in the beta band for the occipital
272 ROI might be a reason why correlations between GABA/Cr concentrations and beta peak

273 frequencies were only found for the sensorimotor cortex. This interpretation, however, cannot
274 account for the lack of a significant correlation in right sensorimotor areas, since we found clear
275 peaks in the right sensorimotor cortex for all subjects. Because GABA/Cr concentrations across
276 MRS ROIs did not differ significantly, it is also unlikely that GABA/Cr concentrations are
277 responsible for the unilaterality. Since 12 of 15 subjects in the present study were classified as
278 right-handed, handedness might be an explanation for the unilaterality of the correlation.
279 However, correlations remained significant even after correcting for handedness. This finding
280 suggests that handedness alone is unlikely to account for the differences between left and right
281 sensorimotor cortices. Handedness, however, is known to lead to asymmetries with respect to
282 hand representations in the sensorimotor cortex [37–39]. Such asymmetries might lead to
283 regional differences in GABA/Cr concentration and/or generators of beta frequencies in left and
284 right sensorimotor areas. The rather large size of the MRS ROIs poses an additional challenge,
285 since for such voxel sizes it is not possible to separately measure GABA/Cr concentrations for
286 motor and somatosensory cortex. Although smaller voxel sizes are possible [21], they result in
287 extended measurement time for a comparable signal to noise ratio. Thus, although GABA/Cr
288 concentrations did not significantly differ between left and right sensorimotor MRS ROIs, our
289 method might have measured more GABA/Cr concentrations that are unrelated to beta
290 frequency generations in right sensorimotor cortex (i.e., more “noise”). More fined-grained
291 analyses might resolve this problem and shed further light on the relation between GABA
292 concentration and beta peak frequencies. In addition, it would be interesting to assess both left
293 and right-handed populations in future studies to further elucidate the effect of handedness on
294 GABAergic concentrations in sensorimotor cortices.

295 A general limitation of GABA measurements via MRS is that this method is unable to
296 differentiate between synaptic and extra-synaptic GABA concentrations [22]. Nonetheless,
297 GABA concentrations measured by MRS might primarily reflect extra-cellular GABA
298 concentrations, i.e., the general GABAergic tone [40]. Contrary to intra-cellular GABA
299 concentrations, extra-cellular GABA concentrations would include synaptic concentrations. Beta
300 band oscillations would be primarily related to synaptic GABA concentrations, since this
301 represents the synaptically active neurotransmitter pool [15]. Thus, our results represent
302 correlations with the overall GABA/Cr concentration of a given voxel, not exclusively for the
303 synaptically active GABA concentration. Despite all potential limitations, we were able to
304 demonstrate a significant positive correlation between GABA/Cr concentration and beta peak
305 frequency. In addition, various studies using parameters similar to the present study proved
306 that GABA MRS in sensorimotor and occipital cortices yields feasible results (reviewed in [22]).
307 The general feasibility of GABA MRS is further supported by studies that link MRS-derived
308 neurotransmitter concentrations to functional and behavioral measurements [21].

309 Neuronal oscillations are thought to depend on the balance between excitatory (i.e.,
310 glutamatergic synaptic input) and inhibitory (i.e., GABAergic synaptic input) network
311 components [12,41,42]. For beta band activity in the sensorimotor cortex, a connection
312 between GABAergic tone and beta band oscillations is supported by studies reporting increases
313 in somatosensory beta band power as an effect of GABAergic modulation by means of
314 GABAergic agonists (e.g., benzodiazepine) [7,12,15,17]. The relation between GABAergic
315 agonists and beta peak frequencies, however, is less clear. While, Jensen and colleagues [12]
316 reported a small decrease (~1.6 Hz) in resting-state beta peak frequency in bilateral

317 sensorimotor cortices after the administration of benzodiazepine, Baker and Baker [17] found
318 no modulation of beta peak frequency after the administration of benzodiazepine. The
319 GABAergic agonist benzodiazepine is considered to enhance the synaptic GABAergic drive [12].
320 Simplified, an enhanced GABAergic drive could be related to an increased GABAergic
321 concentration, which would contradict the positive correlation between beta peak frequency
322 and GABA/Cr levels in the left sensorimotor cortex observed in the present study. Yet, various
323 differences between the studies have to be taken into account. First, Jensen et al. [12] and
324 Baker and Baker [17] measured the influence of pharmacological GABA modulations on beta
325 peak frequencies on the within-subject level. The present study measured non-modulated GABA
326 concentrations and investigated correlations on a between-subject level. Further, while we
327 report a correlation for the left sensorimotor cortex, Jensen and colleagues [12] averaged beta
328 peak frequency over bilateral sensorimotor cortices (thereby not investigating lateral
329 differences). Finally, we measured mostly right-handed subjects, so that an influence of
330 handedness cannot be excluded. The abovementioned studies do not report handedness of
331 their subjects, making a direct comparison difficult.

332 Gaetz and colleagues [16] found no correlation between beta peak frequency during post-
333 movement beta-rebound and endogenous GABA concentrations for the left motor cortex. Post-
334 movement beta-rebound, however, is intrinsically different from resting state beta activity, as
335 measured in our study. Any differences found between our study and Gaetz et al. [16] might
336 thus be related to different tasks. Taken together, the few existing studies focusing on the
337 connection between beta peak frequency and GABA concentrations in sensorimotor cortex

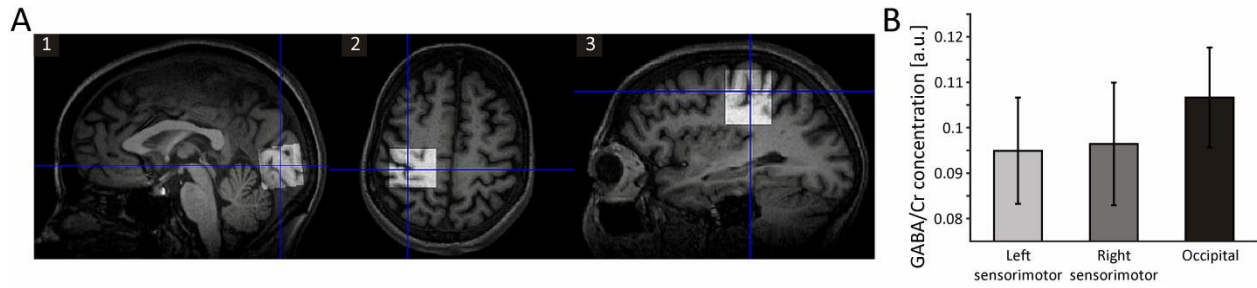
338 areas strongly vary in experimental setting and assessed parameters, thereby complicating a
339 comparison to our results.

340 For future studies, it would be interesting to determine how sensorimotor beta peak frequency
341 and GABA concentration both relate on a behavioral level. There is evidence that higher
342 sensorimotor GABA concentrations correlate with slower reaction times in a motor sequence
343 learning task [43]. Here, slower reaction has been interpreted as a result of higher levels of
344 inhibition. Furthermore, higher concentrations of sensorimotor GABA have been related to
345 lower discrimination thresholds in a tactile frequency discrimination task [21]. The authors
346 associated higher GABA concentrations with a potentially higher temporal resolution of tactile
347 perception, which would enable neurons to more closely tune their responses to the stimulus
348 cycles. Such an adjustment of neuronal response to stimulus frequency is considered as the
349 underlying mechanism of the connection between sensorimotor GABA levels and frequency
350 discrimination and to result in lower frequency discrimination thresholds. The influence of
351 oscillatory beta activity on behavioral parameters is less clear. Studies relating individual beta
352 peak frequencies to measures of functional performance apart from motor-related tasks are
353 scarce. Differences in the phase of ongoing beta band oscillations in the somatosensory cortex
354 have been shown to predict the temporal perception of subsequently presented tactile stimuli
355 [44]. Here, the specific beta band frequency showing the biggest phase differences predicted
356 the temporal resolution of tactile perception. Perfetti and colleagues [45] found beta power
357 variations to successfully predict mean reaction time in a visually guided motor task, with a
358 decrease of beta power in left sensory-motor areas corresponding to faster reaction times. In
359 line with this, lower beta-power levels during the time of stimulus presentation were related to

360 a faster reaction towards this stimulus [46]. Taken together, these results suggest an
361 involvement of GABA concentrations and beta band activity within the sensorimotor cortex in
362 the temporal dimension of tactile perception. Thus, further research should investigate if GABA
363 concentration and beta band activity show similar connections to behavioral parameters
364 assessed in parallel.

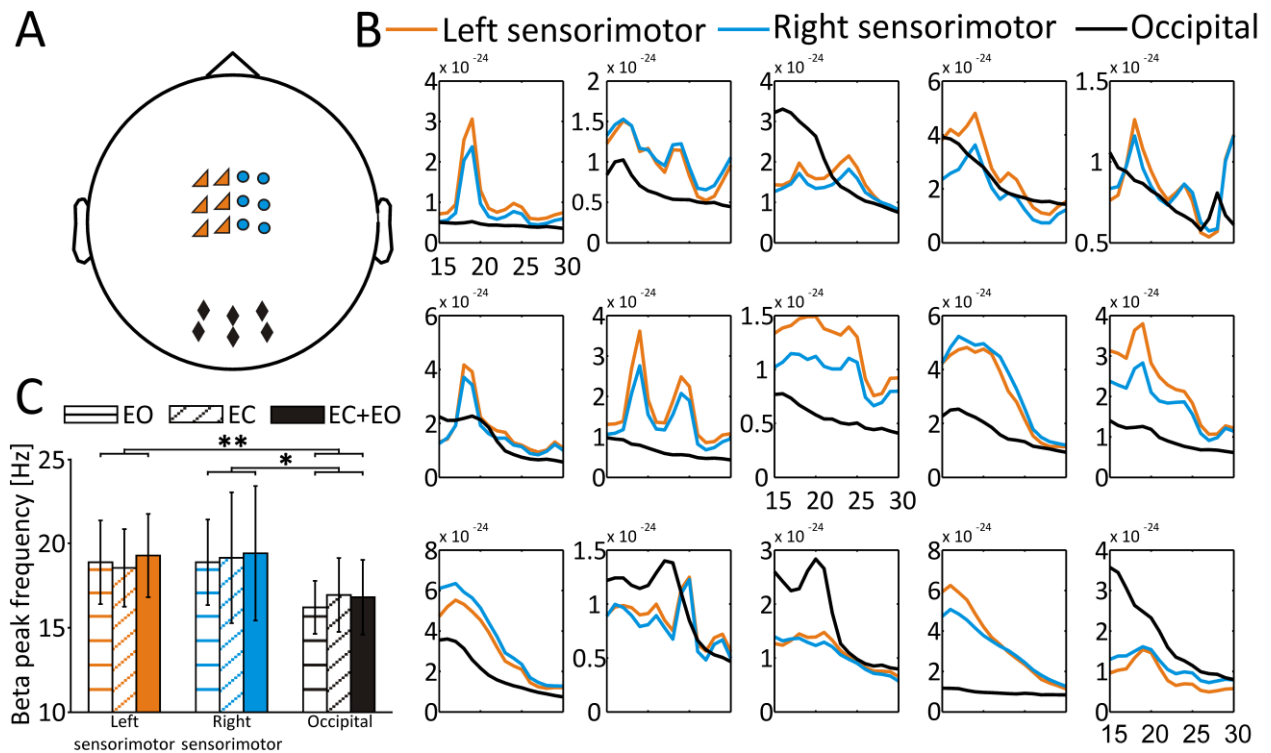
365 In conclusion, the present study shows a significant linear correlation between beta peak
366 frequency at rest and non-modulated endogenous GABA concentration measured by spectrally
367 edited MRS. Significant correlations were restricted to the left sensorimotor cortex area. While
368 previous studies revealed connections between GABA concentrations and beta band power, our
369 results provide a novel connection between GABA concentrations and peak frequencies in the
370 beta band. In line with previous results from studies using pharmacological modulation of GABA
371 concentrations, these results support a specific role of GABAergic inhibition in the generation of
372 oscillatory beta-band activity within the sensorimotor system.

373 **Figures**



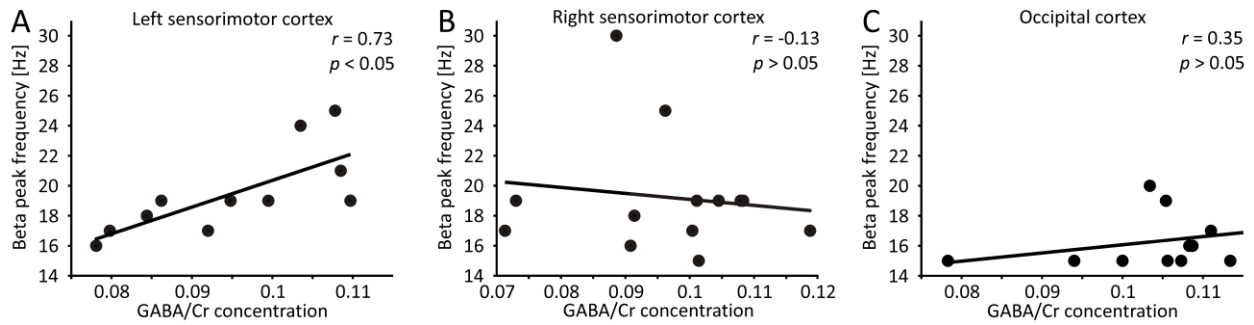
374
 375 Fig 1. Localization of MRS ROIs and average GABA/Cr concentrations across MRS ROIs. A) Placement of
 376 the occipital voxel in the sagittal plane (1), placement of the left sensorimotor voxel, centered on the
 377 hand knob, in the axial (2) and sagittal (3) planes. B) Average GABA/Cr concentrations for the left and
 378 right sensorimotor and occipital MRS ROIs. Error bars represent standard deviations. No significant
 379 difference between voxels was found ($p \geq 0.16$).

380



381
 382 Fig 2. Sensor selection for respective MEG ROIs, individual beta peak frequencies and average
 383 beta peak frequencies across MEG ROIs. A) Sensors for left sensorimotor MEG ROI (orange
 384 triangles), right sensorimotor MEG ROI (blue dots) and occipital MEG ROI (black diamonds). B)
 385 Individual beta peak frequencies for all 15 subjects (EC+EO condition) for left sensorimotor MEG
 386 ROI (orange lines), right sensorimotor MEG ROI (blue lines) and occipital MEG ROI (black lines).

387 C) Average beta peak frequencies separately for all conditions (EO, EC, EC+EO) and all MEG
 388 ROIs. Error bars represent standard deviations. *: $p < 0.01$; **: $p < 0.05$.
 389



390
 391 Fig 3. Correlation of beta peak frequencies and GABA/Cr concentration. (A) Beta peak
 392 frequencies calculated for the left sensorimotor MEG ROI and the EC+EO condition correlated
 393 with GABA/Cr estimates from the left sensorimotor MRS ROI. (B) Same as (A), but now for right
 394 sensorimotor MEG and MRS ROI. (C) Same as (A), but now for occipital MEG and MRS ROI.

Subject	GABA/Cr		
	Left Sensori-motor	Right Sensori-motor	Occipital
1	0.1097	0.1083	0.1054
2	0.0798	0.0713	0.1197
3	0.1035		0.1087
4	0.0995	0.1011	0.1056
5	0.0844	0.0886	0.0940
6		0.0914	0.1213
7		0.0730	0.1134
8		0.1004	0.1166
9			0.1110
10	0.0948	0.1045	0.1073
11	0.0920	0.1187	0.1083
12	0.1078	0.0962	
13	0.1085	0.1014	0.1034
14	0.0781	0.0908	0.0783
15	0.0862	0.1079	0.1000
Mean	0.0949	0.0964	0.1066
SD	0.0117	0.0135	0.0110

395 Table 1: GABA/Cr values per MRS ROI

Beta peak frequency (Hz)									
Subject	Left Sensorimotor			Right Sensori-motor			Occipital		
	EO	EC	ECEO	EO	EC	ECEO	EO	EC	ECEO
1	19	19	19	19	19	19	19	19	19
2	17	17	17	18	16	17	17	17	17
3	24	18	24	24	18	24	15	17	16
4	19	16	19	19	19	19	16	15	15
5	18	18	18	18	30	30	15	15	15
6	18	18	18	18	18	18	17	19	19
7	19	19	19	19	19	19	15	15	15
8	18	19	20	18	17	17	16	15	16
9	17	18	18	17	20	17	17	17	17
10	19	19	19	19	19	19	15	15	15
11	17	17	17	15	17	17	16	16	16
12	25	25	25	25	25	25	15	22	22
13	18	21	21	18	15	15	20	20	20
14	16	15	16	17	15	16	15	17	15
15	19	19	19	19	20	19	15	15	15
Mean	18.87	18.53	19.27	18.87	19.13	19.4	16.2	16.93	16.8
SD	2.47	2.29	2.46	2.53	3.87	3.98	1.57	2.17	2.21

397 Table 2: Beta peak frequencies per MEG ROI and condition

398

399 **References**

400

- 401 1. Salmelin R, Hari R. Spatiotemporal characteristics of sensorimotor neuromagnetic rhythms related
402 to thumb movement. *Neuroscience*. 1994; 60:537–50.
- 403 2. Murthy VN, Fetz EE. Oscillatory activity in sensorimotor cortex of awake monkeys: synchronization
404 of local field potentials and relation to behavior. *Journal of Neurophysiology*. 1996; 76:3949–67.
- 405 3. Pfurtscheller G, Stancák A, JR., Neuper C. Post-movement beta synchronization. A correlate of an
406 idling motor area? *Electroencephalography and Clinical Neurophysiology*. 1996; 98:281–93.
- 407 4. Kilavik BE, Zaepffel M, Brovelli A, MacKay WA, Riehle A. The ups and downs of beta oscillations in
408 sensorimotor cortex. *Special Issue: Neuronal oscillations in movement disorders*. 2013; 245:15–26.
- 409 5. Neuper C, Pfurtscheller G. Event-related dynamics of cortical rhythms: frequency-specific features
410 and functional correlates. *Thalamo-Cortical Relationships*. 2001; 43:41–58.
- 411 6. Jurkiewicz MT, Gaetz WC, Bostan AC, Cheyne D. Post-movement beta rebound is generated in
412 motor cortex: Evidence from neuromagnetic recordings. *NeuroImage*. 2006; 32:1281–89.
- 413 7. Hall SD, Barnes GR, Furlong PL, Seri S, Hillebrand A. Neuronal network pharmacodynamics of
414 GABAergic modulation in the human cortex determined using pharmaco-
415 magnetoencephalography. *Human Brain Mapping*. 2010; 31:581–94.
- 416 8. Muthukumaraswamy S, Myers J, Wilson S, Nutt D, Lingford-Hughes A, Singh K, et al. The effects of
417 elevated endogenous GABA levels on movement-related network oscillations. *NeuroImage*. 2013;
418 66:36–41.
- 419 9. Kilavik BE, Ponce-Alvarez A, Trachel R, Confais J, Takerkart S, Riehle A. Context-Related Frequency
420 Modulations of Macaque Motor Cortical LFP Beta Oscillations. *Cerebral Cortex*. 2012; 22:2148–59.
- 421 10. Neuper C, Pfurtscheller G. Evidence for distinct beta resonance frequencies in human EEG related
422 to specific sensorimotor cortical areas. *Clinical Neurophysiology*. 2001; 112:2084–97.
- 423 11. Salenius S, Portin K, Kajola M, Salmelin R, Hari R. Cortical Control of Human Motoneuron Firing
424 During Isometric Contraction. *Journal of Neurophysiology*. 1997; 77:3401–05.
- 425 12. Jensen O, Goel P, Kopell N, Pohja M, Hari R, Ermentrout B. On the human sensorimotor-cortex
426 beta rhythm: Sources and modeling. *NeuroImage*. 2005; 26:347–55.
- 427 13. Yamawaki N, Stanford IM, Hall SD, Woodhall GL. Pharmacologically induced and stimulus evoked
428 rhythmic neuronal oscillatory activity in the primary motor cortex in vitro. *Neuroscience*. 2008;
429 151:386–95.
- 430 14. Roopun AK, Middleton SJ, Cunningham MO, LeBeau FEN, Bibbig A, Whittington MA, et al. A beta2-
431 frequency (20–30 Hz) oscillation in nonsynaptic networks of somatosensory cortex. *Proceedings of*
432 *the National Academy of Sciences*. 2006; 103:15646–50.
- 433 15. Hall SD, Stanford IM, Yamawaki N, McAllister CJ, Rönqvist KC, Woodhall GL, et al. The role of
434 GABAergic modulation in motor function related neuronal network activity. *NeuroImage*. 2011;
435 56:1506–10.
- 436 16. Gaetz W, Edgar J, Wang D, Roberts T. Relating MEG measured motor cortical oscillations to resting
437 γ -Aminobutyric acid (GABA) concentration. *NeuroImage*. 2011; 55:616–21.
- 438 17. Baker MR, Baker SN. The effect of diazepam on motor cortical oscillations and corticomuscular
439 coherence studied in man. *The Journal of Physiology*. 2003; 546:931–42.
- 440 18. Durst CR, Michael N, Tustison NJ, Patrie JT, Raghavan P, Wintermark M, et al. Noninvasive
441 evaluation of the regional variations of GABA using magnetic resonance spectroscopy at 3 Tesla.
442 *Magnetic Resonance Imaging*. 2015; 33:611–17.
- 443 19. Muthukumaraswamy SD, Edden RA, Jones DK, Swettenham JB, Singh KD. Resting GABA
444 concentration predicts peak gamma frequency and fMRI amplitude in response to visual
445 stimulation in humans. *Proceedings of the National Academy of Sciences*. 2009; 106:8356–61.

- 446 20. Cousijn H, Haegens S, Wallis G, Near J, Stokes MG, Harrison PJ, et al. Resting GABA and glutamate
447 concentrations do not predict visual gamma frequency or amplitude. *Proceedings of the National*
448 *Academy of Sciences*. 2014; 111:9301–06.
- 449 21. Puts NAJ, Edden RAE, Evans CJ, McGlone F, McGonigle DJ. Regionally Specific Human GABA
450 Concentration Correlates with Tactile Discrimination Thresholds. *The Journal of Neuroscience*.
451 2011; 31:16556–60.
- 452 22. Stagg CJ. Magnetic Resonance Spectroscopy as a tool to study the role of GABA in motor-cortical
453 plasticity. *NeuroImage*. 2014; 86:19–27.
- 454 23. Oeltzschner G, Butz M, Baumgarten T, Hoogenboom N, Wittsack H, Schnitzler A. Low visual cortex
455 GABA levels in hepatic encephalopathy: links to blood ammonia, critical flicker frequency, and
456 brain osmolytes. *Metabolic Brain Disease*. 2015:1-10. doi: <http://dx.doi.org/10.1007/s11011-015-9729-2>
- 457
- 458 24. Steingrüber H. *Hand-Dominanz-Test*. Göttingen: Hogrefe; 2011.
- 459 25. Yousry TA, Schmid UD, Alkadhi H, Schmidt D, Peraud A, Buettner A, et al. Localization of the motor
460 hand area to a knob on the precentral gyrus. A new landmark. *Brain*. 1997; 120:141–57.
- 461 26. Mescher M, Merkle H, Kirsch J, Garwood M, Gruetter R. Simultaneous in vivo spectral editing and
462 water suppression. *NMR in Biomedicine*. 1998; 11:266–72.
- 463 27. Edden RA, Puts NA, Harris AD, Barker PB, Evans CJ. Gannet: A batch-processing tool for the
464 quantitative analysis of gamma-aminobutyric acid-edited MR spectroscopy spectra. *Journal of*
465 *Magnetic Resonance Imaging*. 2014; 40:1445–52.
- 466 28. Mullins PG, McGonigle DJ, O’Gorman RL, Puts NA, Vidyasagar R, Evans CJ, et al. Current practice in
467 the use of MEGA-PRESS spectroscopy for the detection of GABA. *NeuroImage*. 2014; 86:43–52.
- 468 29. Haegens S, Cousijn H, Wallis G, Harrison PJ, Nobre AC. Inter- and intra-individual variability in alpha
469 peak frequency. *NeuroImage*. 2014; 92:46–55.
- 470 30. Oostenveld R, Fries P, Maris E, Schoffelen J. FieldTrip: Open Source Software for Advanced Analysis
471 of MEG, EEG, and Invasive Electrophysiological Data. *Computational Intelligence and*
472 *Neuroscience*. 2011; 2011:9.
- 473 31. Liu Z, Zwart JA de, van Gelderen P, Kuo L, Duyn JH. Statistical feature extraction for artifact
474 removal from concurrent fMRI-EEG recordings. *NeuroImage*. 2012; 59:2073–87.
- 475 32. Abbasi O, Dammers J, Arrubla J, Warbrick T, Butz M, Neuner I, et al. Time-frequency analysis of
476 resting state and evoked EEG data recorded at higher magnetic fields up to 9.4T. *Journal of*
477 *Neuroscience Methods*. 2015. doi: 10.1016/j.jneumeth.2015.07.011
- 478 33. Haegens S, Nacher V, Hernandez A, Luna R, Jensen O, Romo R. Beta oscillations in the monkey
479 sensorimotor network reflect somatosensory decision making. *Proceedings of the National*
480 *Academy of Sciences*. 2011; 108:10708–13.
- 481 34. van Ede F, Jensen O, Maris E. Tactile expectation modulates pre-stimulus β -band oscillations in
482 human sensorimotor cortex. *NeuroImage*. 2010; 51:867–76.
- 483 35. Lange J, Halacz J, van Dijk H, Kahlbrock N, Schnitzler A. Fluctuations of Prestimulus Oscillatory
484 Power Predict Subjective Perception of Tactile Simultaneity. *Cerebral Cortex*. 2012; 22:2564–74.
- 485 36. van Dijk H, van der Werf J, Mazaheri A, Medendorp WP, Jensen O. Modulations in oscillatory
486 activity with amplitude asymmetry can produce cognitively relevant event-related responses.
487 *Proceedings of the National Academy of Sciences*. 2010; 107:900–05.
- 488 37. Volkman J, Schnitzler A, Witte OW, Freund H. Handedness and Asymmetry of Hand
489 Representation in Human Motor Cortex. *Journal of Neurophysiology*. 1998; 79:2149–54.
- 490 38. Sörös P, Knecht S, Imai T, Gürtler S, Lütkenhöner B, Ringelstein EB, et al. Cortical asymmetries of
491 the human somatosensory hand representation in right- and left-handers. *Neuroscience Letters*.
492 1999; 271:89–92.
- 493 39. Triggs WJ, Subramaniam B, Rossi F. Hand preference and transcranial magnetic stimulation
494 asymmetry of cortical motor representation. *Brain Research*. 1999; 835:324–29.

- 495 40. Rae C. A guide to the metabolic pathways and function of metabolites observed in human brain 1H
496 magnetic resonance spectra. *Neurochemical Research*. 2014; 39:1-36.
- 497 41. Brunel N, Wang X. What Determines the Frequency of Fast Network Oscillations With Irregular
498 Neural Discharges? I. Synaptic Dynamics and Excitation-Inhibition Balance. *Journal of*
499 *Neurophysiology*. 2003; 90:415–30.
- 500 42. Buzsáki G. *Rhythms of the brain*. Oxford ;, New York: Oxford University Press; 2006.
- 501 43. Stagg CJ, Bachtar V, Johansen-Berg H. The Role of GABA in Human Motor Learning. *Current*
502 *Biology*. 2011; 21:480–84.
- 503 44. Baumgarten TJ, Schnitzler A, Lange J. Beta oscillations define discrete perceptual cycles in the
504 somatosensory domain. *Proceedings of the National Academy of Sciences*. 2015; 112:12187–92.
- 505 45. Perfetti B, Moisello C, Landsness EC, Kvint S, Pruski A, Onofrj M, et al. Temporal Evolution of
506 Oscillatory Activity Predicts Performance in a Choice-Reaction Time Reaching Task. *Journal of*
507 *Neurophysiology*. 2011; 105:18–27.
- 508 46. Tzagarakis C, Ince NF, Leuthold AC, Pellizzer G. Beta-Band Activity during Motor Planning Reflects
509 Response Uncertainty. *Journal of Neuroscience*. 2010; 30:11270–77.
- 510